2017-08-07

Pathways Involved in Recognition and Induction of Trained Innate Immunity by Plasmodium falciparum

Jacob E. Schrum
University of Massachusetts Medical School

PATHWAYS INVOLVED IN RECOGNITION AND INDUCTION OF TRAINED INNATE IMMUNITY BY *PLASMODIUM FALCIPARUM*

A Dissertation Presented By

JACOB EDWIN SCHRUM

Submitted to the Faculty of the
University of Massachusetts Graduate School of Biomedical Sciences, Worcester
in partial fulfillment of the requirements for the degree of

DOCTOR OF PHILOSOPHY

August 7th, 2017

M.D., Ph.D. Program

PATHWAYS INVOLVED IN RECOGNITION AND INDUCTION OF TRAINED INNATE IMMUNITY BY *PLASMODIUM FALCIPARUM*

A Dissertation Presented By

JACOB EDWIN SCHRUM

This work was undertaken in the Graduate School of Biomedical Sciences
M.D., Ph.D. Program

The signature of the Thesis Advisor signifies validation of Dissertation content

Douglas Golenbock, M.D., Thesis Advisor

The signatures of the Dissertation Defense Committee signify completion and approval as to style and content of the Dissertation

Katherine Fitzgerald, Ph.D., Member of Committee

Ricardo Gazzinelli, D.Sc., D.V.M., Member of Committee

Vladimir Litvak, Ph.D., Member of Committee

Clare Bryant, Ph.D., External Member of Committee

The signature of the Chair of the Committee signifies that the written dissertation meets the requirements of the Dissertation Committee

Neal Silverman, Ph.D., Chair of Committee

The signature of the Dean of the Graduate School of Biomedical Sciences signifies that the student has met all graduation requirements of the School.

Anthony Carruthers, Ph.D., Dean of the Graduate School of Biomedical Sciences

August 7th, 2017

Dedication

For Mom and Dad

Acknowledgements

It may take a village to raise a child, but it takes an entire institution to raise an MD/PhD student. As I reflect on my past six years at UMass—four of which I spent in the Golenbock Lab—I'm struck by just how many people have helped me get to this point in my training. To start, I'd like to thank all the current and former members of the Golenbock Lab. Jenny, Donghai, Parisa, Elizabeth, Warrison, Nelsy, and Michelle, thank you for answering the (literally) hundreds of questions I had when I started in the lab and stumbled my way through over the past four years. I had plenty of difficulties when I started my PhD, but finding someone willing to help was not one of them. As time passed and I became one of the longer-tenured lab members answering questions myself, I hope I was able to pay forward a little of the help you all gave me. I'd especially like to thank Kristen for fielding my many reagent requests at all hours of the day and night—almost always for something I needed the next day. I hope by the end of year four you found my planning at least a little bit better. (You'd probably say no.) Carolina, the cGAS work would have languished much longer if it wasn't for your initiative and work ethic—thank you for helping to push that project along. Juliet, you came into the lab and the trained immunity project at just the right time. Having you as an extra pair of hands and another immunologist to bounce ideas off was invaluable to finishing up this work.

UMass fosters a fantastic, collaborative environment, and plenty of postdocs and students outside my lab were instrumental in this work and my development as a scientist. Greg and Shruti, I call you my scientific parents for good reason: you both

helped to raise me as a scientist. Greg, your organized and methodical approach to experimental design and execution was something I adopted early in my PhD, and I know my work is stronger as a result. Shruti, you were always happy to sit and discuss experimental ideas, troubleshoot issues, and interpret results with me. You may have given me a hard time every now and then, but your input absolutely made me a better scientist. Jennie and Rosane, you both helped me learn how to grow malaria in a dish—a surprisingly difficult task considering how easily it grows in infected individuals. Yves, you always encouraged me to think big, and then you challenged my ideas to make sure I had thought them through. Maninjay, I found our discussions of ChIP and gene regulation extremely useful. Mike, thank you for going through multiple NanoString heatmap revisions with me. I'm sure I'm missing others—thank you all.

In keeping with the collaborative spirit, I'm pretty sure every member of the Department of Medicine faculty has helped me directly at some point. I'd especially like to thank Evelyn for attending our lab meetings and having a generous open-door policy—your insights into my work have been extremely valuable. Stu, Sanjay, Steve, and Reed, thank you for letting me tag along and see patients with you when you were on service. Thanks to your teachings, I feel so much more prepared to return to medical school. To my thesis research advisory committee—Neal, Ann, Vladimir, and Kate—thank you for sitting through all my negative results and guiding me towards the promised land of publication. Ricardo, thank you for being a collaborator and serving on my dissertation examination committee. Your work provides the foundation for much of my own.

I'd also like to thank Mihai Netea for generously accepting our request to collaborate, and to his mentees Siroon, Rob, and Bas for helping me to get the trained immunity project up and running. Clare Bryant crossed an ocean to be my external examiner—thank you for your insightful comments and questions that ultimately made this dissertation better. Without my blood donors, I'd have no data. Thank you for committing part of yourselves—literally—to my cause.

I have amazing coworkers and research mentors, but I would not be here today without my family and friends. Too often, I left lab dejected after yet another failed experiment, but you all kept me going. To all my friends in the graduate school, thank you for being there and providing an outlet to vent. Whether through volleyball, softball, or just hanging out, we managed to get out of the lab and have some fun. To Apu and Dennis, thanks for being great friends during our med school experiences and beyond. If you ever end up as my attendings, please show me some mercy. Michael, our runs, workouts, and dinners provided much-needed balance to my life. Adam, Dave, Ben, Corbin, Emily: our friendships span decades and time zones. I'm grateful to have you all in my life.

Kathryn, you are one of the sweetest and most loving individuals I have ever met. I don't know if I could have done this without you—luckily, I didn't have to. I love you. To Joyce and Jill, sometimes a boy just needs a mother, biology be damned. I love you. To my mother, father, and sister, words cannot express how much you mean to me. You've raised me and helped me to become the man I am today, and for that I am grateful beyond measure. I love you.

Finally, I'd like to thank my mentors, Kate and Doug. Kate, there's no way I finish my PhD without your guidance. As chair of my TRAC committee, you kept my work focused and were one of my strongest advocates. Over the past year, you've become a *de facto* co-mentor for me. Thank you for letting me present in your lab meetings and mine your mentees for help. If you had a dollar for every time I knocked on your door these past few months as I raced to finish my dissertation and prepare my work for publication, you'd never have to apply for an NIH grant again. Thank you.

Last, but certainly not least, thank you, Doug. I can't imagine a better mentor. Not only were you invested in my project and results, but you were truly invested in me as a budding physician-scientist and a person. Thank you for sending me to conferences and research sites all over the world, introducing me to your colleagues along the way. My development as a scientist and physician is enriched for it. Thank you for being such a strong advocate for me. The training to become an MD/PhD is long and arduous, but knowing you're in my corner makes all the difference. Thank you.

Abstract

Malarial infection in naïve individuals induces a robust innate immune response, but our understanding of the mechanisms by which the innate immune system recognizes malaria and regulates its response remain incomplete. Our group previously showed that stimulation of macrophages with *Plasmodium falciparum* genomic DNA (gDNA) and AT-rich oligodeoxynucleotides (ODNs) derived from this gDNA induces the production of type I interferons (IFN-I) through a STING/TBK1/IRF3-dependent pathway; however, the identity of the upstream cytosolic DNA receptor remained elusive. Here, we demonstrate that this IFN-I response is dependent on cyclic GMP-AMP synthase (cGAS). cGAS produced the cyclic dinucleotide 2'3'-cGAMP in response to *P. falciparum* gDNA and AT-rich ODNs, inducing IRF3 phosphorylation and *IFNB* transcription. In the recently described model of innate immune memory, an initial stimulus primes the innate immune system to either hyperrespond (termed "training") or hyporespond ("tolerance") to subsequent immune challenge. Previous work in mice and humans demonstrated that infection with malaria can both serve as a priming stimulus and promote tolerance to subsequent infection. In this study, we demonstrate that initial stimulation with *P. falciparum*-infected red blood cells (iRBCs) or the malaria crystal hemozoin (Hz) induced human adherent peripheral blood mononuclear cells (PBMCs) to hyperrespond to subsequent Toll-like receptor (TLR) challenge. This hyperresponsiveness correlated with increased H3K4me3 at important immunometabolic promoters, and these epigenetic modifications were also seen in monocytes from Kenyan children naturally infected with malaria. However,

the use of epigenetic and metabolic inhibitors indicated that malaria-induced trained immunity may occur via previously unrecognized mechanism(s).

Table of Contents

List of Tables

List of Figures

List of Abbreviations

[3-(4,5-dimethylthiazol-2-yl)-5-(3-carboxymethoxyphenyl)-2-(4-sulfophenyl)-2H-tetrazolium, inner salt] (MTS)
5’-methylthioadenosine (MTA)
absent in melanoma 2 (AIM2)
AIM2-like receptor (ALR)
allophycocyanin (APC)
antigen-presenting cell (APC)
apoptosis-associated speck-like protein containing a caspase-recruitment domain (ASC)
bacille Calmette-Guérin (BCG)
base pair (bp)
blood-brain barrier (BBB)
bone marrow derived macrophage (BMDM)
bovine serum albumin (BSA)
C-type lectin receptor (CLR)
cerebral malaria (CM)
chromatin immunoprecipitation (ChIP)
clustered regularly interspaced short palindromic repeats (CRISPR)
cyclic GMP-AMP (2’3’-cGAMP)
cytomegalovirus (CMV)
damage-associated molecular pattern (DAMP)
double-stranded DNA (dsDNA)
Dulbecco’s modified Eagle’s medium (DMEM)
enzyme-linked immunosorbent assay (ELISA)
ethylenediaminetetraacetic acid (EDTA)
experimental cerebral malaria (ECM)
fetal bovine serum (FBS)
fluorescein isothiocyanate (FITC)
genomic DNA (gDNA)
glycosylphosphatidylinositol (GPI)
GMP-AMP synthase (cGAS)
hemozoin (Hz)
herpes simplex virus (HSV)
histone H3 lysine 4 (H3K4me3)
human immunodeficiency virus (HIV)
hypoxia-induced factor 1α (HIF1α)
IFNα receptor (IFNAR)
immune complex (IC)
infected red blood cell (iRBC)
interferon regulatory factor (IRF)
interferon-stimulated gene (ISG)
interferon-stimulatory DNA (ISD)

interleukin (IL)
Lipopolysaccharide (LPS)
liquid chromatography-tandem mass spectrometry (LC-MS/MS)
lithium chloride (LiCl)
macrophage colony-stimulating factor (M-CSF)
major histocompatibility complex (MHC)
mammalian target of rapamycin (mTOR)
mitochondrial antiviral-signaling protein (MAVS)
monocyte derived macrophage (MDM)
myelin and lymphocyte protein (MAL)
myeloid differentiation primary response gene 88 (MYD88)
natural killer (NK)
NOD-like receptor (NLR)
nuclear factor kappa-light-chain-enhancer of activated B cells (NF-κB)
nucleotide-binding domain, leucine-rich repeat–containing, pyrin domain containing 3 (NLRP3)
oligodeoxynucleotide (ODN)
pathogen-associated molecular pattern (PAMP)
pattern recognition receptor (PRR)
peridinin-chlorophyll-Cy5.5 (PerCP-Cy5.5)
peripheral blood mononuclear cell (PBMC)
peritoneal exudate cell (PEC)
phenazine methosulfate (PMS)
phorbol 12-myristate 13-acetate (PMA)
phosphate-buffered saline (PBS)
phycoethrin-cyanine7 (PE-Cy7)
Plasmodium berghei ANKA (PbA)
polymerase chain reaction (PCR)
red blood cell (RBC)
red pulp macrophages (RPMs)
Regulated on Activation, Normal T cell Expressed and Secreted (RANTES)
RIG-I-like receptor (RLR)
RPMI with 10% human serum (RPMI+)
Sendai virus (SeV)
severe malarial anemia (SMA)
stimulator of interferon genes (STING)
systemic inflammatory response syndrome (SIRS)
T-cell receptor (TCR)
TANK binding kinase-1 (TBK1)
Toll-like receptor (TLR)
Toll/interleukin-1 receptor-domain-containing adapter-inducing IFNβ (TRIF)
TRIF-related adaptor molecule (TRAM)
Tris-EDTA (TE)
tumor necrosis factor-α (TNFα)

type I interferons (IFN-I)
uninfected red blood cell (uRBC)
wild-type (WT)
Y-form short DNA (YSD)

Chapter I: Introduction

Malaria: A primer

Malaria, along with HIV/AIDS and tuberculosis, remains one of the world's most pressing infectious disease-related global health issues. According to the World Health Organization's most recent *World Malaria Report*, although the malaria incidence rate has decreased by over 40% and 17 nations have eradicated malaria since the year 2000, there were still an estimated 212 million new cases of malaria worldwide in 2015, with nine in ten of those occurring in Africa (1). These cases resulted in over 400,000 deaths, 92% of which occurred in Africa and the majority in children under the age of five (1). Malarial disease in humans is primarily caused by infection with one of four parasite species from the protozoan genus *Plasmodium*: *Plasmodium falciparum, Plasmodium vivax, Plasmodium ovale, and Plasmodium malariae*. *P. falciparum* infection is the most common infection worldwide and is responsible for 99% of fatalities due to malaria (1). Infection with *P. vivax* has the second highest prevalence, and although the WHO estimates that only 4% of new malaria infections in 2015 were due to *P. vivax*, more than 40% of malarial infections outside of Africa were due to *P. vivax*, primarily in southern and southeast Asia, islands of the western Pacific, and central and South America (1).

The malarial life cycle is complex, involving development in both human and mosquito hosts. For simplicity, the stages of human infection are briefly summarized here. Infection is transmitted when *Plasmodium* sporozoites are injected into the skin through the bite of an infected *Anopheles* mosquito. The sporozoite then invades the

vasculature and travels to the liver, where it invades a hepatocyte and begins to divide asexually. After several cycles of asexual reproduction during this liver stage of infection, the hepatocyte ruptures, releasing the daughter malaria parasites—now called merozoites—into the bloodstream. These merozoites then each infect a red blood cell (RBC), where they continue to replicate asexually. During this blood stage of replication, which takes 48-72 hours depending on the species of parasite (2), the merozoites develops sequentially into a ring form, then a trophozoite, which then reproduces asexually to produce many daughter merozoites. The resulting schizont—the RBC containing the daughter merozoites—ruptures, releasing these merozoites into the bloodstream to each infect a new RBC. In *P. vivax* and *P. ovale*, some of the parasites reinfect the liver, where they remain dormant as hypnozoites. These hypozoites, through reactivation and escape from the hepatocyte, can then cause relapse after clearance of the original blood stage infection. For all species of malarial parasites, the infection is propagated when an *Anopheles* mosquito takes a blood meal from an infected individual which includes both male and female gametocytes, which can also develop from blood stage parasites. The gametocytes combine sexually in the mosquito, where through further developmental processes in the mosquito [thoroughly reviewed in (3)], sporozoites mature and migrate to the mosquito salivary gland for infection of a new human host.

Human malarial disease is believed to be the result of blood stage infection. General symptoms of uncomplicated blood stage infection include fevers, chills, rigors, malaise, and other flu-like symptoms. The majority of malarial infections remain

uncomplicated; however, some infections—most commonly in children under the age of five or naïve individuals—become severe and potentially life-threatening. Symptoms of severe malaria include, but are not limited to, respiratory distress, convulsions, severe anemia, loss of consciousness, and circulatory collapse (4). The majority of severe malaria cases fall into one of three groups: malaria with metabolic disturbances/respiratory distress, severe malarial anemia (SMA), and cerebral malaria (CM) (5, 6).

Of these three, CM, which affects over 575,000 children in Sub-Saharan Africa annually (7), is arguably the most dangerous, as it can progress rapidly and has an ultimate fatality rate of 15-20% (4). CM is defined by the World Health Organization as a coma lasting longer than one hour after the cessation of convulsions that is associated with *P. falciparum* parasitemia and cannot be explained by any other etiology (4). Based on early postmortem anatomical and histological specimens, sequestration of *P. falciparum* infected red blood cells (iRBCs) resulting in obstruction of the cerebral microvasculature was determined to be the primary mechanism behind CM pathogenesis (8), and it has also been implicated in other forms of severe malarial illness (6). While iRBC sequestration is still believed to be one of the main drivers of CM, further research indicates that CM pathogenesis is more complex. A postmortem study of 31 patients diagnosed clinically with CM found that 18 of the patients had cerebral histopathology typical of CM—sequestered iRBCs, parenchymal hemorrhage, and leukocyte accumulation—while six had sequestration only and seven had no iRBC sequestration at all (9). Conversely, cerebral iRBC sequestration can also be seen in malaria patients who

do not have clinical symptoms of CM (10). Breakdown of the blood-brain barrier (BBB) appears to be important in CM pathogenesis, and mononuclear cells have been identified at these lesions (11), suggesting a potential role for the immune system in CM pathogenesis.

As mentioned previously, immunologically naïve individuals are most at risk for severe malarial disease. However, for individuals in endemic area, the risk of severe malaria drops precipitously with age as the individual is exposed more frequently to the parasite. It has been estimated that the risk of severe malaria—excluding cerebral malaria—largely disappears after only one or two infections (12). Although it is less likely that children over the age of five will contract severe malaria in endemic areas, they are still at risk for uncomplicated malaria, with the flu-like symptoms discussed earlier (13). By the time individual reach the age of thirty, they are largely immune to clinical malaria (13). However, it is not uncommon for adults and older children in endemic areas to have asymptomatic parasitemia; that is, they have detectable levels of parasite in the bloodstream—crucially, at high enough levels to transmit the parasite through a mosquito blood meal—but remain afebrile and appear healthy. This phenomenon of malarial tolerance will be explored later in this Chapter. But first, we need to introduce the immune system, with special focus on innate immunity.

Introduction to innate immunity

The immune system is traditionally divided into two interconnected arms: the innate immune system and adaptive immune system. According to this paradigm, first

elucidated by Charles Janeway in his landmark 1989 *Cold Spring Harbor Symposia on Quantitative Biology* paper (14), the innate immune system is composed of cells that express a limited number of germline-encoded pattern recognition receptors (PRRs), which recognize pathogen-associated molecular patterns (PAMPs) found exclusively on infectious organisms and non-self cells. Triggering these PRRs on cells such as macrophages and dendritic cells indicates to the innate immune system that a pathogen has been encountered. The innate immune system responds in two main ways: it activates an inflammatory response primarily through the production of proinflammatory cytokines in an effort to contain the infection, and it also activates B and T cells of the adaptive immune system. These adaptive immune cells contain unique receptors that are the product of somatic recombination at the V(D)J locus. The wide variety of receptors that can be generated by this process provides the adaptive immune system with the ability to respond quite specifically, but first these cells must be activated. This activation of the adaptive immune system requires two signals from a cell of the innate immune system: presentation of a protein component of the pathogen, termed an antigen, on a major histocompatibility complex (MHC) expressed on the antigen-presenting cell (APC) surface, and expression of a co-stimulatory molecule. Activation of the adaptive immune system then produces a clonal response that is specific to the invading pathogen, leading to its eradication from the body. The maintenance of memory B and T cells also allows the adaptive immune system to respond more immediately if the pathogen is encountered at a later time point.

Janeway's main contribution to this paradigm was the idea that "the immunologist's dirty little secret"—his term for the dead bacteria-containing, immune-stimulating adjuvants required to initiate an adaptive response—may do so by triggering these PRRs (14). Triggering of these PRRs would then cause the expression of co-stimulatory molecules, so that the adaptive immune system would only be triggered in the presence of a non-self challenge. The first PRR was discovered a few years later, in 1996, when Jules Hoffman's group demonstrated that the transmembrane protein Toll was required to protect *Drosophilia melanogaster* from fatal fungal infection (15). A year later, Janeway, along with his mentee Ruslan Medzhitov, demonstrated that the human version of Toll—later renamed Toll-like receptor (TLR) 4—activated the NF-κB pathway, led to the production of proinflammatory cytokines, and induced the expression of costimulatory molecules on the cell surface (16).

These landmark studies helped to open the floodgates of innate immunity research, and in the 20 years since the publication of Medzhitov and Janeway's work on human Toll, the list of PRRs involved in innate immune recognition and signaling has exploded. After Toll, multiple members of what became known as the TLR family were described. Most of the TLRs are located on the plasma membrane or in an endosomal compartment. The nucleic-acid recognizing TLRs, including double-stranded RNA-sensing TLR3 (17), single-stranded RNA-sensing TLR7 and TLR8 (18), and CpG motif-containing DNA-sensing TLR9 (19), recognize their ligands in and signal from an endosomal compartment. Additionally, homodimers of TLR12 or TLR11/12 heterodimers, depending on the cell type, recognize a profilin protein from *T. gondii* in

the endosome (20, 21), while uropathogenic *Escherichia coli* are recognized by TLR11 alone (22). On the plasma membrane, TLR2 recognizes lipoproteins (23, 24) through the formation of heterodimers with TLR1 (25) or TLR6 (26). TLR2 also recognizes peptidoglycan (27) and GPI anchors from *Toxoplasmosis gondii* (28), while TLR4 is the receptor for lipopolysaccharide (LPS) (29) with CD14 and MD-2 functioning as co-receptors (30). Bacterial flagellin is recognized by TLR5 (31). These TLRs, once they recognize their cognate PAMP (or damage-associated molecular pattern—DAMP), dimerize and initiate a signaling cascade that begins with one of a handful of adaptor proteins— myeloid differentiation primary response gene 88 (MYD88), myelin and lymphocyte protein (MAL), Toll/interleukin-1 receptor-domain-containing adapter-inducing IFNβ (TRIF), and TRIF-related adaptor molecule (TRAM)—and ends with the activation of a specific combination of transcription factors, such as nuclear factor kappa-light-chain-enhancer of activated B cells (NF-κB) or interferon regulatory factors (IRFs), depending on the TLR(s) stimulated (32).

The TLR family was the first PRR family discovered and is perhaps one of the evolutionarily oldest PRR families—the sea urchin, for example, has gene sequences for 222 TLRs in its genome (33)—but it is far from the only PRR family. The C-type lectin receptor (CLR) family of PRRs are also expressed on the plasma membrane. Primarily known for their ability to recognize carbohydrates in fungal cell walls, they also play a role in the immune response to a variety of other pathogens (34). The NOD-like receptor (NLR) family, named for the central nucleotide-binding oligomerization domain shared by all of its members, is a family of cytosolic receptors that plays multiple roles in

pathogen sensing and proinflammatory signaling (35), although they are arguably best known for their roles as inflammasome sensors, which are critical for activating caspase-1 to cleave pro-IL-1β and pro-IL-18 into their active forms (36).

Cytosolic nucleic acids represent a potent family of PAMPs and DAMPs, and there are two intracellular PRR families dedicated to recognizing them. The RIG-I-like receptor (RLR) family is a family of helicases best known for inducing type I interferon (IFN-I) expression after binding to various RNA species (37). The final major PRR family is united not by structural similarity but by functional similarity: the cytosolic DNA receptors. This family includes absent in melanoma 2 (AIM2), which binds to double-stranded DNA (dsDNA) through its HIN200 domain and activates an apoptosis-associated speck-like protein containing a caspase-recruitment domain (ASC)-containing inflammasome complex (38, 39); IFI16, a fellow HIN-containing protein that has been proposed, along with its mouse ortholog p204, to form the AIM2-like receptor (ALR) family (40); RNA polymerase III, which detects poly(dA:dT) and synthesizes a special RNA species for detection by RIG-I (41); and cyclic GMP-AMP synthase (cGAS), which catalyzes the synthesis of 2’3’-cGAMP after binding directly to DNA, leading to IFN-I production in a stimulator of interferon genes (STING)-dependent manner (42-45). Now we will turn our attention to the PRRs, PAMPs, and pathogenesis inherent in the innate immune recognition of malaria.

The innate immune response to malaria

As discussed earlier, uncomplicated malarial illness is characterized by fever, malaise, and other flu-like symptoms. These symptoms, the hallmarks of malarial disease, are believed to be the result of robust proinflammatory cytokine production induced by widespread innate immune activation. Multiple PRRs are involved in recognizing malarial parasites and PAMPs. TLR2 recognizes *P. falciparum* glycosylphosphatidylinositol (GPI) anchors by forming heterodimers with TLR1 or TLR6 in macrophages (46). TLR2 also appears to recognize sporozoites in the *P. yoelii* mouse malaria model (47). Injection of hemozoin (Hz) crystals—the end product of heme metabolism by the malaria parasite—into mice causes the recruitment of monocytes to the area of injection, as well as the production of IL-1β, IL-6, and multiple chemokines (48). Work performed by our group and collaborators demonstrated that TLR9 recognizes Hz crystals coated with *Plasmodium* genomic DNA (gDNA) in the phagolysosome (49). Originally, it was believed that Hz was directly recognized by TLR9 (50), but our group demonstrated that DNase treatment of these crystals completely abrogated Hz-induced TLR9 activation (49). In recent years, other laboratories have demonstrated that TLR9 recognizes DNA/protein complexes from malaria parasites (51), and later work demonstrated that these DNA/protein complexes were actually parasite nucleosomes (52).

Hz crystals can also destabilize the phagolysosome and allow *Plasmodium* DNA to access the cytosol, where it is recognized by the AIM2 inflammasome and is an important component for IL-1β production in malarial infection (53). Hz itself is able to

activate the NLRP3 inflammasome, leading to robust cleavage of pro-IL-1β into its active form (53). The NLRP12 inflammasome is also activated—as evidenced by the presence of NLRP12 containing inflammasome specks in patient peripheral blood—during natural malarial infection(54). An additional cytosolic DNA receptor senses AT-rich stem-loop structures in *Plasmodium* genomes and produces IFN-I in a manner independent of p204, RNA pol III, and TLR9, but dependent on the STING/TANK binding kinase-1 (TBK1)/IRF3/IRF7 axis (55). Innate immunity in *Plasmodium* infection does benefit the host by limiting parasitemia, clearing infected red blood cells (iRBCs), and assisting in the activation of adaptive immunity (56); however, innate immune activation is not without drawbacks.

The proinflammatory cytokinemia resulting from infection with malaria has been well-defined, and even implicated in the development of severe pathology like cerebral malaria (57). A landmark 1989 study in the *New England Journal of Medicine* reported that serum tumor necrosis factor-α (TNFα) were higher in children who died of severe malaria than those that survived severe malaria, and that mortality rate was positively correlated with serum TNFα (58). Additionally, they found that TNFα levels were significantly higher in patients with parasite burdens greater than 10^6 trophozoites/μl than patients with parasite levels below this (58). In another study comparing serum cytokine levels between patients with severe malaria, uncomplicated malaria, and healthy controls with no parasites on blood smear (which does not rule out asymptomatic, submicroscopic infection), interleukin (IL)-6 and IL-10 levels were highest in patients with CM, significantly higher in severe malaria patients than uncomplicated malaria patients, and

these levels were higher in uncomplicated malaria patients than healthy controls, although surprisingly IL-6 levels were significantly lower in patients with $5x10^5$ parasites/μl than patients with higher parasite burdens (59). TNFα and IL-12 levels were significantly higher in severe malaria patients than healthy controls, while there were no significant differences between the groups for IL-1β or IL-8 (59).

Despite many studies examining the effects of the immune system on CM pathogenesis (57, 60) a definitive role for immune cells and the cytokines they produce has yet to be determined. Since human studies of CM are largely limited to analysis of peripheral blood and postmortem tissue samples, interventional studies to determine the causative agent(s) of CM pathogenesis are restricted to animal models of CM. Using mouse models of malaria also allows for the determination of definite roles for various innate immune components in pathogenesis, but these models may not completely correspond to human disease.

The *Plasmodium berghei* ANKA (PbA)-induced murine experimental cerebral malaria (ECM) model mimics many of the symptoms—including convulsions, seizures and coma—and histopathological changes of human CM (57). In this model, which involves infection of C57BL/6 mice with either PbA liver-stage forms called sporozoites or PbA iRBCs, multiple immune cell types and cytokines have been identified as essential for ECM pathogenesis. Conventional dendritic cells (cDCs), primarily $CD8^+$ cDCs (61, 62), phagocytose iRBCs in the spleen and cross-present parasite antigens to $CD8^+$ T cells, which are activated to a cytotoxic phenotype in a largely parasite antigen-specific manner (63). These activated $CD8^+$ T cells also express the chemokine receptor

CXCR3, which is required for effective trafficking to the brain (64). Once in the brain, activated $CD8^+$ T cells recognize their cognate antigen cross-presented in the cerebral microvasculature (65) and damage the BBB—thus inducing ECM—in a perforin- and granzyme B-dependent manner (66, 67).

Both $CD4^+$ T cells and $CD8^+$ T cells are required for ECM pathogenesis (68). Depletion of $CD4^+$ T cells just before onset of ECM symptoms is not protective; however, depletion of $CD8^+$ T cells at the same time point confers ECM resistance, indicating that $CD8^+$ T cells are the primary cellular effectors in ECM (69). Although IFNγ has long been known to be necessary for the development of ECM (70), recent work showed that IFNγ expression by $CD4^+$ T cells was sufficient to make previously resistant $IFN\gamma^{-/-}$ mice susceptible to ECM, and $CD4^+$ T cell-derived IFNγ was important for $CD8^+$ T cell trafficking to the brain (71). In addition to IFNγ, multiple recent studies have shown that type I interferons are also essential for ECM pathogenesis (55, 72-74).

Interferons were so-named because of their ability to interfere with viral replication (75). Interferons can be divided into two classes: type II interferons, of which IFNγ is the only member; and type I interferons (IFN-I), which in humans include 13 isoforms of IFNα and one isoform each of IFNβ, IFNε, IFNκ, and IFNω (reviewed in (76)). Induction of IFN-I begins with the sensing of microbial- and danger-associated molecular patterns—primarily nucleic acids—by PRRs on the cell surface, in endosomes, and in the cytosol. These receptors then trigger signaling cascades through one of four adaptor molecules: mitochondrial antiviral-signaling protein (MAVS), MYD88, STING, and TRIF. These signaling cascades lead to the phosphorylation of the transcription

factors IRF3 and IRF7, which translocate to the nucleus and promote transcription of IFN-I. All IFN-I signal through the IFNα receptor (IFNAR), a heterodimer of IFNAR1 and IFNAR2. In addition to their importance in host antiviral defense, IFN-I function in host response to bacterial infection and modulation of both the innate and adaptive immune systems ((77, 78)).

In patients, IFNα levels in the blood positively correlate with parasitemia in *Plasmodium falciparum* infection (79), and polymorphisms in *IFNAR1* are associated with protection from CM (72, 80). Recently, multiple groups have shown that deletion of *Ifnar1* or both *Irf3* and *Irf7* protect mice from ECM (55, 72-74). Although daily administration of exogenous IFNα throughout PbA infection drastically decreased parasitemia and protected most mice from ECM (81), the ECM protection conferred by *Ifnar1* deletion does not appear to depend on parasitemia, as various groups have found a decrease (74), no change (55, 73), or increase (72) in parasitemia in ECM-resistant *Ifnar1*$^{-/-}$ mice compared to ECM-susceptible wild-type (WT) mice. Adoptive transfer of *Ifnar1*$^{+/+}$ CD8^{+} splenocytes, but not *Ifnar1*$^{-/-}$ CD8^{+} splenocytes, from PbA-infected mice is sufficient to make *Ifnar1*$^{-/-}$ mice susceptible to ECM; however, IFN-I do not appear to be necessary for activation of CD8^{+} T cells, as similar numbers of activated CD8^{+} T cells accrue in the spleens of WT and *Ifnar1*$^{-/-}$ mice (72). IFN-I have also been implicated in modulation of the adaptive immune system. One group found that deleting *Ifnar* lead to a decrease in parasitemia in both the PbA and *P. chaubaudi* mouse malaria models because IFN-I inhibited IFNγ production by CD4+ T cells (82). In a later paper, this group found that IFN-I block proinflammatory cytokine production by human PBMCs taken from

individuals experimentally infected with *P. falciparum* and then rechallenged *ex vivo* with iRBCs as well as promote the production of $CD4^+$ IL-10 producing type 1 regulatory T (Tr1) cells (83).

Multiple cell types and signaling pathways have been implicated in production of IFN-I during *Plasmodium* infection. In experimental human infection with *P. falciparum*, increased numbers of $CD56^+$ cells are IFN-I positive compared to pre-infection (83). Hepatocytes produce IFN-I in response to PbA sporozoite RNA in a MAVS-dependent manner, and these IFN-I help the host control the liver-stage parasite burden (84). Both cDCs and plasmacytoid dendritic cells (pDCs) produce IFN-I in the spleen during PbA infection (85, 86), and splenic red pulp macrophages (RPMs) drive early production of IFN-I during infection with the related parasite *P. chabaudi*, which does not cause ECM (87). However, these RPMs are not required for control of *P. chabaudi* parasitemia (87), and only cDCs, not pDCs, are necessary for PbA-induced ECM (85), so it is unclear if these IFN-I are relevant to malaria-induced pathology. Recent work on CD11c-Cre *Ifnar1*$^{fl/fl}$ mice, in which *Ifnar1* is deleted almost exclusively in cDCs, showed that these mice were completely resistant to ECM, and this protection correlated with a 50% drop in serum IFNα as compared to ECM-susceptible *Ifnar1*$^{fl/fl}$ littermate control mice (86). This drop in serum IFNα is almost certainly due to interruption of a positive feedback loop in cDCs. The endosomal DNA sensor TLR9, which is important for production of IFN-I in pDCs, recognizes *Plasmodium* DNA bound to Hz (49), and the endosomal RNA sensor TLR7 is essential for early production of IFN-I induced by *P. chabaudi* (88). Although the drug E6446, which inhibits both TLR7 and TLR9, protects mice from PbA-induced

ECM (89), deletion of *Tlr7* or *Tlr9* provides little to no protection from ECM (90-92), and TLR7 is dispensable for *P. chabaudi* parasite control (88), so E6446 may function as a general blocker of nucleic acid sensing rather than a specific inhibitor of TLRs 7 and 9. At the adaptor level, the importance of MYD88, which is downstream of both TLR7 and TLR9, to ECM pathogenesis is unclear, as some research has shown either a partial or complete protection from ECM for *Myd88*$^{-/-}$ mice (90, 92, 93), while other experiments have shown that *Myd88*$^{-/-}$ mice remain susceptible to ECM (91). The adaptor TRIF, required for induction of IFN-I downstream of TLR3 and TLR4, is completely dispensable for ECM pathogenesis (90, 91). STING, an adaptor protein important for cytosolic DNA sensing, is essential for recognition of a common AT-rich motif found within *Plasmodium* genomic DNA, and mice expressing a non-functional hypomorph of TBK1—which normally phosphorylates IRF3 downstream of STING (94)—are completely resistant to ECM (55). Still, the upstream signaling pathway essential for production of these IFN-I remains unknown. Given the discovery of cGAS and its well-described role in detecting cytosolic DNA, **we hypothesize that cGAS is the sensor for cytosolic *P. falciparum* gDNA and AT-rich ODNs and is required for the resulting expression of IFN-I.**

Innate immune memory

Traditionally, it was believed that immune memory was exclusively a component of the adaptive immune system. However, multiple studies in the past few years have demonstrated memory phenotypes in innate immune cells. Mihai Netea and colleagues

demonstrated that initial stimulation of human monocytes with β-glucan—a component of fungal cell walls—followed by washing of the cells and a rest period with no stimulus, provoked increased cytokine production upon secondary stimulation with TLR ligands (95). Similarly, administration of the bacille Calmette-Guérin (BCG) vaccination—the primary vaccine against tuberculosis—to healthy volunteers induced increased monocyte responsiveness to both bacterial and fungal pathogens up to three months after vaccination (96). In both instances, this memory phenotype appeared to be mediated by epigenetic modifications, specifically increased trimethylation at histone H3 lysine 4 sites (H3K4me3), because treatment with a methyltransferase inhibitor to prevent histone methylation abrogated this training effect in both studies. Netea and colleagues coined the term “trained immunity” to described these increased, non-specific secondary innate immune responses (97). The converse of trained immunity, tolerance, occurs when an initial stimulation renders innate immune cells hyporesponsive to subsequent immune challenge. Lipopolysaccharide (LPS) tolerance is a classical example, and this tolerance is seen clinically in sepsis and systemic inflammatory response syndrome (SIRS) (98). An increasing amount of evidence supports the idea that post-sepsis tolerance is at least partially due to epigenetic changes in traditional innate immune cell lineages (99). In opposition to trained immunity, LPS tolerance appears to be regulated in part by loss of H3K4me3 at proinflammatory promoters upon secondary challenge (100). Global epigenomic and transcriptomic analysis of β-glucan-trained and LPS-tolerized macrophages discovered differential regulation of gene modules between these two functional states (101). Trained immunity seems to be at least in part dependent on

cellular metabolism, as the phenotype is correlated with a shift toward aerobic glycolysis, and chemical inhibition of the AKT/mammalian target of rapamycin (mTOR)/hypoxia-induced factor 1α (HIF1α) pathway blocks training (102). Blocking BCG-induced training using the mTOR inhibitor rapamycin also blocks the increase in H3K4me3 at proinflammatory promoters (103), while tolerant monocytes from patients with septic shock have defective glycolytic and oxidative phosphorylation pathways (104). Interestingly, tolerance and training appear to be two ends of the same spectrum, as LPS and other ligands that induce tolerance can also induce training at much lower concentrations (105). This can be summarized by the following model: an initial immune challenge serves as a priming stimulus, which, depending on the nature and concentration of the priming ligand, induces epigenetic and metabolic alterations that result in a trained or tolerized response to subsequent immune challenge.

McCall and colleagues demonstrated that whole blood samples isolated from volunteers infected experimentally with *P. falciparum* produced elevated proinflammatory cytokines upon TLR ligand stimulation; additionally, naïve PBMCs primed *ex vivo* with *P. falciparum* lysate and then immediately re-stimulated with TLR ligands produced increased proinflammatory cytokines than PBMCs primed with media alone (106). Subsequently, our group confirmed that the hyperresponsiveness of malaria-primed PBMCs to TLR ligand stimulation is conserved in naturally acquired febrile *P. falciparum* infection, and, through the use of *P. chabaudi* infection in mice, demonstrated that this priming is IFNγ- and at least partially TLR9-dependent (107). Children who presented to a Gabonese hospital with uncomplicated malaria and whose PBMCs

produced IFNγ after stimulation with malarial proteins had lower rates of malaria reinfection than children with severe malaria or children with mild malaria whose PBMCs did not produce IFNγ to malarial protein challenge (108). Similarly, Eleanor Riley's group demonstrated that febrile malaria patients whose PBMCs produced IFNγ upon stimulation with iRBCs were less likely to have malarial disease and infection on follow-up (109). These results indicate that this IFNγ-dependent, malaria-induced priming could induce a memory component.

On the other hand, a lengthier exposure to malarial infection can also induce tolerance to subsequent infection (110). A recent reanalysis of historical experimental *P. falciparum* infection data demonstrated that the pyrogenic threshold—the level of parasitemia required to provoke fever—was higher for individuals after reinfection compared to initial infection (111). In holoendemic areas, where malaria is transmitted year-round, many individuals have blood parasitemias that would cause fever in naïve or occasionally exposed individuals, but they remain asymptomatic. The tolerance induced by malarial infection also extends to non-malarial infection or immune challenge. In the Gambia, recent malarial infection appeared to predispose children to nontyphoid *Salmonella* bacteremia (112). Acute malarial disease inhibited the immune response to *Salmonella typhi* or meningococcal vaccination, and this depressed response to meningococcal vaccination persisted one month after presentation of febrile malaria (113). Analogous to LPS tolerance, individuals with experimental *P. vivax* malaria (114) or malaria as fever therapy for neurosyphilis (115) exhibited depressed febrile responses to subsequent experimental endotoxin challenge. As discussed by McCall and colleagues

(106), these endotoxin challenge studies differed from the studies demonstrating priming in that the endotoxin challenges were performed during recovery from the peak febrile response, while the priming studies were performed during the febrile response. Similarly, DCs isolated from spleens of mice on day 17 post-infection with *P. chabaudi* showed depressed proinflammatory cytokine production upon TLR ligand stimulation, while this depression was not seen in DCs isolated three days after infection (116). Given that malaria induces priming early *in vivo* and *in vitro* and can induce tolerance after prolonged infection or multiple infective episodes, **we hypothesize that *P. falciparum* can also induce trained innate immunity in an *in vitro* model of innate immune memory.**

Chapter II: Materials and Methods

Ethics statement

The protocol and consent forms for experiments with human samples were approved by the Institutional Research Boards from the University of Massachusetts Medical School (IRB H-14839 and H-10368), Centro Internacional de Entrenamiento e Investigaciones Medical-CIDEIM (CIEIH-1249), University Hospitals Cleveland Medical Center IRB (06-11-22), and the Kenya Medical Research Institute Ethical Review Committee (SSC No: 2207). All experiments involving animals were performed in accordance with guidelines set forth by the American Association for Laboratory Animal Science and were approved by the Institutional Animal Care and Use Committee (A-1332) at the University of Massachusetts Medical School.

Malaria cultures and iRBC/hemozoin isolation

Plasmodium falciparum clone 3D7 was cultured utilizing a candle jar technique as described previously (117), substituting AlbuMAX II (Gibco) for human serum. iRBCs were isolated by passing the *P. falciparum* culture through a magnetic field (MACS LD column, Miltenyi Biotec); this resulted in enrichment consistently ≥90% iRBCs in the trophozoite or schizont stage. Enrichment was performed on the day the iRBCs were to be used, and they were then kept on ice until used to stimulate immune cells. Similarly, Hz was isolated by passing discarded malaria culture media through an LD column. The

Hz was then dried, weighed, resuspended in phosphate-buffered saline (PBS), and frozen at -20°C until use.

Isolation of *P. falciparum* genomic DNA (gDNA)

P. falciparum culture (~30% parasitemia) observed by Giemsa stain under light microscopy to be at the trophozoite stage was harvested and parasites from iRBCs were released by treatment with 0.2% saponin. The released parasites were pelleted at 3000 x *g* for 20 min, washed with cold PBS, and incubated in PBS with proteinase K (25 μg/ml) at 56 °C for 10 min. The resultant *P. falciparum* gDNA-containing solution was then extracted with phenol/chloroform/isoamyl alcohol and centrifuged at 10,000 x *g* for 10 min. The parasite DNA was precipitated overnight with NaOAc and absolute ethanol at -80°C, then washed with 70% ethanol and suspended in nuclease and endotoxin-free water. After determining DNA concentration by absorption at 260 nm, the *P. falciparum* gDNA was stored at -20°C. The purity of *P. falciparum* gDNA was confirmed by PCR using primers for *Plasmodium* 18S RNA as described previously (118) and human *TLR7* genes.

Human primary cell isolation and preparation (for Chapter III)

Peripheral blood mononuclear cells (PBMCs) from healthy human donors were obtained as described previously using Ficoll gradient separation (119). Human primary $CD14^+$ monocytes were purified from PBMC using the Pan Monocyte isolation kit (Miltenyi

Biotec) and magnetic separation according to the manufacturer's instructions. Monocyte derived macrophages (MDMs) were obtained by adherence and differentiation of adherent PBMCs in RPMI 1640 containing 10% fetal bovine serum (FBS) for 7 days.

Mouse primary cell isolation and preparation

Primary bone marrow derived macrophages (BMDMs) from C57BL/6 mice were generated as described previously (120) utilizing L929 conditioned media as the source for macrophage colony-stimulating factor (M-CSF) and cultured in Dulbecco's modified Eagle's medium (DMEM) (GIBCO-BRL) supplemented with 2 mM glutamine and 10% FBS. Mouse non-thioglycollate-elicited peritoneal exudate cells (PECs) were prepared as described previously (121) For stimulations, poly(dA:dT), interferon stimulatory DNA (ISD), *P. falciparum* gDNA, Hz, and AT-rich ODNs were transfected at the indicated concentrations using Lipofectamine 2000 (Invitrogen) according to the manufacturer's instructions. Sendai virus (SeV, Cantrell strain, 20 U/ml) was used as a control where indicated. DNase digestion of *P. falciparum* gDNA and hemozoin was performed using DNase I (Qiagen) according to the recommended protocol. Primary cells and cell lines were stimulated as stated and collected after the described time points for RNA extraction or cell lysate preparation.

Human cell lines

Human pro-monocyte THP-1 cells (WT [$cGAS^{+/+}$/$IFI16^{+/+}$], $cGAS^{-/-}$, and $IFI16^{-/-}$) were generated as previously described using clustered regularly interspaced short palindromic repeats (CRISPR)/Cas9 genome editing technology (122). WT and knockout THP-1 cells were grown in RPMI 1640 supplemented with 2 mM L-glutamine with 10% FBS. THP-1 cells were differentiated into macrophages by treating with 100 nM phorbol 12-myristate 13-acetate (PMA) (Chapter III) or 5 ng/mL PMA (Chapter IV) for 48 hrs (123). BLaER1 cells were grown and transdifferentiated as described previously (124).

Kenyan field samples

Pediatric malaria samples were obtained as part of a longitudinal cohort study conducted at the Chulaimbo Sub-County Hospital outpatient clinic in Kisumu County, Kenya. Participants enrolled in this observational cohort included children aged 1-10 years with acute uncomplicated malaria diagnosed by light microscopy. All cases of uncomplicated malaria were febrile (temperature ≥ 37.5°C) and without signs or symptoms of severe malaria. Thick and thin blood smears were prepared from all blood samples. A slide was deemed negative when no parasites were seen after counting microscopic fields containing at least 200 leukocytes. Children with acute uncomplicated malaria were treated with artemether/lumefantrine per Kenyan Ministry of Health guidelines and followed up at 2 and 6 weeks. At 2 weeks, finger prick blood samples were obtained for blood smear to ensure parasite clearance. Venous blood samples were obtained from

cases with acute malaria at the time of presentation (before administration of the first dose of artemether-lumefantrine) and 6 weeks following treatment. Submicroscopic blood stage infections were detected at 6 week recovery visits by a nested polymerase chain reaction (PCR) assay targeting *P. falciparum*-specific small subunit ribosomal RNA genes (118). PBMCs were separated by Ficoll-Hypaque density gradient centrifugation and cryopreserved as previously described (125). Monocytes were negatively selected from thawed PBMCs using the Pan Monocyte Isolation Kit (Miltenyi Biotec).

Human adherent PBMC isolation and stimulation (trained immunity assay)

Leukopaks (enriched leukapheresis products; New York Biologics) or whole blood drawn from healthy human donors was diluted 1:1 with sterile PBS (Gibco) and layered over Ficoll-Paque PLUS (GE) for density gradient centrifugation. The buffy coat was then harvested, washed twice with sterile medium, and incubated for 3 min in RBC lysis buffer (Roche). To remove any residual platelets, cells were washed 3x in PBS supplemented with 2% FBS and centrifuged 10 min at 120xg with no break. The washed PBMCs were resuspended in RPMI 1640 media (Gibco) supplemented with sodium pyruvate (Sigma), L-glutamine (Gibco), and gentamicin (Gibco) to concentrations of 10 mM, 10 mM, and 10 ng/mL, respectively. PBMCs were then plated at $5x10^5$ cells/well (in 96-well round-bottom plates) or $10x10^6$ cells/well (in 6- or 12-well flat-bottom plates) and incubated at 37°C for ≥1 hr, after which the non-adherent cells were removed by washing 3x with warm PBS. The adherent PBMCs were then incubated in similarly

supplemented RPMI with 10% human serum (RPMI+) and stimulated for 24 hours. Cells were then washed with warm PBS and allowed to rest in RPMI+ for three or five days. After the rest period, cells were either harvested for chromatin immunoprecipitation (ChIP) analysis or challenged with 10 μg/mL Pam3CSK4 (Invivogen) or 10 ng/mL LPS (Sigma) for 4-24 hours. Stimulated cells were harvested for mRNA analysis or supernatants were frozen at -20°C for subsequent cytokine measurement (Fig. 2.1).

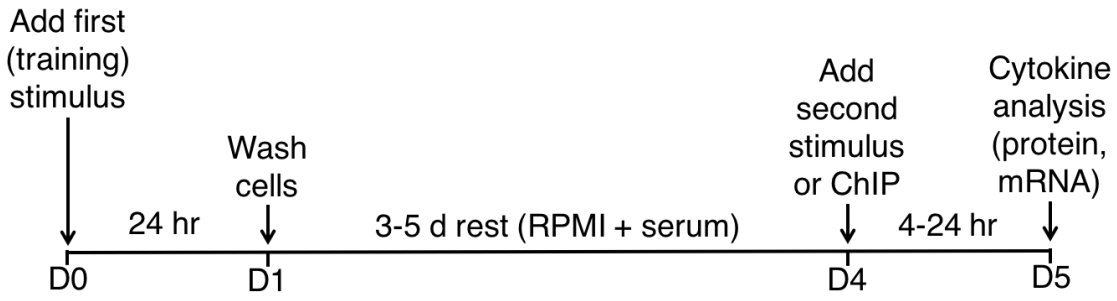

Figure 2.1. Schematic of *in vitro* trained immunity assay. Cells were treated with media alone (RPMI+), iRBCs, uRBCs, or Hz for 24 h and then washed 3x with warm PBS. Cells were then rested for 3-5 d in RPMI+. At the conclusion of the rest period, cells were either harvested for ChIP analysis or challenged with the TLR ligands LPS (10 ng/mL) or Pam3CSK4 (10 μg/mL) for 4-24 h, after which mRNA was harvested from cells or supernatants were assayed by ELISA.

Negative selection of monocytes (Chapter IV)

The trained immunity assay was also performed on a population of enriched, negatively selected monocytes. This population was obtained by using the EasySep Human Monocyte Enrichment Kit without CD16 depletion (STEMCELL Technologies) according to the manufacturer's instructions.

Enzyme-linked immunosorbent assays (ELISAs)

Chapter III: ELISA for mouse IFNß protein was performed as described in detail previously (126).

Chapter IV: Production of human TNFα and IL-6 or mouse TNFα and Regulated on Activation, Normal T cell Expressed and Secreted (RANTES) were measured in the cell supernatants after 24 hrs of Pam3CSK4 or LPS stimulation with ELISA kits (R&D) according to the manufacturer's specifications. A MTS tetrazolium dye assay [3-(4,5-dimethylthiazol-2-yl)-5-(3-carboxymethoxyphenyl)-2-(4-sulfophenyl)-2H-tetrazolium, inner salt] (Promega) was used according to the manufacturer's instructions to determine relative cell number post stimulation. Briefly, after removing supernatants from cells, cells were incubated with 120 µl/well RPMI+ with 20% of MTS/phenazine methosulfate (PMS) (Sigma) mixture and incubated for 2-20 h at 37°C. Solutions were then transferred to ELISA plates and read at 490 nm. Absorbance values were normalized by subtracting the absorbance values for no-cell blank wells. Relative cell numbers were determined by

dividing each absorbance value by the mean absorbance value for RPMI+ trained/RPMI+ challenged wells. Cytokine values were then normalized to these relative cell numbers.

Flow cytometry

After primary stimulation and three-day rest, supernatants were removed and adherent PBMCs incubated in PBS containing 1 mM ethylenediaminetetraacetic acid (EDTA) for 10-15 min at 37°C. Contents of the wells were pipetted up and down vigorously for ~5 min to detach adherent PBMCs from the wells. Cells were transferred to new tubes and efficient cell removal from plates was confirmed by inspection under light microscopy. Cells were then washed in PBS containing 1% bovine serum albumin (BSA), resuspended in PBS with 1% BSA, and stained for 20-30 min on ice with the following fluorescently-labeled antibodies according to the manufacturer's instructions: anti-CD3-phycoethrin-cyanine7 (PE-Cy7), anti-CD4-allophycocyanin (APC), anti-CD8-PE, anti-CD14-Pacific Blue, anti-CD19-fluorescein isothiocyanate (FITC), anti-CD45-APC-Cy7, and anti-CD56-peridinin-chlorophyll-Cy5.5 (PerCP-Cy5.5), as well as live-dead Aqua stain. All flow cytometry experiments were performed on a LSR II flow cytometer (BD Biosciences) with compensation levels set using single-antibody controls. Data was analyzed using FlowJo software (Tree Star).

mRNA expression

Total RNA was extracted using the Trizol (Invitrogen) or the RNeasy Mini Kit (Qiagen) according to the manufacturer's instructions. RNA was then quantified using a NanoDrop spectrophotometer (Thermo). cDNA synthesis and qPCR assay were performed using an iScript cDNA synthesis kit and iQ SYBR Green supermix (both Bio-Rad), respectively. Data was normalized to *ACTB* and/or *GAPDH* expression and analyzed using Bio-Rad software. NanoString analysis was performed using the nCounter Human Inflammation v2 Codeset, and the data was analyzed using NanoString software. Hierarchical clustering heatmaps of the NanoString expression data were prepared in R using a package described here: https://cran.r-project.org/web/packages/heatmap3/heatmap3.pdf.

Detection of IRF3 phosphorylation

Cell lysates were prepared in RIPA lysis buffer as described previously (127), subjected to SDS-PAGE and visualized by Western Blotting using antibodies against phospho-IRF3 (S386) (Abcam), total IRF3 (D614C) (Cell Signaling Technology), and ß-actin (Sigma).

Preparation of Cytosol for Analysis of Endogenous 2'3'-cGAMP

THP-1 cells were transfected with *P. falciparum* gDNA and cytosolic extracts from ~1.8 x 10^7 cells were prepared by hypotonic lysis. Briefly, cells were incubated in hypotonic buffer (10mM Tris-HCl (pH 7.4), 10 mM KCl, 1.5 mM $MgCl_2$) for 30 minutes and then

dounce-homogenized x 100 strokes. Cell lysates were heated at 95°C for 5 min and then centrifuged at 17,000 x *g* for 10 min to remove denatured proteins. The heat resistant supernatant was recovered and stored at -80°C until LC-MS/MS analysis.

Quantification of 2'3'-cGAMP by Liquid Chromatography-Tandem Mass Spectrometry (LC-MS/MS)

Quantification of 2'3'-cGAMP was performed by LC-MS/MS as described previously (122). Briefly, extraction of 2'3'-cGAMP from cell lysates was performed with acetonitrile/methanol/water (2/2/1, vol/vol/vol) buffer. 5 ng of heavy-labeled 2'3'-cGAMP was added to each sample as an internal standard. The samples were then heated to 95°C for 10 min, cooled on ice for 10 min, and then centrifuged at 17,000 x *g* for 10 min to remove denatured proteins. The remaining supernatants were dried in a roto Speedvac, and the lyophilized material from each sample was resuspended in 50 µl water. 10 µl of sample was then injected per technical replicate. Ratios of endogenous 2'3'-cGAMP to heavy-labeled 2'3'-cGAMP were compared to a standard curve of light:heavy 2'3'-cGAMP prepared in human PBMCs to quantify endogenous 2'3'-cGAMP in each sample.

Neutralizing antibodies and inhibitors

Mouse anti-human IL-12p40 IgG1 was from R&D. Both mouse anti-human IFNγ IgG1 and mouse IgG1 isotype control were from Biolegend. 5'-methylthioadenosine (MTA) and rapamycin were from Sigma.

Chromatin precipitation (ChIP) analysis

ChIP was performed using a rabbit anti-human H3K4me3 IgG antibody (Diagenode) and ChIPed DNA was then further analyzed via qPCR as described previously (96). Briefly, cells were fixed in 1% formaldehyde for 10 min and then quenched with glycine. Cells were then washed, counted, and resuspended in lysis buffer and sonicated using a Bioruptor UCD-300 (Diagenode) for four cycles of 10 x (30 sec ON, 30 sec OFF) on the HIGH setting. ChIP was performed on the sonicated chromatin using either a rabbit anti-human H3K4me3 IgG antibody (Diagenode) or a control rabbit IgG antibody (Abcam) conjugated to Sheep anti-rabbit Dynabeads (Life Technologies). After ChIP, chromatin:bead complexes were washed 2x in each of low salt, high salt, lithium chloride (LiCl)-containing, and Tris-EDTA (TE) buffers. Chromatin was then eluted from the beads and decrosslinked to isolate the DNA. DNA was then purified and quantified using qPCR as described above. For all ChIP experiments, qPCR values were normalized as percent recovery of the input DNA.

Statistical Analysis

Chapter III: Differences in paired groups were analyzed with paired *t*-tests. When ratios to controls were compared, one sample paired *t*-tests (H_0 log(ratio)=0) were performed on log-transformed ratio values. Otherwise, data were analyzed using an unpaired, two-tailed Student's t test correcting for multiple comparisons using the Holm-Sidak method. Analyses were performed with GraphPad Prism 7 software (GraphPad Inc., San Diego, CA).

Chapter IV: For experiments with multiple replicates for an individual donor performed on different days, several sensitivity analyses were carried out. Four different statistical analyses were performed for the experiments represented in Fig. 1*B*-*C*: a mixed model regression analysis, a Wilcoxon signed-rank test with clustering (analysis at the replicate level accounting for correlation of data within donor), a Wilcoxon signed-rank test using one averaged value per donor (mean of all replicates), and a paired *t*-test using one averaged value per donor. All four tests provided nearly identical hypothesis decisions with an α=0.05, so paired *t*-tests using one value per donor was used for all other experiments. When ratios to controls were compared, one sample *t*-tests (H_0 log(ratio)=0) were performed on log-transformed ratio values. For experiments comparing three groups a non-parametric ANOVA was used (Kruskal-Wallis).

Chapter III: Cyclic GMP-AMP Synthase (cGAS) is the cytosolic sensor of *Plasmodium falciparum* genomic DNA and activates type I interferons in malaria

Carolina Gallego-Marin[*, † 1], Jacob E. Schrum[* 1], Warrison A. Andrade[*], Scott A. Shaffer[* ‡], Lina F. Giraldo[†], Alvaro M. Lasso[†], Kate A. Fitzgerald[*], Evelyn A. Kurt-Jones[*] and Douglas T. Golenbock[*]

* Division of Infectious Diseases and Immunology, Department of Medicine, University of Massachusetts Medical School, Worcester, MA 01605

† Centro Internacional de Entrenamiento e Investigaciones Medical-CIDEIM, Cali, Colombia

‡ Proteomics and Mass Spectrometry Facility and Department of Biochemistry and Molecular Pharmacology, University of Massachusetts Medical School, Worcester, MA 01605

[1] C.G-M. and J.E.S. contributed equally to this work

Corresponding author:

Phone: 1-508-856-5982

Fax: 1-508-856-5463

e-mail: douglas.golenbock@umassmed.edu

Grant support:

This work received support by the National Institute of Allergy and Infectious Diseases grant R21AI124171 (to E.A.K-J., D.T.G. and C.G.) and R01AI079293 (K.A.F. and D.T.G.). A.M.L and L.F.G were supported by the Departamento de Ciencia y Tecnologia – Colciencias-CIDEIM grant 0234-2014 and 0552-2015 and the NIH/Fogarty International Center training grant D43TW006589.

Attributions

This Chapter represents an expanded version of a paper submitted to *The Journal of Immunology* with the same title listed above, on which J.E.S is co-first author. C.G.-M. and W.A.A. performed the experiments shown in Figure 3.1A. C.G.-M. performed the experiments shown in Figure 3.2 and Figures 3.3B and D. C.G.-M. transfected the cells in Figure 3.5A and B, and S.A.S. performed the LC-MS/MS analysis. C.G.-M. wrote the first draft of the text of this paper, and all authors edited and/or reviewed the text. All other experiments, analysis, and editing of the most recent version manuscript into the format seen in this Chapter were performed by J.E.S.

Abstract

Innate immune receptors have a key role in the sensing of malaria and initiating immune responses. As a consequence, systemic inflammation emerges and is directly related to signs and symptoms during acute disease. Here we demonstrate that *Plasmodium falciparum* genomic DNA delivered to the cytosol of human monocytes binds and activates the cytosolic DNA receptor cGAS. Activated cGAS synthesizes 2'3'-cGAMP, which we subsequently detect using mass spectrometry. 2'3'-cGAMP acts as a second messenger for STING activation and triggers STING/TBK1/IRF3 activation, resulting in type IFN-I production in human cells. This induction of IFN-I was independent of the IFI16 receptor. Access of DNA to the cytosolic compartment is mediated by hemozoin, since incubation of cultured malaria hemozoin pigment with DNase abrogated IFNß induction. Collectively, these observations implicate cGAS as an important cytosolic sensor of *Plasmodium falciparum* DNA and reveal the role of the cGAS/STING pathway in the induction of IFN-I in response to malaria parasites.

Introduction

Malaria remains a major cause of morbidity and mortality worldwide. The World Health Organization has estimated that there were ~212 million cases of malaria globally in 2016 and about 429,000 deaths, primarily (~70%) occurring in children under age 5 (1). Despite many gains against the disease, the problems associated with malaria eradication remain significant. These include increasing resistance of insect vectors to insecticides and the emerging resistance of *Plasmodium* to the most efficacious antimalarial drugs (128). Current evidence indicates that drug resistance to artemisinin derivatives, the last generation treatment for asexual blood-stage infection, has developed in Southeast Asia and Africa (129-131). Despite these setbacks, the efforts continue with the objective to achieve the global elimination of malaria.

Our understanding of the pathogenesis of malaria is still limited (132). Therefore, a top priority in basic research is to dissect the mechanisms involved in malaria disease development and provide new approaches for therapeutic and prophylactic interventions since a highly effective malaria vaccine is still unavailable. An important component of the pathogenesis of malaria is the host innate immune response to the parasite. The activation of innate immune cells and the associated systemic inflammation leads to the initial signs and symptoms of disease and can influence the development of severe disease (133). Inflammatory mediators during malaria infection are produced as a result of direct recognition of malarial PAMPs (pathogen-associated molecular patterns) by innate immune receptors, including TLRs (133), NLRs and other nucleic acid sensors

(55). Concomitant with TLR activation, expression of sensor proteins including NLRs is augmented and NLR-containing inflammasomes are assembled. Pro-inflammatory cytokines and mediators like TNFα, IL-12, caspase-1 and IL-1ß are then released (53). Elevated expression of interferon-stimulated genes (ISGs) in innate immune cells is also characteristic during *Plasmodium* infection (55, 134).

The recognition of microbial DNA by the immune system provides a general mechanism for the detection of pathogens (135, 136). Delivery of foreign or self DNA into the cytoplasm (which is largely free of self DNA) through microbial infection or cell damage can activate cytosolic DNA sensors (137). *Plasmodium* DNA represents a major trigger of innate immunity during infection (49, 51, 55). The *Plasmodium* genome contains highly stimulatory CpG motifs, which are thought to activate TLR9 when carried into the phagolysosomal compartment by the malaria pigment hemozoin (Hz) (49, 51). However, CpG-rich motifs are relatively rare in *Plasmodium falciparum* (*P. falciparum)*. In contrast, AT-rich DNA motifs are present in abundance and induce IFN-I via a pathway that is independent of TLRs, DAI, RNA polymerase III and IFI16/p204 but dependent on STING (138, 139), TBK1 (120, 140), and IRF3 and IRF7 (55, 141).

The enzyme cyclic GMP-AMP synthase (cGAS) has been identified as a cytosolic DNA sensor whose activation results in the subsequent activation of STING (42, 43). Specifically, in the presence of cytosolic double-stranded DNA, cGAS catalyzes the synthesis of cyclic GMP-AMP (2’3’-cGAMP) from ATP and GTP. 2’3’-cGAMP then functions as a second messenger that binds to and activates STING. Activated STING leads to IRF3 phosphorylation and IFN-I production and expression of ISGs (44). Here,

we report that cGAS has an important role as a sensor of *P. falciparum* genomic DNA. Our data suggest that 2’3’-cGAMP acts as a second messenger after the sensing of *P. falciparum* genomic DNA and other malaria PAMPs to induce IFN via the cGAS/STING pathway. We suggest that cGAS detection of cytosolic malaria DNA is an important molecular feature of malaria pathogenesis.

Results

IFN-I are induced in human primary myeloid cells in response to P. falciparum gDNA

In our previous work, we demonstrated that *Plasmodium falciparum* iRBCs—but not uninfected RBCs (uRBCs)—stimulated *IFNB* expression in human PBMCs, and *IFNB* expression was also induced by the transfection of *P. falciparum* genomic DNA (gDNA) in these cells (55). We extended these studies to determine the direct effect of *P. falciparum* on IFN-I induction in purified human myeloid cells. $CD14^+$ monocytes were stimulated with iRBCs or with uRBCs as controls. A significant induction of *IFNB* mRNA was observed with iRBC stimulation. Although stimulation of $CD14^+$ monocytes with heterologous uRBCs did induce slightly increased expression of *IFNB* mRNA as compared to media-stimulated controls, stimulation with iRBCs induced significantly increased *IFNB* expression as compared to uRBCs (Fig. 3.1A). The induction of *IFNB* by iRBCs was similar to that elicited by transfection of *P. falciparum* gDNA (Fig. 3.1A). IFNα was also induced at the mRNA level (data not shown).

Previous results from our group demonstrated that Hz presents *Plasmodium* DNA to TLR9 (49). Like $CD14^+$ monocytes, monocyte-derived macrophages (MDMs) expressed *IFNB* mRNA in response to transfection of *P. falciparum* gDNA (Fig. 3.1B). We also determined whether other malarial products would induce *IFNB* expression in MDMs. Hz strongly stimulated *IFNB* expression in a dose-dependent manner when delivered into the cytosol of MDMs (Fig. 3.1B). Likewise, other known IFN-I inducers—poly (dA:dT), ISD, and Sendai virus (SeV)—as well as AT-rich ODNs containing secondary stem-loop structure (AT5 and AT5 3x) significantly promoted *IFNB*

expression in MDMs (Fig. 3.1C). Collectively, these data indicate that both malaria parasites and malarial PAMPs (*P. falciparum* gDNA, Hz, AT-rich ODNs) activate IFN-I in human primary myeloid cells.

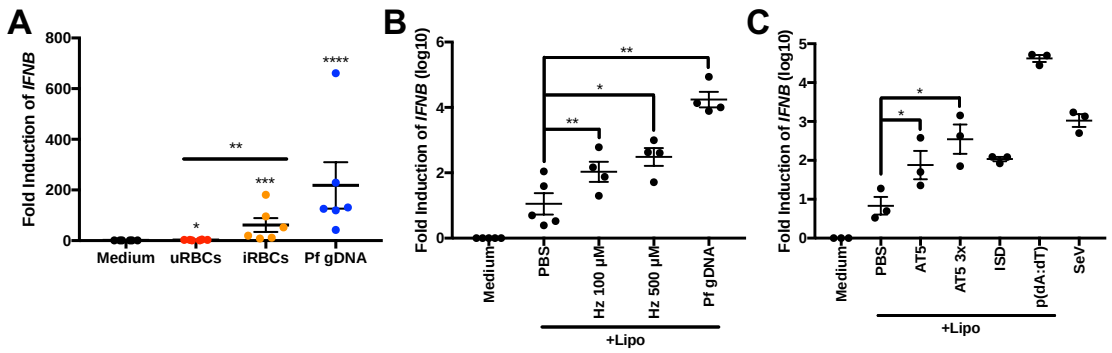

Figure 3.1. Human primary myeloid cells express *IFNB* in response to *P. falciparum* iRBCs and malarial DNA ligands. (**A**) CD14+ monocytes were isolated from healthy human donor PBMCs by magnetic bead selection and incubated with uRBCs, iRBCs, or transfected with *P. falciparum* gDNA (10 µg/ml). RNA was prepared 6 h later and *IFNB* was measured by qRT-PCR. (**B-C**) Human monocyte-derived monocytes were transfected with PBS alone, natural hemozoin (Hz), or *P. falciparum* gDNA (B). AT-rich oligodeoxynucleotides (ODNs) AT5 and AT5 3x (3 µM) were also transfected into MDMs, and interferon-stimulatory DNA (ISD), p(dA:dT) and Sendai virus (SeV) were used as positive controls (C). *IFNB* levels measured as in (A). Each dot represents a single donor. Each horizontal bar represents mean ± SEM for six donors (A), four or five donors (B) or three donors (C) (all comparisons in (A) to medium-stimulated cells unless otherwise indicated, *p<0.05, **p<0.01, ***p<0.001, ****p<0.0001, paired *t*-test).

IFN-I are induced after cytosolic delivery of malarial DNA

We determined the role of cytosolic delivery of DNA in the ability of Hz to induce *IFNB* expression in THP-1 cells. Hz significantly induced *IFNB* expression in a dose-dependent manner when transfected into cells. This activity was abolished when Hz was pretreated with DNase I (Fig. 3.2A). Similarly, purified *P. falciparum* gDNA induced *IFNB* when delivered to the cytosol of THP-1 cells in a dose and time-dependent manner (Figs. 3.2B and 3.2C).

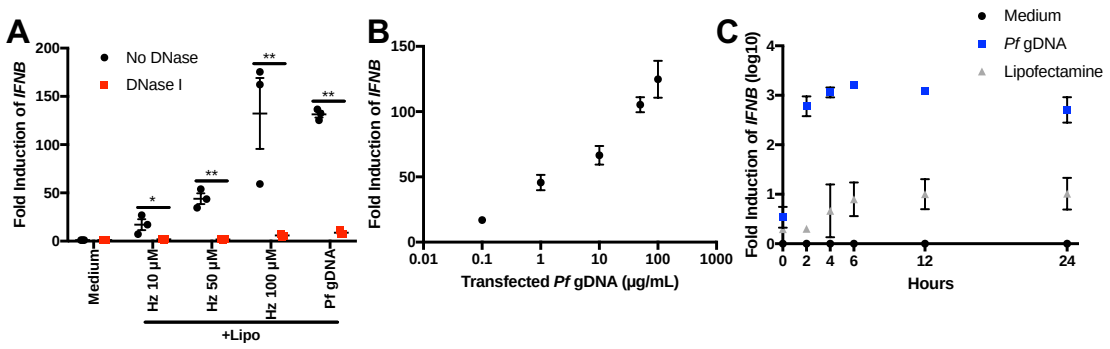

Figure 3.2. IFN-I are induced by *P. falciparum* gDNA. (**A**) The indicated amounts of Hz or *P. falciparum* gDNA (10 µg/mL) were either treated with DNase I or not treated, and then transfected into THP-1 cells for 6 h followed by measurement of *IFNB* mRNA expression by qRT-PCR. Each dot represents the result of an individual experiment, and horizontal bars represent mean ± SEM for three independent experiments (all comparisons between No DNase and DNase I-treated cells, *p<0.05, **p<0.01, paired *t*-test). (**B**) THP-1 cells were transfected with the indicated concentrations (µg/ml) of *P. falciparum* gDNA for 6 h followed by measurement of *IFNB* mRNA by qRT-PCR. Dots represent mean ± SEM for two independent experiments. (**C**) Time course of induction of *IFNB* mRNA in THP-1 cells transfected with 50 µg/ml of *P. falciparum* gDNA or lipofectamine alone for the indicated time periods. Dots represent mean ± SEM for two or three independent experiments.

IFN-I induction by P. falciparum *gDNA is dependent on cGAS.*

cGAS is a DNA sensor that catalyzes the synthesis of 2'3'-cGAMP to drive activation of STING, resulting in the induction of IFN-I and other inflammatory genes (42, 43). In order to determine the involvement of cGAS as a sensor for *Plasmodium* DNA, *IFNB* expression was assessed in cGAS KO and WT THP-1 cells. Transfection of cultured Hz or *P. falciparum* gDNA induced expression of *IFNB* mRNA in WT but not in cGAS-deficient THP-1 cells (Fig. 3.3A). Detection of phosphorylated IRF3, an indicator of STING activation and an upstream readout for IFN-I induction, revealed phosphorylation of IRF3 in WT but not cGAS KO cells when transfected with Hz or *P. falciparum* gDNA (Fig. 3.3B). Cytosolic delivery of AT-rich oligonucleotides (whose design was based on sequences from the *P. falciparum* genome) also induced *IFNB* in WT THP-1 cells but did not induce *IFNB* expression in cGAS KO cells (Fig. 3.3C). Finally, transfection of IFI16 knockout cells with *P. falciparum* gDNA induced equivalent levels of *IFNB* mRNA to WT cells (Fig. 3.3D), suggesting that IFI16 is not required for detection of *P. falciparum* gDNA. Altogether, these results indicate that cGAS is the cytosolic sensor of *P. falciparum* gDNA and is required for the induction of *IFNB* by *P. falciparum* DNA or malaria hemozoin.

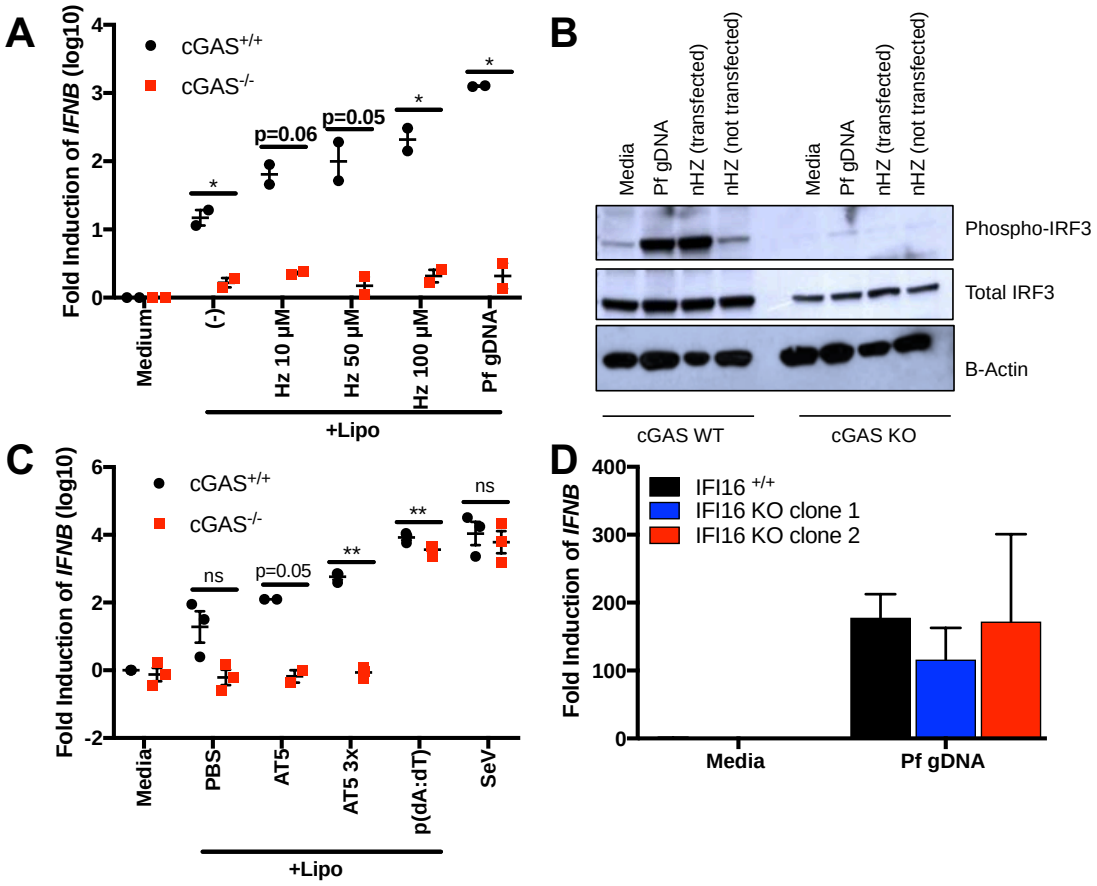

Figure 3.3. *P. falciparum* gDNA induces *IFNB* expression through the cGAS-STING pathway. (**A**) cGAS$^{+/+}$ and cGAS$^{-/-}$ THP-1 cells were transfected with the indicated quantities of Hz or *P. falciparum* gDNA for 6 h followed by detection of *IFNB* mRNA by qRT-PCR. Each dot represents the result of an individual experiment, and horizontal bars represent mean ± SEM for two independent experiments (all comparisons between cGAS$^{+/+}$ and cGAS$^{-/-}$ cells for each stimulus, *p<0.05, paired *t*-test) (**B**) Phosphorylation of IRF3 and total IRF3 were detected by SDS-PAGE followed by western blot. Detection of ß-actin was used as loading control. (**C**) cGAS$^{+/+}$ and cGAS$^{-/-}$ THP-1 cells were transfected with AT-rich ODN (AT5 and AT5 3x, 3 µM each) or poly(dA:dT) for 6 h followed by detection of *IFNB* mRNA by qRT-PCR. Stimulation with Sendai virus was used as a cGAS-independent control. Each dot represents the result of an individual experiment, and horizontal bars represent mean ± SEM for two or three independent experiments (all comparisons between cGAS$^{+/+}$ and cGAS$^{-/-}$ cells for each stimulus, **p<0.01, paired *t*-test) (**D**) Wild type IFI16 (IFI16$^{+/+}$) and IFI16 KO (clones 1 and 2) THP-1 cells were transfected with 10 µg/ml of *P. falciparum* gDNA for 6 h and *IFNB* mRNA was measured by qRT-PCR. Bars represent mean ± SD of technical duplicates from one experiment.

The cGAS-STING pathway is involved in the induction of IFN-I in response to malaria DNA

To corroborate the involvement of the cGAS-STING pathway in the production of IFNß, we measured IFNß protein secreted by mouse BMDMs stimulated with *P. falciparum* DNA ligands. Cytosolic delivery of *P. falciparum* gDNA or AT-rich ODNs induced the secretion of IFNß from WT BMDMs (Fig. 3.4). This induction of IFNß protein secretion was not observed in either STING KO or cGAS KO macrophages (Fig. 3.4). These data indicate the involvement of the cGAS-STING pathway in the induction of IFN-I in response to the sensing of *P. falciparum* DNA.

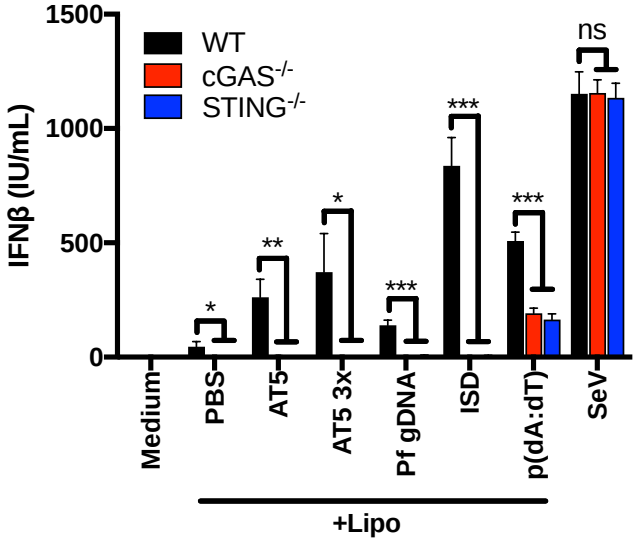

Figure 3.4. IFN-I are produced through the activation of the cGAS-STING pathway in response to *P. falciparum* DNA ligands in mouse primary cells. Bone marrow-derived macrophages (BMDMs) from WT, STING$^{-/-}$ and cGAS$^{-/-}$ mice were transfected with *P. falciparum* gDNA (1 µg/ml) or the AT-rich ODNs AT5 and AT5 3x (3 µM). Supernatants were recovered after 18 h stimulation and levels of mouse IFNß were measured by ELISA. ISD, poly(dA:dT) and SeV were used as controls. Bars represent mean ± SD of quadruplicate stimulations of BMDMs from 1 mouse per genotype and are representative of 3 independent experiments (all comparisons to WT cells for each stimulus, *p<0.05, **p<0.01, ***P<0.001, unpaired *t*-test corrected for multiple comparisons using the Holm-Sidak method).

2’3’-cGAMP is induced after sensing of P. falciparum *gDNA*

cGAS catalyzes the synthesis of cyclic GMP-AMP (2’3’-cGAMP) in the presence of cytosolic DNA (43). To further characterize this activity in response to *Plasmodium* DNA, we transfected THP-1 cells with *P. falciparum* gDNA and measured 2’3’-cGAMP production. We began by heat-treating total extracts of transfected cells, as 2’3’-cGAMP is heat-stable. We confirmed the induction of 2’3’-cGAMP in cells transfected with *P. falciparum* gDNA by LS-MS/MS, consistent with the cGAS-dependent induction of *IFNB* shown before in response to *P. falciparum* gDNA (Fig. 3.3). 2’3’-cGAMP was produced in *P. falciparum* gDNA-transfected THP-1 cells (Fig. 3.5A, panel 2) but not in control THP-1 cells (Fig. 3.5A, panel 1; 2’3’-cGAMP peak is represented by one asterisk). As a positive control, the lysate from untreated THP-1 cells was spiked with synthetic 2’3’-cGAMP (Fig. 3.5A, panel 3). All lysates also included an internal standard of 3’3’-cGAMP (500 pg per sample; represented by two asterisks). MS/MS of the 2’3’-cGAMP peak revealed several fragmented ions with the expected *m/z* values for product ions of 2’3’-cGAMP which were observed in similar ratios in DNA transfected samples and spiked controls (Fig. 3.5B), confirming the induction of 2’3’-cGAMP by transfected *P. falciparum* gDNA. To corroborate this result in primary cells, we transfected *P. falciparum* gDNA into MDMs from two donors and used LC-MS/MS to quantify the amount of 2’3’-cGAMP produced (Fig. 3.5C). Together our data indicate that the cGAS-*P. falciparum* DNA complex activates 2’3’-cGAMP synthesis and consequently the induction of IFNß. The data also suggest that cGAS is an important sensor for *P. falciparum* gDNA.

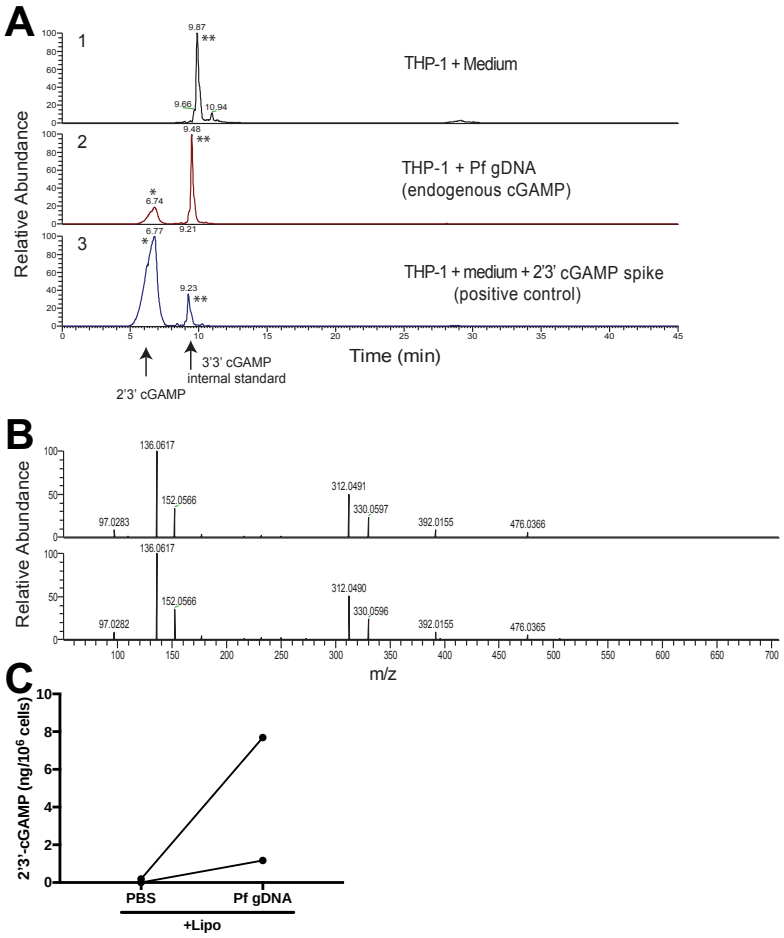

Figure 3.5. 2'3'-cGAMP is induced by transfection of *P. falciparum* genomic DNA. (**A, B**) LC-MS/MS profile from THP-1 isolates. Lysates from THP-1 cells left untreated (medium) or transfected with 50 µg/ml of *P. falciparum* gDNA for 6 h were heated at 95°C for 5 min to denature proteins. The heat-resistant supernatants were recovered after 17,000 x *g* centrifugation. As positive control, lysate from untreated THP-1 cells was spiked with 100 nM 2'3'-cGAMP. (A) 1. THP-1 cells untreated (medium), 2. THP-1 cells transfected with *P. falciparum* gDNA and 3. THP-1 cells untreated and spiked with synthetic 2'3'-cGAMP. Reconstructed ion chromatograms of cGAMP fragment ion at *m/z* 312.049 following LC-MS/MS fragmentation of cGAMP protonated ion. Peaks marked with a single asterisk are from endogenous or positive control 2'3'-cGAMP; double asterisks indicate 3'3' cGAMP spiked at 500 pg to each isolate as internal standard. (B) Tandem mass spectra (MS/MS) of the peak observed at 6.7 min (from corresponding panels A2 and A3). Peaks are 2'3'-cGAMP fragment ions and are observed in similar ratios. (**C**) Quantitation of 2'3'-cGAMP by LC-MS/MS from human MDMs transfected with PBS alone or *P. falciparum* gDNA for 6 h and then processed as described in (A). Each dot represents an individual donor.

Discussion

Much progress has been made in our understanding of how phagocytes sense *Plasmodium* and their associated host receptors that elicit inflammation (133). Three major *P. falciparum* PAMPs have been described: GPI anchors (46), hemozoin crystals (53) and *P. falciparum* gDNA (49, 55). Still, the receptor or family of receptors for *Plasmodium* DNA-driven IFN-I responses has been elusive. In previous reports, we described "unknown" cytosolic DNA sensor(s) that coupled to a STING, TBK1 and IRF3-IRF7 signaling pathway. This receptor or family of receptors acted as a sensor for *Plasmodium* DNA and oligonucleotides containing the AT-rich motif, leading to IFN-I production (55). We also revealed that the induction of IFN-I is driven by a pathway that did not involve TLR9, DAI, RNA polymerase-III or IFI16/p204 (55). In this report, we demonstrate that *Plasmodium* gDNA induces IFN-I production through cGAS, a cytosolic DNA activated enzyme that drives activation of the STING pathway, raising the role of IFN-α/ß in malaria pathogenesis.

The sensing of pathogen-derived DNA is a central strategy used by the innate immune system to initiate immune responses following microbial invasion (135). cGAS is a cytosolic DNA sensor that activates innate immune responses through production of the second messenger 2'3'-cGAMP, which in turn activates the adaptor STING and leads to IFN-I production (136). The importance of this cytosolic DNA sensor and IFN-I release is now being appreciated in the context of various infectious diseases beyond their traditional roles in antiviral immunity. A growing list of pathogens as diverse as *Neisseria gonorrhoeae* (122), Cytomegalovirus (142), *Mycobacterium tuberculosis* (143),

human immunodeficiency virus (HIV) (144), *Streptococcus agalactiae* (145), *Listeria monocytogenes* (146), and *Chlamydia trachomatis* (147) all induce IFN-I through the cGAS/STING pathway. The data in this paper demonstrate a similar mechanism for *Plasmodium falciparum.*

Exogenous DNA that gains access to the cytosol is a particularly potent and clear danger signal for the innate immune system (136). We have previously demonstrated that natural hemozoin activates TLR9 due the delivery of Plasmodial DNA to the endosomal compartment (49). However, a TLR9-independent response also occurs when purified hemozoin acts as vehicle to deliver Plasmodial DNA into the cytosol leading to IFNß production (55). Experimentally, we addressed this hypothesis by transfecting *P. falciparum* genomic DNA with lipofectamine. In contrast to our experimental *in vitro* conditions, hemozoin crystals appear to destabilize the phagolysosome during infection, which allows the delivery of phagosomal contents including DNA to the cytosol (53). This highlights a mechanism by which hemozoin-associated cargo such as Plasmodial DNA might access the cytosol and suggest that *P. falciparum* gDNA can drive IFNß production upon access to the cytosolic compartment.

Data presented in this study identify the basis of IFN-I production mediated by the sensing of cytosolic Plasmodial DNA by cGAS and subsequent activation of the cGAS/STING pathway. The consequences of IFN-I induction during malarial infection are currently under investigation in several laboratories. Several reports have revealed the ability of *Plasmodium spp* to induce IFN-I and a IFN-I gene signature (49, 83, 88, 134, 148). Previous reports have shown that exogenous recombinant IFNα can even inhibit

experimental cerebral malaria and reduce parasite burden in mice infected with *P. berghei* ANKA (PbA) (149). However, other studies demonstrate that signaling via the IFN-I receptor impairs DC function and T cell responses that control parasitemia in mouse models of malaria (74). Our studies in the PbA model have demonstrated that the TBK1, IRF3-IRF7 dependent production of IFN-I is central to the progression of experimental cerebral malaria, given that mice deficient in these factors survived longer than wild-type mice (55). A recent report in human malaria identifies an immunological regulatory effect of IFN-I during blood-stage *P. falciparum* infection. IFN-I were found to suppress IL-6 but not TNFα production by blood monocytes, promote IL-10-producing CD4+ T cells and generate regulatory Tr1 cells (83). Altogether, these data indicate the relevant and complex involvement of IFN-I in the pathogenesis of malaria.

The activation of innate immune cells and consequent systemic inflammation lead to the initial signs and symptoms of malaria, and can also influence the development of the more severe forms of the disease. The data presented in this paper corroborate the role of *Plasmodium* DNA as a potent PAMP during malaria infection and identify cGAS as an important cytosolic sensor that activates the second messenger 2’3’-cGAMP. We also reveal the role of the cGAS/STING pathway in the consequent IFN-I production. Our results suggest that any attempts at immunomodulatory therapy for patients with severe malaria will need to take into account the role of DNA-induced IFN-I and its impact on pathogenesis.

Acknowledgments

The authors are grateful to Elizabeth J. Thatcher for assistance with sample preparation and data analysis.

Chapter IV: *Plasmodium falciparum* induces trained innate immunity

Jacob E. Schrum,[*] Juliet N. Crabtree,[*] Katherine R. Dobbs,[†] Michael C. Kiritsy,[*] George W. Reed,[*,‡] Ricardo T. Gazzinelli,[*,§,¶] Mihai G. Netea,[‖] James W. Kazura,[#] Arlene E. Dent,[†,#] Katherine A. Fitzgerald,[*,1] and Douglas T. Golenbock[*,1]

*****Division of Infectious Diseases and Immunology, Department of Medicine, University of Massachusetts Medical School, Worcester, MA 01605

†Division of Pediatric Infectious Diseases, Department of Pediatrics, Rainbow Babies and Children's Hospital, Cleveland, OH 44106

‡Corrona, LLC, Southborough, MA 01772

§Departamento de Bioquímica e Imunologia, Universidade Federal of Minas Gerais, Belo Horizonte, MG, Brazil

¶Centro de Pesquisas René Rachou, Fundação Oswaldo Cruz, Belo Horizonte, MG, Brazil

‖Department of Internal Medicine, Radboud University Medical Center, 6525 GA, Nijmegen, the Netherlands

#Center for Global Health and Disease, Case Western Reserve University School of Medicine, Cleveland, OH 44106

[1]These authors contributed equally to this work

Address correspondence and reprint requests to Dr. Douglas Golenbock, Division of Infectious Diseases and Immunology, University of Massachusetts Medical School, LRB Room 328, 364 Plantation St, Worcester, MA 01605. E-mail address: douglas.golenbock@umassmed.edu

Footnotes:

This work was funded by NIH grants R01AI079293 (DTG, KAF, RTG, GWR), R01NS098747 (RTG), U19AI0089681 (DTG, RTG) T32AI095213 (JES), R01AI095192 (JWK, AED, KRD) and R01AI130131 (JWK).

Attributions

This Chapter represents an expanded version of a paper submitted to *The Journal of Immunology* with the same title listed above for consideration as a *Cutting Edge* publication. J.N.C. performed the flow cytometry experiments (Fig. 4.10B, C), K.R.D. completed some of the ChIP-qPCR analyses (Fig. 4.12A), G.W.R. provided statistical assistance, and M.C.K produced the NanoString heatmap (Fig. 4.6C, D) and resulting table (Table 4.1). All other experiments, analysis, and writing were performed by J.E.S.

Abstract

Malarial infection in naïve individuals induces a robust innate immune response. In the recently described model of innate immune memory, an initial stimulus primes the innate immune system to either hyperrespond (termed “training”) or hyporespond (“tolerance”) to subsequent immune challenge. Previous work in both mice and humans demonstrated that infection with malaria can both serve as a priming stimulus and promote tolerance to subsequent infection. In this study, we demonstrate that initial stimulation with *Plasmodium falciparum* iRBCs or the malaria crystal Hz induced human adherent PBMCs to hyperrespond to subsequent stimulation of TLR receptors. This hyperresponsiveness correlated with increased H3K4me3 at important immunometabolic promoters, and these epigenetic modifications were also seen in Kenyan children naturally infected with malaria. However, the use of epigenetic and metabolic inhibitors indicated that the induction of trained immunity by malaria and its ligands may occur via previously unrecognized mechanism(s).

Introduction

A hallmark of malaria is robust proinflammatory cytokine production induced by widespread innate immune activation. Multiple innate immune receptors are involved in the recognition of *Plasmodium* iRBCs and other malarial ligands [reviewed in (133)]. For example, the malaria crystal Hz, which becomes coated with *Plasmodium*-derived PAMPs including genomic DNA as a result of parasite turnover, activates TLR9 in the phagolysosome (49). These Hz crystals can also induce phagolysosomal rupture resulting in the activation of the nucleotide-binding domain, leucine-rich repeat–containing, pyrin domain containing 3 (NLRP3) inflammasome as well as deliver *Plasmodium* DNA to the cytosol, where it is recognized by the AIM2 inflammasome and a cytosolic DNA receptor that senses AT-rich stem-loop structures in *Plasmodium* genomes (53, 55). This innate immune response, although beneficial through limiting parasitemia and assisting in the activation of adaptive immunity (56), induces the systemic symptoms of fever, nausea, and malaise. Additionally, proinflammatory cytokinemia has been implicated in the development of cerebral malaria (57).

Multiple studies over the past decade have demonstrated memory phenotypes in innate immune cells (95, 96, 100). In the prevailing model of innate immune memory, an initial stimulus primes the innate immune system, which, depending on the type and concentration of the stimulus, induces epigenetic and metabolic changes that result in an increased or decreased response—termed training and tolerance, respectively—to a subsequent challenge occurring days to months after the priming challenge (150). Malarial infection serves as a robust priming stimulus, as whole blood samples from

experimentally infected individuals and PBMCs from naturally infected individuals with acute febrile disease are hyperresponsive to *ex vivo* TLR ligand stimulation—a phenotype that can be recapitulated by stimulating naïve donor PBMCs with iRBC extract *in vitro* (106, 107).

Malarial infection can induce tolerance to subsequent malaria infection or other immune challenge [reviewed in (110)]. A reanalysis of experimental *P. falciparum* infection data demonstrated that the pyrogenic threshold—the level of parasitemia required to provoke fever—was higher for individuals after reinfection compared to initial infection (151). In an area of Mali with malaria transmission only during the rainy season, nearly 50% of healthy asymptomatic individuals had detectable parasitemia at the end of the dry season (152). Individuals infected with malaria as fever therapy for neurosyphilis and then challenged 2-3 days post final defervescence with heat-killed *Salmonella* exhibited depressed febrile responses (115). Interestingly, tolerance and training appear to be two ends of the same spectrum, as LPS and other ligands induce tolerance at higher concentrations but produce training at much lower concentrations (105). Therefore, we hypothesized that malarial stimulation would also induce trained immunity and set about to evaluate this possibility directly using human PBMCs.

Results

Primary stimulation of leukopak adherent PBMCs with malaria parasites or ligands induces increased proinflammatory cytokine production in response to secondary TLR stimulation

Adherent PBMCs were generated from leukopaks (leukapheresis product with concentrated PBMCs) by isolating PBMCs via density gradient centrifugation and allowing the PBMCs to adhere to tissue-culture treated polystyrene plates for ≥ 1 hour. After washing the plates 3x with warm PBS to remove non-adherent cells, the adherent PBMCs were stimulated with media containing 10% human serum (RPMI+) alone, *Plasmodium falciparum* iRBCs, uninfected red blood cells (uRBCs) or Hz for 24 hours. The cells were then washed and allowed to rest in RPMI+ for three days or five days. At this point, the cells were stimulated with the TLR2 ligand Pam3CSK4 or the TLR4 ligand LPS for 24 hours, at which point the supernatants were removed and TNFα and IL-6 levels were measured by ELISA. Since different training stimuli seemed to consistently induce higher or lower levels of adherent PBMCs by the end of the experiment (data not shown), we controlled for cell number by performing an MTS assay on the cells after removing the supernatants, and we normalized the cytokine values to relative cell numbers determined by the MTS assay. Training with either $1x10^5$ or $1x10^6$ iRBCs—but not similar quantities of uRBCs—and allowing the cells to rest for three or five days induced increased production of TNFα after a 24 h second stimulation with Pam3CSK4 as compared to control (RPMI+) trained cells (Fig. 4.1A). Although the differences in TNFα production over control-trained cells appeared to be greater after iRBC primary

stimulation and three days of rest than after iRBC stimulation and five days of rest, iRBC-induced training was only significant after the five-day rest. Similarly, primary stimulation with Hz induced increased production of TNFα in a dose-dependent manner following three or five days of rest and Pam3CSK4 restimulation; however, these differences were significantly greater than control only when training with 10 μM of Hz paired with three-day rest or 100 μM of Hz paired with five-day rest (Fig. 4.1A). Only training with the lower concentration of iRBC before either duration of rest induced increased IL-6 post-Pam3CSK4 stimulation, and this training effect was only significant after three days' rest (Fig. 4.1B). As seen with TNFα, training with Hz induced increased production of IL-6 in a largely dose-dependent manner after TLR2 challenge. This Hz-induced training was significant for the 100 and 10 μM Hz doses after three days' rest and for the 10 μM Hz dose after 5 days' rest. (Fig 4.1B).

When LPS was given as the second stimulus, the training effects of iRBCs and Hz were not as robust. There were trends towards increased TNFα production after iRBC training, three-day rest, and LPS challenge, but these trends were not seen if LPS challenge came five days after iRBC training (Fig. 4.1C). Similarly, primary stimulation with any of the three concentrations of Hz had no effect on TNFα production as a result of LPS challenge. Training with iRBCs or higher concentrations of Hz increased IL-6 production after three-day rest and LPS challenge, but this was only significant for training with 10^5 iRBCs, and no significant training was seen with a rest duration of 5 days (Fig. 4.1D). Based on these results, we decided to use a three-day rest period for all future experiments.

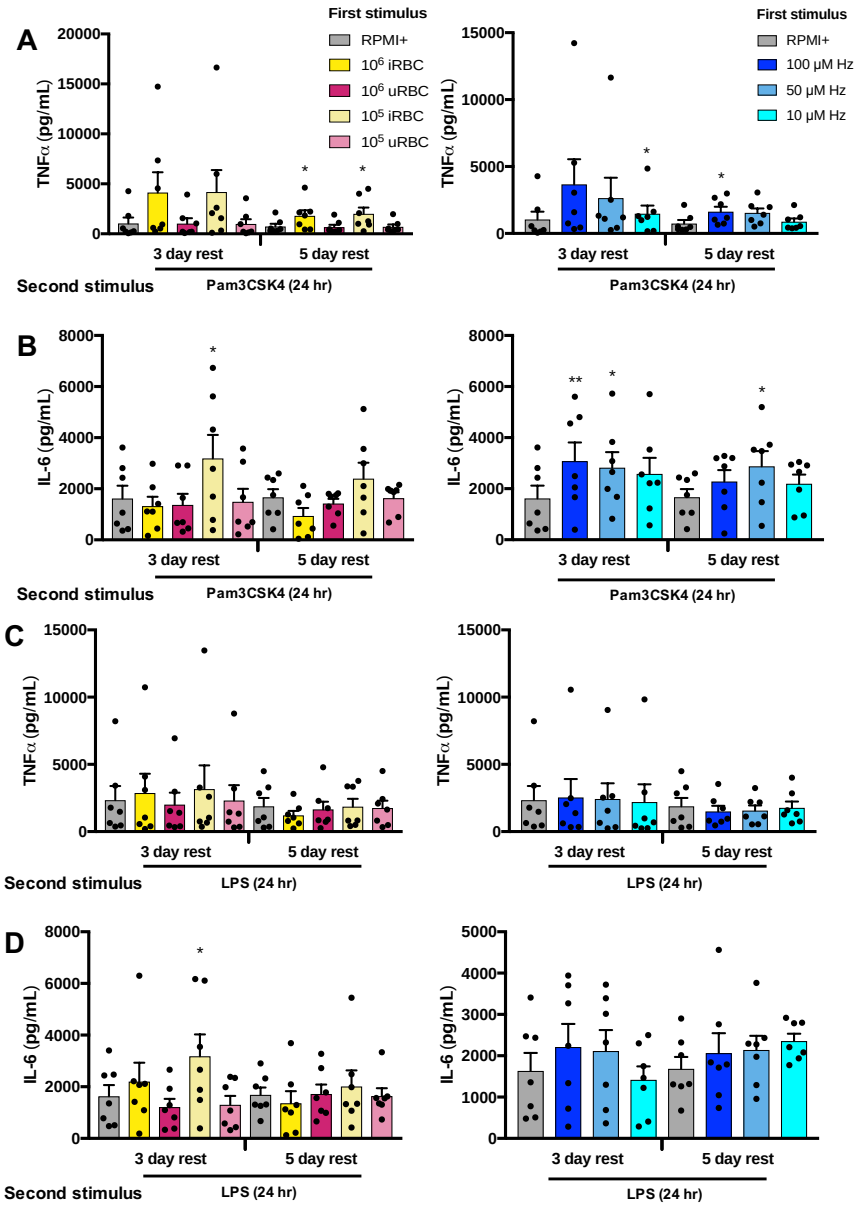

Figure 4.1. Effect of pretreatment ("training") with *P. falciparum* iRBCs or Hz three or five days before TLR ligand stimulation of human adherent PBMCs isolated from leukopaks. (**A-D**) TNFα (A, C) and IL-6 (B, D) ELISA measurements of supernatants from leukopak adherent PBMCs trained for 24 h with iRBCs, uRBCs, or Hz, rested for 3 d or 5 d, then challenged with Pam3CSK4 (A, B) or LPS (C, D) for 24 h. Bars represent mean ± SEM for seven donors (all comparisons to RPMI+ trained for similar duration of rest, *p<0.05, **p<0.01, paired *t*-test).

Induction of trained innate immunity by Plasmodium falciparum appears to be lost in a purer monocyte population

For the experiments described in Figure 4.1, we utilized adherent PBMCs, as this was the cell population used in earlier descriptions of trained immunity (95, 96). Examination of these populations via light microscopy showed a heterogeneous mix of cells; therefore, we decided to repeat some of the experiments shown in Figure 4.1 in a purer monocyte population. For these experiments, we again isolated PBMCs from leukopaks. For each leukopak, some of the PBMCs were allowed to adhere to polystyrene dishes as described above to produce adherent PBMCs, while the rest of the leukopak PBMCs underwent monocyte enrichment via negative selection using the EasySep Human Monocyte Enrichment Kit without CD16 depletion (STEMCELL Technologies). The training assay was then performed as described above with a three-day rest.

In general, the results for the adherent PBMCs look quite similar to those in Figure 4.1. Training with iRBCs and Hz resulted in increased TNFα production after secondary Pam3CSK4 stimulation, but this increased TNFα production was not significant for any training stimulus (Fig. 4.2A), presumably because of the relatively small sample size of three individual donors. Interestingly, increased TNFα after iRBC or Hz pretreatment was not seen in the negatively selected monocytes (Fig 4.2A). This difference in training between adherent PBMCs and monocytes was seen regardless of the training stimulus or challenge stimulus. For example, training with 10^5 iRBCs appeared to induce increased IL-6 after Pam3CSK4 second stimulus in adherent PBMCs, but this training effect was not seen in monocytes (Fig 4.2B). After primary stimulation

with 10^6 iRBCs and LPS challenge, negatively selected monocytes actually produced decreased levels of IL-6 as compared to media-trained, LPS-challenged monocytes (Fig. 2D). Although the small sample size precludes the making of any robust conclusions, these data suggest that *P. falciparum*-induced training is not seen in negatively selected monocytes.

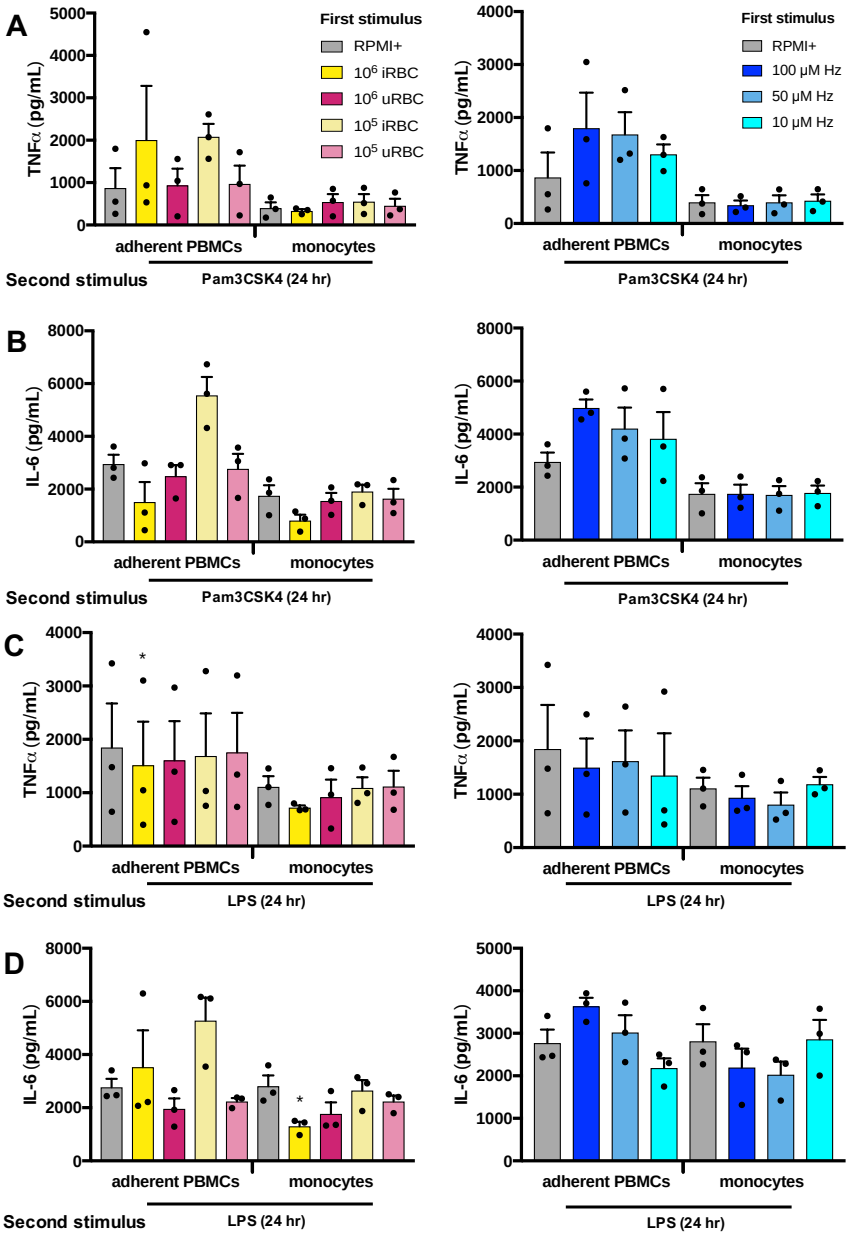

Figure 4.2. Comparison of *P. falciparum* innate immune memory assay in adherent PBMCs and monocytes. (**A-D**) TNFα (A, C) and IL-6 (B, D) ELISA measurements of supernatants from leukopak adherent PBMCs or negatively-selected monocytes trained for 24 h with iRBCs, uRBCs, or Hz, rested for 3 d, and then challenged with Pam3CSK4 (A, B) or LPS (C, D) for 24 h. Bars represent mean ± SEM for three donors (all comparisons to RPMI+ trained for similar cell populations, *p<0.05, **p<0.01, paired *t*-test).

Training with P. falciparum iRBCs and Hz induces increased proinflammatory cytokine production after Pam3CSK4 challenge in adherent PBMCs drawn from the same donor on different days

For the previous experiments, we used adherent PBMCs or monocytes from leukopaks because leukopaks were a relatively cheap and easy source for large numbers of PBMCs. However, the interdonor variability was quite large. Although a recent paper demonstrated the extent of interdonor variability in PBMC responses to common pathogens and TLR ligands, including Pam3CSK4 and LPS (153), we wondered if some of the variability in our assay could be due to the fact that our leukopaks came from out-of-state and were shipped overnight at ambient temperatures. In an attempt to minimize this variability, we performed our trained immunity assay on adherent PBMCs taken from the same donor on eight different days over the course of roughly thirteen months. Significant increases in both TNFα (Fig. 4.4A) and IL-6 (Fig 4.4B) post-Pam3CSK4 challenge were seen in adherent PBMCs trained with either iRBCs or Hz. Training with malaria ligands had no effect on TNFα production (Fig. 4.4C) and mild effects on IL-6 production (Fig. 4.4D) post-LPS challenge.

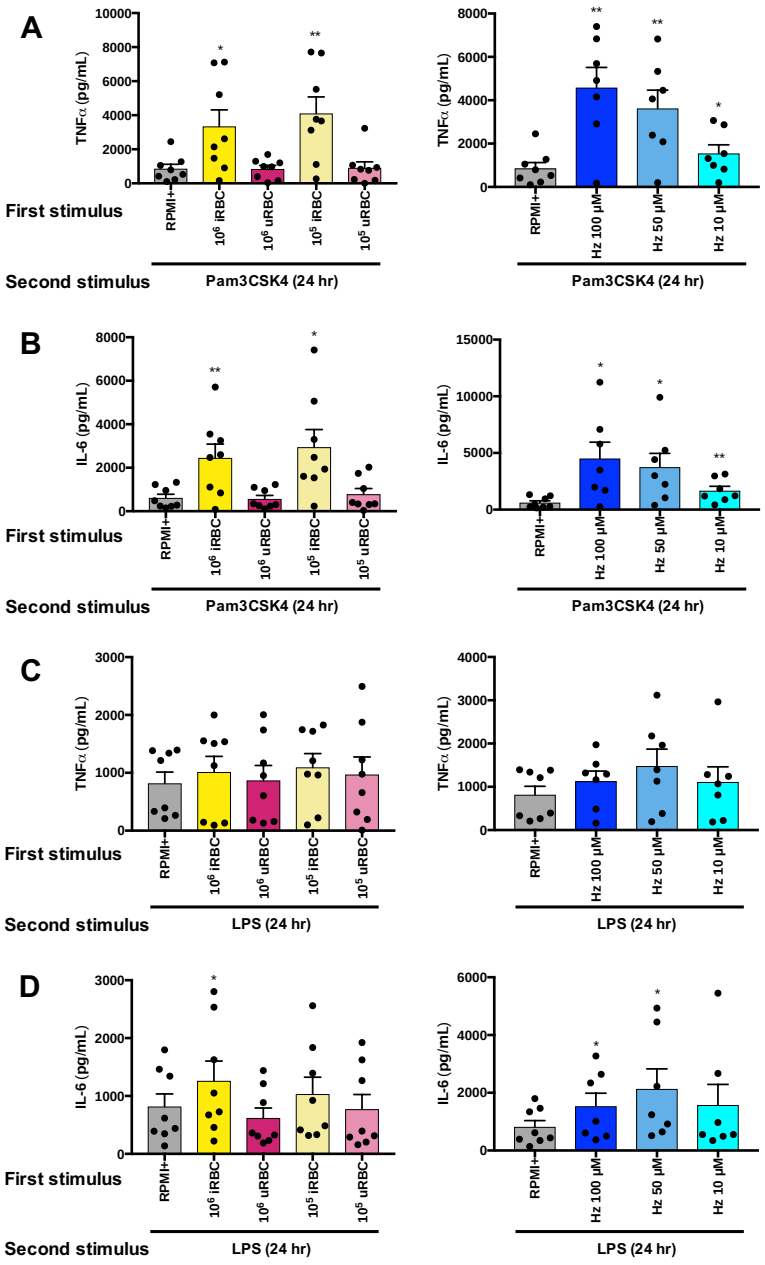

Figure 4.3. *P. falciparum* iRBCs and Hz induce trained immunity in adherent PBMCs from a single donor. (**A-D**) TNFα (A, C) and IL-6 (B, D) ELISA measurements of supernatants from adherent PBMCs trained for 24 h with iRBCs, uRBCs, or Hz, rested for 3 d, and then challenged with Pam3CSK4 (A, B) or LPS (C, D) for 24 h. Bars represent mean ± SEM for eight (RBCs) or seven (Hz) experiments using adherent PBMCs drawn from the same donor on different days (all comparisons to RPMI+ trained cells, *p<0.05, **p<0.01, paired *t*-test).

Training freshly-drawn adherent PBMCs with malaria parasites or Hz induces increased proinflammatory and decreased anti-inflammatory cytokine production in response to Pam3CSK4 challenge

Given the reproducibility of malaria-induced training in adherent PBMCs drawn from the same donor on different days, we decided to expand perform our trained immunity assay on adherent PBMCs taken from additional healthy donors. Training with either $1x10^5$ or $1x10^6$ iRBCs induced increased production of both TNFα and IL-6 24 h after secondary stimulation with Pam3CSK4. Similarly, primary stimulation with 100 μM or 10 μM Hz also induced increased production of these proinflammatory (Fig. 4.4A, B). However, training with malarial ligands had little effect on either TNFα and IL-6 production post-LPS secondary stimulation (Fig. 4.4C, D). Conversely, training with iRBCs significantly decreased production of the anti-inflammatory cytokine IL-10 after Pam3CSK4 challenge (Fig. 4.5A). Decreased IL-10 production was also seen after iRBC training/LPS challenge, Hz training/Pam3CSK4 challenge, and Hz training/LPS challenge, but these decreases were not significant (Fig. 4.5A, B).

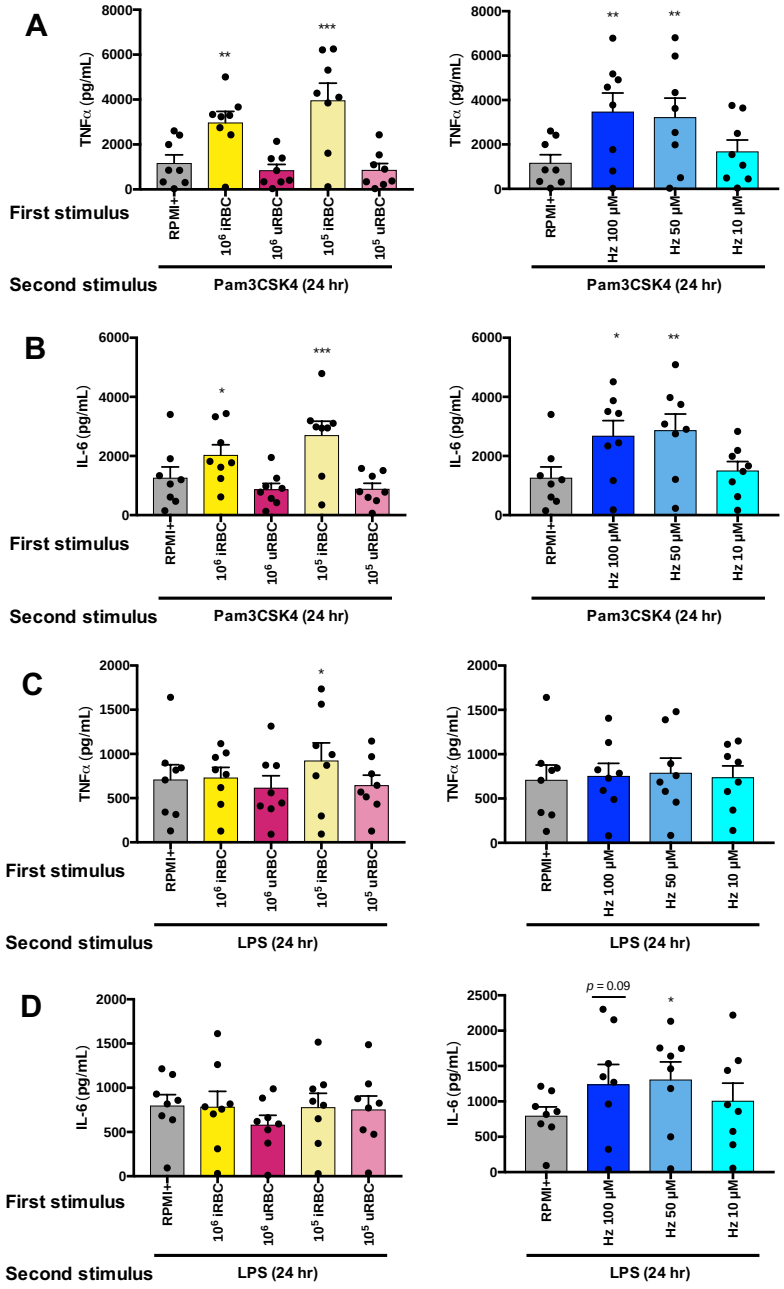

Figure 4.4. *P. falciparum* iRBCs and Hz induce increased proinflammatory cytokine production post-Pam3CSK4 challenge. (**A-D**) TNFα (A, C) and IL-6 (B, D) ELISA measurements of supernatants from freshly-drawn adherent PBMCs trained for 24 h with iRBCs, uRBCs, or Hz, rested for 3 d, and then challenged with Pam3CSK4 (A, B) or LPS (C, D) for 24 h. Bars represent mean ± SEM for eight donors (all comparisons to RPMI+ trained, *p<0.05, **p<0.01, ***p<0.001, paired *t*-test).

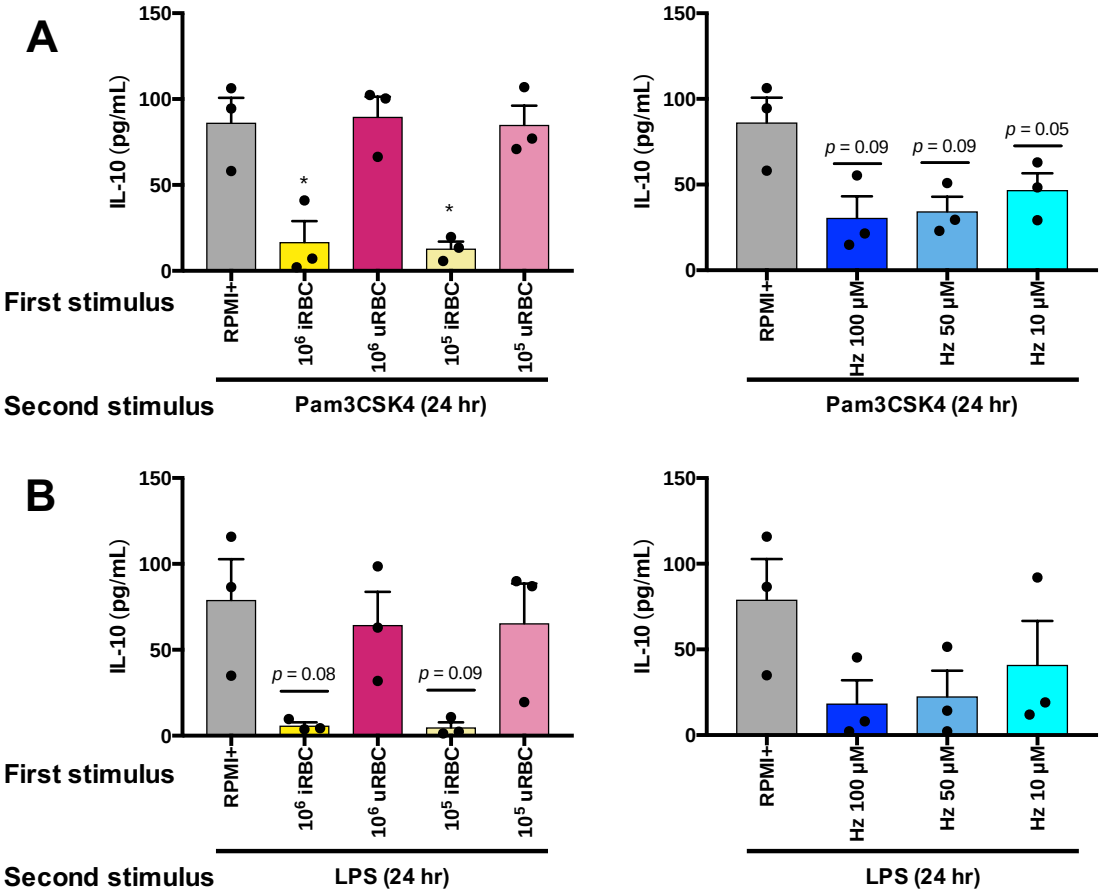

Figure 4.5. *P. falciparum* iRBCs and Hz induce decreased IL-10 production post TLR challenge. (**A, B**) IL-10 ELISA measurements of supernatants from freshly-drawn adherent PBMCs trained for 24 h with iRBCs, uRBCs, or Hz, rested for 3 d, and then challenged with Pam3CSK4 (A) or LPS (B) for 24 h. Bars represent mean ± SEM for three donors (all comparisons to RPMI+ trained, *p<0.05, paired *t*-test).

Malarial training has wide-ranging effects on the inflammatory transcriptome post-TLR second stimulus

The prevailing model of trained immunity is that increased responsiveness to secondary stimuli results from epigenetic remodeling that increases chromatin accessibility. It follows that increased proinflammatory gene transcription should follow secondary stimulation. In our *in vitro* model, stimulation of iRBC- or Hz-trained—but not uRBC-trained—adherent PBMCs with Pam3CSK4 for either 4 or 12 hrs increased transcription at the *TNF* locus as compared to cells trained with media alone (Fig. 4.6A). Interestingly, malarial training did not lead to increased *IL6* transcription after 4 h Pam3CSK4 second stimulation, but there was a trend towards increased *IL6* transcription in iRBC- and Hz-trained cells after 12 h Pam3CSK4 stimulation (Fig. 4.6B). To determine if malarial training has a more global effect on inflammatory gene expression, we performed a NanoString analysis on RNA harvested from malaria-trained cells given Pam3CSK4 as a secondary stimulus for 4 or 12 hrs. For each of the roughly 250 genes analyzed, we normalized the iRBC-, uRBC-, or Hz-trained transcript count to the control-trained transcript count at each secondary stimulus time point. These normalized ratios were log(2) transformed and displayed as a heatmap (Fig. 4.6C), which demonstrated that while uRBC training had little effect on the inflammatory transcriptome, both iRBC and Hz training had wide-ranging and similar effects. Based on hierarchical clustering, the majority of transcripts can be broadly classified into the following cohorts: globally upregulated (C1), upregulated after 4 h Pam3CSK4 stimulation (C2), upregulated after 12 h Pam3CSK4 stimulation (C3), downregulated after 12 h Pam3CSK4 stimulation (C4),

downregulated after 4 h Pam3CSK4 stimulation (C5), or globally downregulated (C6). Individual genes from each cohort previously implicated in malarial pathogenesis and/or trained immunity are listed in parenthesis after the cohort number (154-158). The normalized ratios for each gene found in the same order as in Figure 4.6C can be found in Table 4.1.

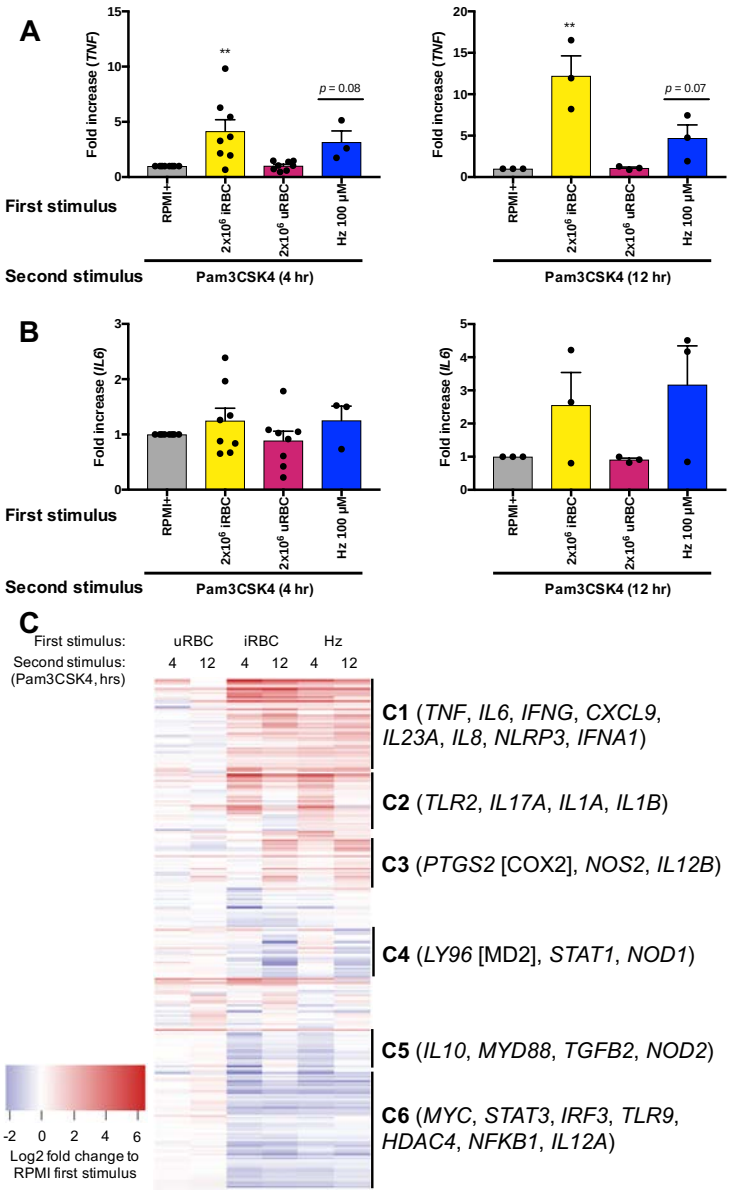

Figure 4.6. Malaria-induced training has wide-range effects on the transcriptional response to subsequent challenge. (**A, B**) mRNA was harvested from adherent PBMCs trained with iRBCs or Hz, rested for 3 d, and challenged with Pam3CSK4 for 4 or 12 h. Expression levels of *TNF* (A) and *IL6* (B) relative to RPMI+ trained cells are shown. Bars represent mean ± SEM for eight (4 h Pam3CSK4) or three (12 h Pam3CSK4) donors (**p<0.01, paired *t*-test). (**C**) Gene expression from cells treated as in (A) and (B) was quantified using NanoString technology. Expression counts were represented as log2 fold change compared to control-trained cells and plotted using hierarchical clustering. Each row represents one gene. Values shown are the means of two independent experiments from one of the donors in (A) and (B).

GENE NAME	URBCS, PAM 4H	URBCS, PAM 12H	IRBCS, PAM 4H	IRBCS, PAM 12H	HZ, PAM 4H	HZ, PAM 12H
IL5	2.92	0.02	7.15	5.74	5.66	4.10
IL13	1.48	0.08	4.43	3.83	2.60	2.69
CCL4	0.41	0.02	1.45	1.71	1.54	1.01
TNFSF14	0.09	-0.37	1.74	1.56	1.84	1.02
CXCL9	1.93	1.84	5.93	6.42	4.55	4.56
TNF	0.83	0.14	2.57	3.57	1.97	1.99
CCL19	0.44	1.27	3.98	3.57	2.56	2.40
IL21	0.27	0.16	4.08	2.90	2.16	2.28
IL23R	1.04	-0.08	1.96	2.24	1.22	0.56
C1R	-0.84	2.23	5.29	4.79	4.93	3.93
CRP	-0.62	0.42	0.99	1.24	0.90	0.55
PTGIR	0.10	0.37	0.79	0.93	1.14	0.83
C7	-2.33	-0.51	-0.26	0.83	0.76	0.35
C7	-2.33	-0.51	-0.26	0.83	0.76	0.35
IFNG	0.87	1.67	3.81	4.57	2.24	3.41
JUN	-0.21	0.17	0.33	0.74	0.12	0.61
CCR4	0.07	0.53	1.08	2.57	0.24	1.15
AREG	-0.06	0.44	2.53	4.22	2.46	3.66
FLT1	-0.03	-0.23	1.91	2.52	1.47	2.34
CCL3	0.30	0.09	1.34	1.98	1.38	1.62
FXYD2	-0.48	-0.85	0.28	1.22	0.37	0.82
C8B	-0.26	0.38	1.49	3.22	1.89	1.95
IL23A	-0.31	-0.05	0.97	3.11	1.13	2.47
CXCL2	0.16	-0.54	1.71	2.68	2.27	2.84
IL8	-0.12	-0.37	0.35	0.81	0.87	0.99
IL6	-0.07	-0.05	0.67	1.61	1.23	2.12
IL9	0.01	0.15	2.65	2.56	2.00	2.97
MBL2	-1.05	-0.53	1.17	1.23	0.90	1.98
IL11	0.50	0.55	0.61	1.45	1.92	2.00
CXCL3	0.01	-0.33	0.50	0.89	1.29	1.68
LTB4R	-0.05	-0.29	0.04	0.30	0.36	0.57
CCL20	-0.39	-0.66	-0.37	0.32	0.42	0.74
ALOX12	-0.83	-0.47	0.19	0.50	1.12	2.09
C2	0.00	-0.12	2.37	1.77	2.46	1.91
MAFF	-0.23	-0.21	1.23	1.05	1.27	0.93

CFB	-0.78	-0.45	2.11	1.64	1.97	1.88
HLA−DRB1	0.24	0.27	1.13	1.34	1.55	1.46
HLA−DRA	0.25	0.19	1.19	1.15	1.60	1.42
IL18	-0.17	-0.21	0.49	0.37	0.60	0.69
NLRP3	0.22	-0.41	0.76	0.78	1.00	1.29
RIPK2	0.23	-0.23	0.71	0.61	0.79	0.85
PTGER1	0.37	-0.02	0.94	1.00	1.13	1.03
IL1RN	0.02	-0.34	1.06	0.86	0.74	1.15
IL3	1.19	0.24	3.60	1.93	2.40	2.77
IFNA1	1.76	-0.66	3.28	0.66	2.74	2.32
PTGFR	0.74	-1.03	0.61	0.32	-0.11	1.00
C1S	1.26	0.67	6.50	4.48	5.77	3.68
IL2	-0.24	1.20	4.48	2.89	4.32	2.27
CSF1	0.18	0.33	2.35	1.08	2.22	1.01
CCL21	1.36	1.00	3.25	1.95	3.46	1.53
ITGB2	0.09	0.09	0.92	0.40	0.96	0.27
C1QA	0.36	0.24	2.36	0.70	2.48	0.41
MMP9	0.81	0.02	2.94	1.28	2.50	0.72
LIMK1	0.06	-0.24	1.47	0.51	1.35	0.70
FOS	-0.09	-0.74	0.95	0.28	1.16	0.27
CEBPB	-0.14	-0.37	0.44	-0.03	0.70	0.32
CCR1	-0.31	-0.11	0.82	0.08	1.18	0.29
MRC1	0.39	-0.28	2.32	-0.16	2.22	0.37
C1QB	0.06	0.17	1.36	-0.10	1.47	0.14
CCL24	0.91	-0.11	2.78	-0.90	2.92	-0.04
TLR2	0.24	-0.08	0.62	-0.17	1.27	0.15
CCL8	0.82	2.43	3.43	1.48	3.23	1.56
CCL13	0.04	1.30	4.11	-0.91	4.95	-1.49
IL17A	0.01	1.03	3.51	1.61	2.39	1.05
TLR8	-0.18	0.32	1.78	0.52	1.34	0.62
KNG1	0.01	-0.14	2.63	0.03	1.16	0.52
CXCL5	0.59	-0.45	0.75	-0.80	1.65	1.00
IL1A	0.34	-0.34	0.16	-0.96	1.20	0.44
PTGS1	0.38	-0.14	0.83	-0.56	1.17	0.54
C3AR1	0.03	0.06	0.33	-0.38	0.80	0.32
CFD	0.26	-0.11	0.07	-0.37	1.03	1.18

C3	-0.24	-0.38	-0.14	-0.72	0.77	0.52
IL1B	0.03	-0.25	0.01	-0.06	0.74	0.68
CCL11	-2.18	-1.10	0.01	-1.67	-0.58	0.85
IL22RA2	0.67	1.36	1.18	1.68	3.19	0.55
PIK3C2G	0.01	0.15	0.03	1.74	1.63	0.55
MASP1	0.01	-0.54	0.03	0.88	2.72	0.88
MYL2	0.01	1.03	0.03	0.33	1.22	0.55
CSF2	0.34	0.08	1.16	3.80	1.91	3.56
PTGS2	-0.19	-0.57	0.40	2.21	0.85	2.45
IL1R1	0.18	-0.67	0.06	2.35	0.84	2.28
CCL16	-0.40	-1.13	0.00	1.34	0.37	1.53
CSF3	-0.79	-1.00	-0.69	2.67	1.02	3.16
MMP3	-0.50	-0.62	-0.54	1.66	0.60	2.52
MAP2K1	0.03	0.01	0.07	0.39	0.09	0.50
MAPKAPK2	0.10	-0.01	-0.06	0.62	0.17	0.28
IL12B	1.35	1.75	1.09	2.45	1.40	2.25
TNFAIP3	0.00	-0.02	-0.16	0.22	-0.02	0.18
MAFK	-0.22	0.04	-0.40	0.63	0.12	0.54
IL15	0.08	0.28	0.03	0.73	0.24	0.94
IL6R	-0.23	0.10	-0.21	0.75	0.26	0.90
RAPGEF2	0.11	0.12	-0.11	0.34	0.14	0.48
NOS2	-0.33	2.08	0.03	3.22	2.12	3.13
C8A	0.01	0.15	0.03	0.33	0.33	0.55
C6	-0.82	0.46	0.70	1.00	0.68	1.55
GNGT1	-0.96	-0.18	-0.23	0.72	0.11	0.84
C9	-0.12	2.26	0.03	3.17	0.44	2.60
OASL	-0.30	0.92	-0.54	2.01	-0.39	1.51
TBXA2R	-0.30	0.87	0.11	1.79	0.36	0.90
BCL2L1	0.37	0.20	-0.15	0.70	-0.15	0.67
TGFB1	0.20	0.04	-0.14	0.58	-0.08	0.65
CD86	-0.19	-0.19	-0.40	-0.15	-0.46	0.53
TSLP	0.13	-0.14	-2.48	1.58	1.16	1.94
CXCR1	-0.53	-0.17	-1.35	0.57	0.35	0.60
MAFG	-0.06	-0.13	-0.36	-0.08	0.14	0.21
GNAQ	-0.25	-0.06	-0.86	-0.50	-0.55	0.02

ATF2	-0.04	0.11	-0.39	0.04	-0.07	0.28
IFNB1	-0.69	0.02	-1.63	-0.30	-0.56	0.21
ELK1	0.06	-0.09	-0.48	-0.04	-0.02	0.11
IL10RB	-0.25	-0.20	-0.89	-0.40	-0.32	-0.08
NFE2L2	-0.05	0.08	-0.57	-0.19	-0.12	-0.09
TLR5	-0.73	0.02	-3.86	-1.09	-1.93	-0.43
ALOX15	0.67	0.21	0.03	0.16	0.33	0.38
SMAD7	0.15	-0.18	-0.27	-0.21	0.14	-0.12
CXCL1	0.23	-0.27	-0.51	-0.78	0.38	0.38
TOLLIP	-0.12	-0.06	-0.47	-0.43	-0.18	0.16
RAC1	-0.20	-0.14	-0.55	-0.40	-0.17	-0.01
PLA2G4A	-0.32	-0.15	-0.88	-1.13	-0.20	-0.11
PTGER2	-0.11	-0.42	-1.14	-1.03	-0.37	-0.14
HIF1A	-0.04	-0.16	-0.93	-0.89	-0.32	0.14
TLR4	-0.28	-0.34	-1.51	-1.60	-0.74	-0.16
IFIT2	0.15	0.97	0.68	0.13	0.22	0.45
OXER1	1.77	0.59	1.84	-0.87	1.92	-2.14
HSH2D	0.13	0.72	0.26	-0.05	-0.13	-0.76
CD4	0.04	0.33	-0.27	-0.27	-0.02	-1.22
IL1RAP	0.44	-0.13	0.35	-1.06	0.30	0.09
ALOX5	-0.04	0.34	0.47	-0.71	0.57	-0.04
LY96	-0.06	-0.07	0.02	-0.99	0.35	-0.30
CCL2	0.19	-0.16	-0.27	-3.73	0.71	-1.79
CD163	0.40	0.55	-0.46	-1.12	0.74	-0.11
TYROBP	0.00	-0.06	-0.71	-0.90	0.16	-0.28
PTGDR2	1.10	1.02	-0.52	-0.43	1.68	-1.39
HSPB1	-0.30	-0.06	-0.36	-1.16	-0.03	-0.95
NOX1	-0.60	0.23	-0.86	-1.76	0.92	-1.44
STAT1	0.66	1.09	0.17	-0.36	0.14	-0.03
NOD1	0.30	0.31	0.01	-0.72	-0.17	-0.27
PLCB1	-0.16	0.05	-1.10	-1.90	-0.75	-1.07
TREM2	0.04	0.08	-1.32	-2.46	-0.37	-1.51
CXCL6	1.45	0.17	-0.18	-3.04	0.80	-1.73
CCL7	0.33	0.20	-0.53	-3.00	-0.05	-1.90
CFL1	0.19	0.15	-0.06	-0.29	0.14	-0.28
CYSLTR2	0.19	0.40	-0.55	-1.28	0.00	-1.70
CCL23	0.25	0.39	-0.49	-0.86	-0.14	-0.82

MAPK3	0.14	0.37	-0.58	-1.39	-0.25	-1.30
CXCR4	0.06	0.15	-0.37	-1.04	-0.48	-0.94
CD55	-0.15	0.07	-0.67	-1.51	-0.80	-1.70
IL4	3.82	3.41	4.72	3.79	3.40	1.79
CCL17	1.84	0.55	3.52	2.33	1.09	-0.90
CXCL10	1.88	2.21	3.06	2.78	1.86	2.17
CCL22	0.89	0.52	1.61	1.98	-0.15	0.32
FASLG	0.66	0.45	0.34	0.57	0.05	-0.42
CD40	0.41	0.26	0.32	0.20	-0.13	-0.06
MAP3K9	1.01	0.16	-0.40	-0.30	-1.14	-0.94
ARG1	1.05	-1.04	-0.24	1.01	-0.52	-0.40
IFIT1	0.14	2.25	0.22	1.61	-0.09	1.42
IRF7	-0.05	0.66	-0.19	0.41	-0.20	0.30
OAS2	0.04	0.98	0.13	0.87	-0.25	0.29
C4A	0.67	1.95	1.21	1.31	-0.25	1.15
CCR2	0.69	1.27	0.25	1.88	-0.10	0.55
HMGB2	-0.78	0.15	-1.23	0.50	-1.32	-0.57
LTA	0.17	0.41	0.12	0.75	-0.32	0.03
TLR7	0.06	0.48	-0.25	0.76	0.01	-0.31
CXCR2	-0.63	1.01	-2.44	-0.18	-1.07	-1.56
IFIT3	-0.14	1.26	0.42	0.71	0.15	0.97
TWIST2	-0.73	1.69	-0.25	0.33	-0.07	0.55
IFI44	0.02	1.15	0.16	0.23	0.05	0.43
MX1	-0.46	0.97	-0.40	0.05	-0.66	-0.06
MASP2	-0.39	0.80	-0.36	0.33	-0.07	0.55
HSPB2	-1.00	1.30	-1.26	1.08	-0.56	0.64
IRF1	0.55	0.80	-0.11	0.23	-0.55	0.24
MEF2D	0.30	0.47	-0.31	0.13	-0.99	0.09
CCR3	3.95	3.65	1.91	3.26	2.41	2.82
MAPK8	0.08	0.02	-0.53	-0.24	-0.33	-0.07
IL10	0.42	0.47	-2.23	-0.20	-1.07	-0.17
DDIT3	-0.08	0.04	-1.42	-0.57	-0.88	-0.45
TLR1	0.20	0.05	-0.96	-0.14	-0.74	0.07
ROCK2	0.08	-0.09	-0.71	-0.31	-0.77	-0.17
SHC1	0.02	0.22	-0.72	-0.31	-0.55	-0.10
BCL6	-0.09	0.12	-1.12	-0.56	-0.87	-0.16
TLR6	0.09	0.41	-1.26	-0.35	-1.16	0.04

RAF1	0.05	0.10	-0.85	-0.42	-0.80	-0.17
MAPK14	0.02	0.13	-1.75	-0.69	-1.65	-0.32
NFATC3	0.04	0.28	-1.65	-0.87	-1.59	-0.81
MYD88	0.08	0.33	-0.90	-0.41	-0.68	-0.30
TRADD	0.05	0.35	-1.71	-0.81	-1.16	-0.52
CREB1	-0.04	0.19	-1.99	-1.10	-1.50	-0.75
NOD2	-0.08	0.33	-0.66	0.39	-1.10	0.31
PRKCB	-0.16	0.10	-0.95	0.18	-0.90	0.15
PDGFA	-0.13	0.67	-1.50	0.78	-1.09	0.15
C5	-0.96	1.25	-4.11	0.61	-2.17	-0.74
MEF2A	-0.16	0.00	-0.77	-0.12	-0.60	-0.20
TGFB2	-0.47	0.82	-2.39	0.01	-1.80	0.04
MEF2BNB−MEF2B	-1.81	-0.61	-3.49	-1.56	-2.92	-1.33
CCL5	0.17	0.54	-0.81	-0.23	-1.05	-1.06
CD40LG	0.00	0.20	-1.19	-0.82	-1.59	-1.55
IL18RAP	0.70	0.90	-0.98	0.33	-0.95	-0.67
MAP2K6	-0.46	0.60	-3.06	-1.39	-2.77	-3.05
TCF4	0.02	0.39	-1.92	-0.97	-1.36	-1.28
CCR7	0.00	0.42	-1.93	-1.18	-1.84	-1.46
PTGER4	0.00	0.43	-0.95	-0.67	-0.62	-0.79
CYSLTR1	-0.14	0.37	-1.55	-1.31	-1.40	-1.45
DEFA1	0.54	1.06	-2.50	-1.82	-2.04	-1.76
MYC	-0.30	0.33	-2.66	-1.90	-2.20	-2.10
HMGB1	0.05	0.19	-0.45	-0.61	-0.68	-0.67
RPS6KA5	0.17	0.17	-0.95	-1.12	-0.97	-1.23
STAT3	0.07	0.29	-0.42	-0.42	-0.52	-0.30
MX2	-0.21	0.71	-0.97	-1.14	-0.98	-0.91
TLR9	-0.07	0.81	-1.12	-1.30	-1.33	-1.25
HDAC4	0.12	0.42	-1.05	-1.14	-1.06	-0.77
PRKCA	0.33	0.59	-1.93	-2.33	-1.94	-1.68
MEF2C	0.29	0.84	-1.40	-1.19	-0.95	-1.04
IRF3	0.18	0.39	-1.38	-1.15	-0.99	-0.92
HMGN1	-0.12	0.08	-1.46	-1.33	-1.19	-1.13
PTGER3	1.09	1.65	0.02	0.34	-0.26	0.68

IL7	0.25	0.72	-0.66	-0.55	-0.93	0.07
RELA	0.05	0.35	-0.39	-0.21	-0.33	-0.09
STAT2	0.26	0.51	-0.21	-0.18	-0.13	0.22
MAP3K5	0.09	0.30	-1.10	-0.64	-0.73	-0.30
TGFBR1	-0.05	0.11	-0.95	-0.71	-0.62	-0.26
NFKB1	0.15	0.05	-0.66	-0.45	-0.34	-0.19
NR3C1	0.01	0.04	-0.88	-0.46	-0.31	-0.25
CDC42	0.06	0.03	-0.38	-0.24	-0.11	-0.15
GRB2	0.26	0.42	-0.97	-0.53	-0.26	-0.22
GNB1	0.12	0.10	-0.68	-0.90	-0.41	-0.40
MKNK1	0.00	-0.10	-1.03	-1.28	-0.71	-0.70
RHOA	0.08	0.11	-0.36	-0.31	-0.07	-0.13
TGFB3	-0.40	-0.17	-1.72	-1.67	-1.11	-1.04
LTB4R2	-0.29	-0.03	-1.96	-1.94	-1.31	-1.21
IL12A	0.30	0.67	-2.20	-1.38	-0.93	-1.75
GNAS	0.03	0.23	-1.00	-0.89	-0.49	-0.71
TLR3	0.41	0.46	-1.45	-1.59	-0.43	-1.21
PTK2	-0.16	0.20	-1.51	-1.89	-1.05	-1.34
LTB	0.02	0.48	-2.23	-2.65	-1.74	-2.47
KEAP1	0.14	-0.04	-0.50	-0.68	-0.57	-0.39
PPP1R12B	0.26	0.11	-1.38	-2.10	-1.45	-0.97
HRAS	0.36	0.16	-0.49	-0.35	-0.27	-0.38
DAXX	0.24	0.06	-0.48	-0.45	-0.52	-0.40
IRF5	0.17	0.02	-0.63	-0.69	-0.64	-0.55
MAPK1	0.09	-0.04	-0.86	-0.59	-0.62	-0.36
MAP2K4	0.22	0.06	-1.50	-1.00	-1.22	-0.56
MAPKAPK5	0.12	-0.01	-1.48	-1.25	-1.34	-0.82
BIRC2	-0.02	-0.07	-1.18	-0.96	-0.90	-0.57
MAP3K7	-0.05	-0.02	-1.23	-0.92	-1.03	-0.59
RELB	0.02	0.24	-1.39	-0.98	-0.91	-0.70
RIPK1	0.12	0.26	-0.83	-0.67	-0.73	-0.37
MAX	0.29	0.36	-0.97	-0.90	-0.86	-0.62
AGER	0.19	0.37	-1.71	-1.46	-1.39	-1.06
TRAF2	0.11	0.20	-1.22	-1.11	-1.06	-0.73

MAP3K 1	-0.03	0.30	-2.65	-2.36	-2.25	-1.53

Table 4.1. Normalized ratios comparing the iRBC-, uRBC-, or Hz-trained NanoString transcript count to the control-trained transcript count. mRNA was harvested from adherent PBMCs trained with iRBCs or Hz, rested for 3 d, and challenged with Pam3CSK4 for 4 or 12 h. NanoString gene expression counts were represented as log2 fold change compared to control-trained cells stimulated for the same duration with Pam3CSK4 and plotted using hierarchical clustering. Each row represents one gene. Shown are the means of two independent experiments from one of the donors in Figure 4.6A and B.

Robust malarial training was not seen in the transdifferentiated BLaER1 or THP-1 human cell lines

We have demonstrated that training with malarial parasites and Hz can induce adherent PBMCs to respond in a more proinflammatory manner to secondary TLR stimulation; however, we have not yet delved into the mechanism by which malaria stimulation does this. Therefore, we sought to identify a cell line that also displayed training characteristics after stimulation with malaria parasites and Hz. If we were successful, we could then engineer genetic knockouts to elucidate what PRRs and downstream signaling cascades were required for this malarial training phenotype.

A recent study described transduction the Seraphina B cell lymphoma cell line with the macrophage lineage transcription factor C/EBPα under the control of the estrogen receptor dependent promoter. When cells of one of the transduced clones, BLaER1, were exposed to estrogen, they transdifferentiated into macrophage-like cells that expressed macrophage cell surface markers, expressed a transcriptome similar to primary macrophages, and became both phagocytic and post-mitotic (159). Veit Hornung's group then demonstrated that these cells respond to LPS in a manner similar to human primary monocytes, including alternative activation of the NLRP3 inflammasome without a traditional second signal. They then utilized CRISPR-Cas9 to generate many knockout BLaER1 cell lines to further explore the mechanism behind this alternative inflammasome activation pathway (124).

We acquired this BLaER1 cell line, and after transdifferentiating the cells into macrophages, we also saw robust proinflammatory cytokine production in response to

LPS stimulation (Fig. 4.7A). We then utilized transdifferentiated BLaER1 cells in our *in vitro* trained immunity assay. We found that training with 10^6 iRBCs induced the BLaER1 cells to produce significantly more TNFα (Fig 4.7B) and IL-6 (Fig 4.7C) post-LPS challenge. However, these cells did not show similarly significant training post Pam3CSK4 challenge (Fig 4.7D), and the levels of TNFα and IL-6 produced post-Pam3CSK4 stimulation were quite low. We tested other TLR2 ligands (peptidoglycan, Pam2CSK4, and MALP-2) with similar results (data not shown).

Since malarial training in adherent human PBMCs is seen more robustly with Pam3CSK4 challenge than LPS challenge (Figs. 4.4, 4.5), we decided to test the THP-1 human monocyte cell line. Training with *P. falciparum* iRBCs or Hz had no effect on proinflammatory cytokine production post TLR challenge (Fig. 4.8).

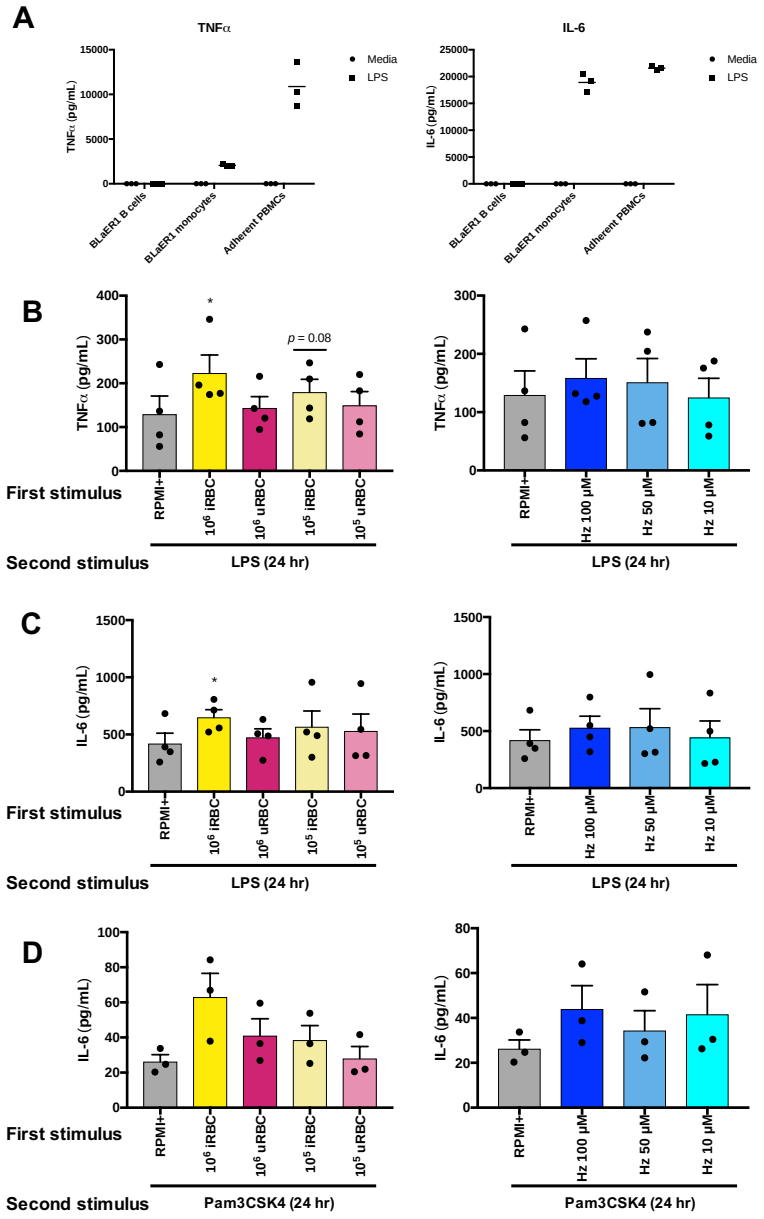

Figure 4.7. Transdifferentiated BLaER1 cells respond to LPS, but do not display robust malarial trained immunity. (**A**) BLaER1 cells prior to transdifferentiation (BLaER1 B cells), post-transdifferentiation (BLaER1 monocytes) and adherent PBMCs were stimulated with media or 200 ng/mL LPS overnight, and cytokine concentrations were measured in the supernatants by ELISA. Data points represent technical replicates for one transdifferentiation experiment or adherent PBMCs from one donor. (**B-D**) TNFα (B) and IL-6 (C, D) ELISA measurements of supernatants from transdifferentiated BLaER1 cells trained with iRBCs or Hz, rested for 3 d, then challenged with LPS (B, C) or Pam3CSK4 (D) for 24 h. Bars represent pooled mean ± SEM from three or four independent experiments (all comparisons to RPMI+ trained, *p<0.05, paired *t*-test).

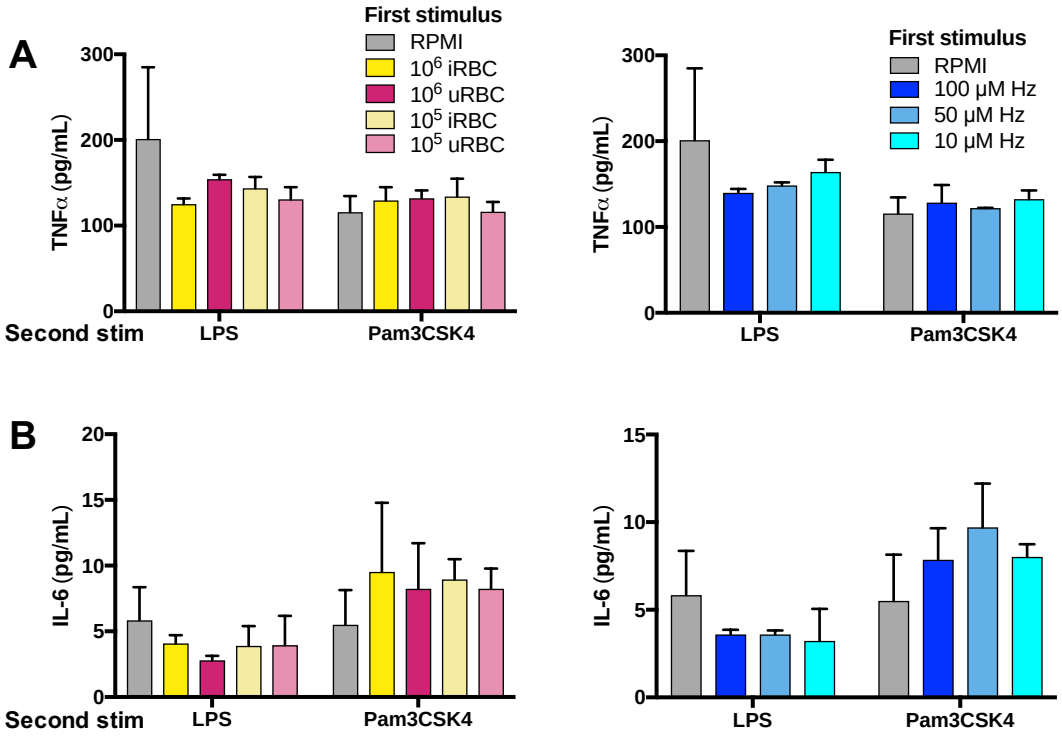

Figure 4.8. *P. falciparum* iRBCs and Hz do not induce trained immunity in THP-1 human monocytes. (**A, B**) TNFα (A) and IL-6 (B) ELISA measurements of supernatants from PMA-differentiated THP-1 cells trained with iRBCs or Hz, rested for 3 d, then challenged with LPS or Pam3CSK4 for 24 h. Bars represent mean ± SD for duplicate stimulations of THP-1 cells from one experiment (all comparisons to RPMI+ trained and not significant, unpaired *t*-test).

P. falciparum-*induced training seen in mouse BMDMs, while iRBCs induce tolerance in mouse peritoneal exudate cells*

In a further attempt to develop an *in vitro* model of malaria-induced trained immunity amenable to genetic manipulation, we performed our trained immunity assay on mouse BMDMs and non-thioglycollate-elicited peritoneal exudate cells (PECs). We did not use thioglycollate elicitation because, although it increases the yield of PECs/mouse, it also induces some non-specific activation of the cell and may partially inhibit phagocytosis (160). Training with iRBCs did not induce increased TNFα in mouse BMDMs post-LPS challenge, although TNFα was slightly increased after training with 100 μM Hz/Pam3CSK4 challenge (Fig. 4.9A). Training with 10^6 iRBCs did promote increased chemokine RANTES after both LPS and Pam3CSK4 challenge (Fig. 4.9B). Pretreatment with $2.4x10^6$ PbA iRBCs for 36 hrs, followed by three-day rest, significantly decreased TNFα production after secondary stimulation with LPS or Pam3CSK4 (Fig. 4.9C), potentially indicating the induction of tolerance.

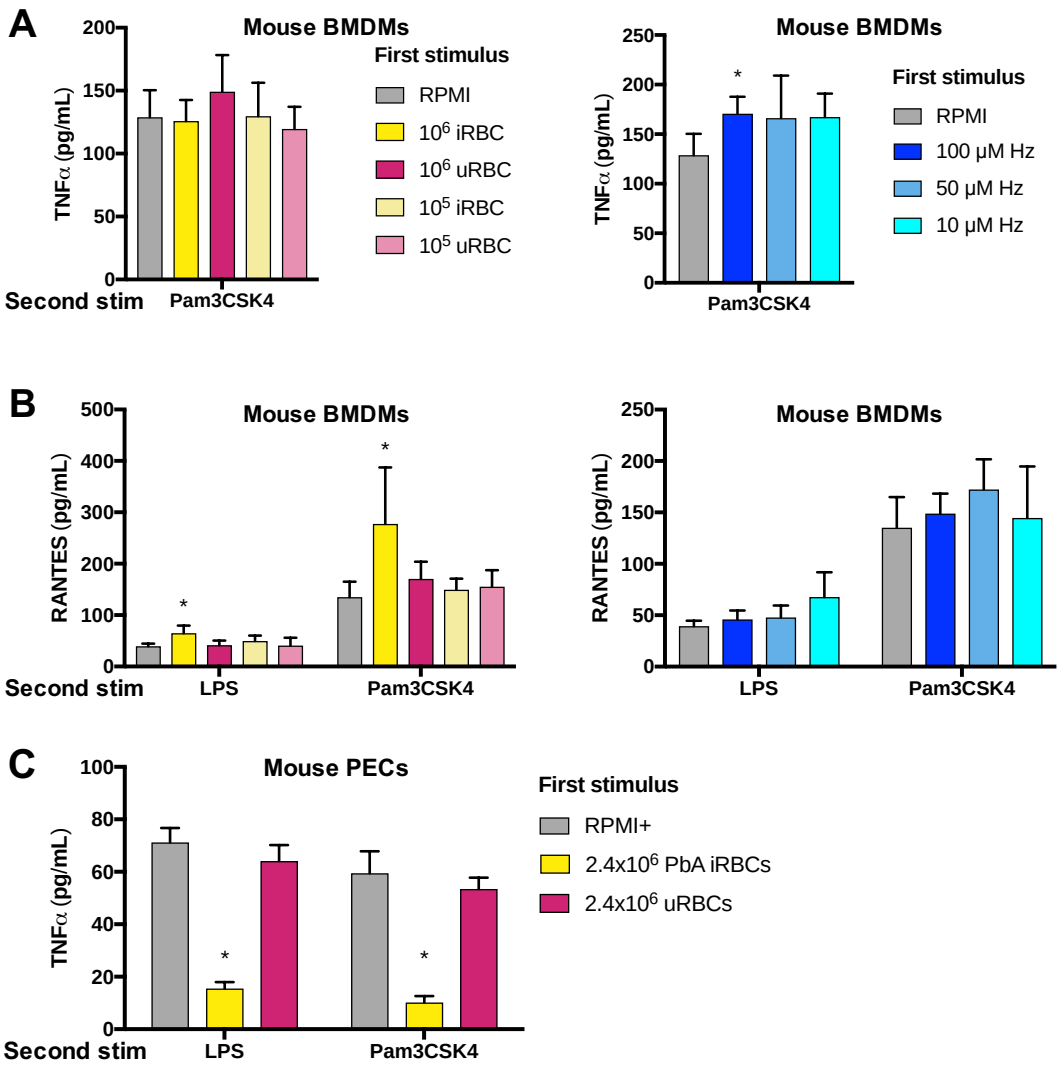

Figure 4.9. *P. falciparum* iRBCs and Hz induce innate immune memory in mouse BMDMs and PECs. (**A, B**) TNFα (A) and RANTES (B) ELISA measurements of supernatants from mouse BMDMs trained with iRBCs or Hz, rested for 3 d, then challenged with LPS or Pam3CSK4 for 24 h. Bars represent mean ± SD for technical quadruplicates from one experiment (all comparisons to RPMI+ trained, *p<0.05, **p<0.01, unpaired *t*-test) (**C**) TNFα ELISA measurements of supernatants from non-thioglycollate-elicited mouse PECs stimulated with PbA iRBCs for 36 h, rested for 3 d, then challenged with LPS or Pam3CSK4 for 24 h. Bars represent mean ± SD for duplicate stimulations of cells from one experiment (all comparisons to RPMI+ trained, *p<0.05, unpaired *t*-test).

Adherent PBMCs contain multiple cell types and malaria-induced training alters the relative proportions of these cell types

As mentioned earlier in this Chapter, training with malaria iRBCs and Hz consistently results in increased numbers of adherent PBMCs as compared to control-trained adherent PBMCs; therefore, we normalized the raw cytokine values to cell numbers estimated by the use of a MTS assay. In addition to increased adherent PBMC numbers, we also saw that the adherent PBMCs trained with malarial ligands were often larger and had more of an activated macrophage phenotype (Fig. 4.10A). To determine the both the composition of the adherent PBMCs and the contribution of adherence to changing the relative makeup of the PBMC population, we perform flow cytometry on freshly isolated PBMCs and the adherent PBMCs remaining after at least 1 h of adherence and three washes with PBS. To our great surprise, the two populations were almost identical for both donors we tested (Fig. 4.10B).

Next, we performed flow cytometry on adherent PBMCs after training and three days' rest. We discovered that training with iRBCs or Hz appears to increase the relative proportion of $CD14^+$ cells with the concomitant decrease in the relative proportion of $CD3^+$ cells (Fig. 4.10C). To determine if the changes in relative cell number within the trained adherent PBMC population affected our results, we normalized the cytokine values determined by ELISA post-secondary TLR challenge to the $CD14^+CD45^+$:$CD14^-CD45^+$ ratio for each training stimulus. As seen in Figure 4.10C, the results of the two normalization techniques were nearly identical, so we continued normalizing our results using the MTS assay.

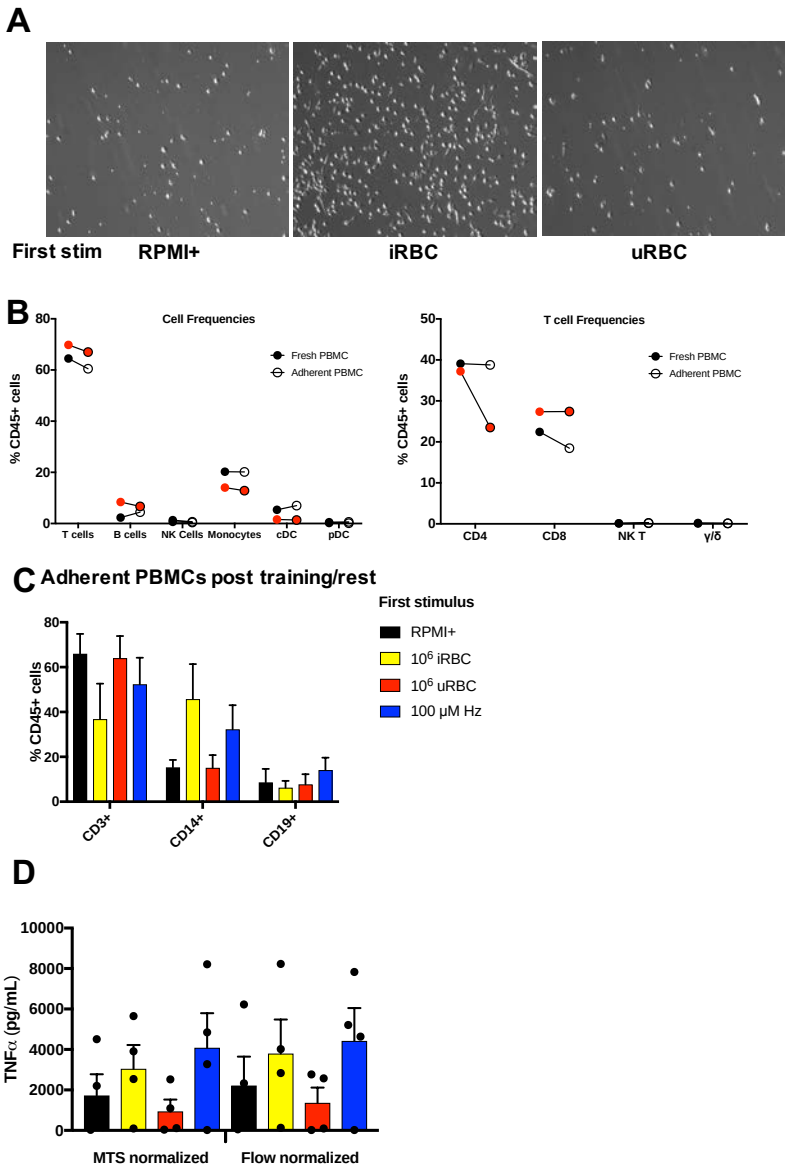

Figure 4.10. *P. falciparum* training effects on cell morphology and adherent PBMC composition. (**A**) Adherent PBMCs were treated with media alone (RPMI+), iRBCs, or uRBCs for 24 h and then washed. After 3 d rest, cells were examined via light microscopy and representative images were selected. (**B**) Flow cytometry was performed on freshly isolated PBMCs and adherent PBMCs post adhesion to plastic for at least 1 h and 3x washed to remove non-adherent cells. Each donor is represented by a different color. (**C**) Flow cytometry were performed on adherent PBMCs treated as in (A). (**D**) ELISA values post-Pam3CSK4 challenge were normalized using MTS values, or using the ratio of $CD14^{+}CD45^{+}$:$CD14^{-}CD45^{+}$. Images in (A) are from one donor, (B) is from two donors, and (C and D) bars represent mean ± SD (C) or SEM (D) for four donors.

Malarial training may not depend on IL-12p40 or IFNγ signaling

As demonstrated in Figure 4.6D, IFNγ was one of the cytokines highly upregulated by malarial training. Natural killer (NK) cells produce IFNγ starting as little as 6 hours post-iRBC stimulation in an IL-12- and IL-18-dependent manner, although this NK-dependent IFNγ production is heterogeneous between donors (161-163). In a murine malaria model, malarial priming was IL-12- and IFNγ-dependent (107). Interestingly, IFNγ plays a necessary role in *Candida albicans*-induced trained immunity, and this IFNγ-dependent training was blocked by pretreatment with the αIL-12p40 antibody ustekinumab (164). Transcription of the IL-12p40 subunit (*IL12B*) was slightly elevated in our NanoString dataset (Fig. 4.6D), and the IL-23p19 subunit (*IL23A*), which dimerizes with IL-12p40 to make a functional IL-23 molecule, was highly upregulated after malarial training. To test the role of these cytokines in malaria-induced trained immunity, we utilized neutralizing antibodies against either IFNγ or IL-12p40. Treatment of adherent PBMCs with anti-IFNγ IgG during the 24 h first stimulation did not appear to inhibit iRBC- or Hz-induced training (Fig. 4.11A). Additionally, treatment of adherent PBMCs with anti-IL-12p40 IgG continuously during the first stimulation, 3 d rest, and second stimulation did not appear to substantively inhibit malaria-induced training (Fig. 4.11B). However, these are only the results of two donors. Although these results may indicate that signaling via these cytokines was dispensable for malarial training, these experiments must be repeated with additional donors in order to conclude that these cytokines are not required for training in our model.

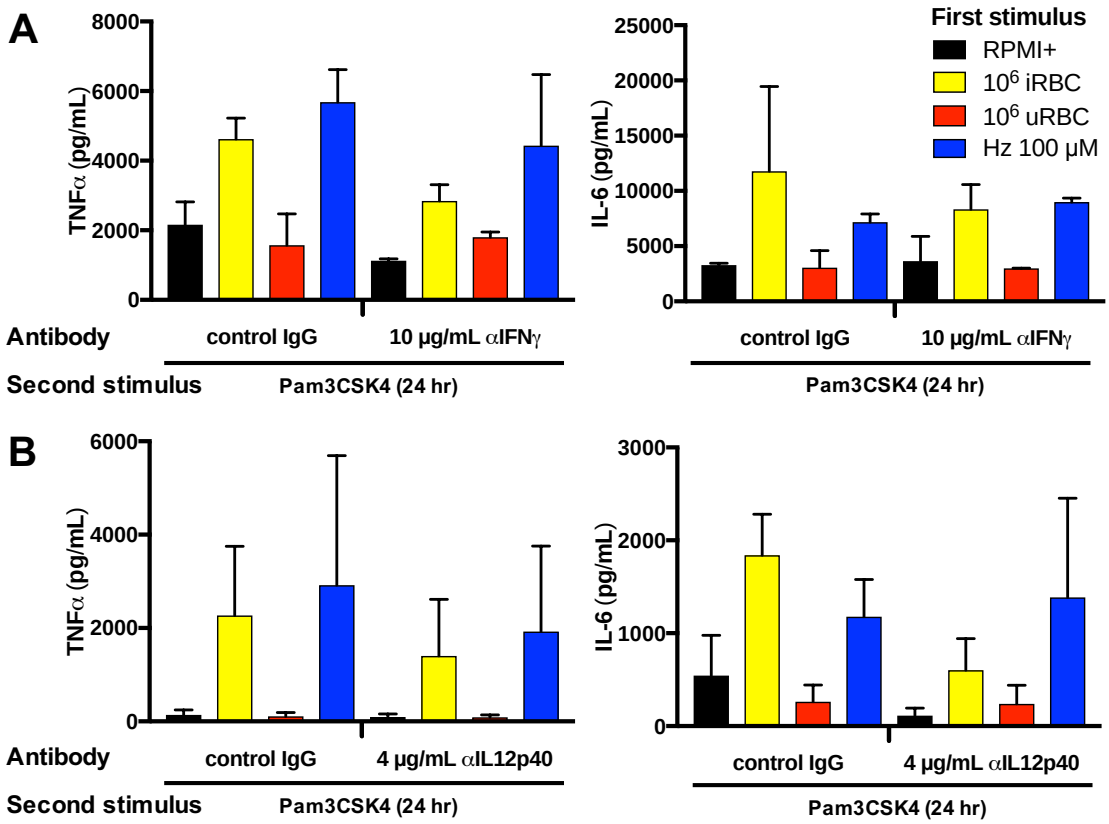

Figure 4.11. Malaria-induced training does not appear to be inhibited by co-treatment with anti-IFNγ or anti-IL12p40 neutralizing antibodies. (**A, B**) TNFα and IL-6 ELISA measurements of supernatants from adherent PBMCs trained with iRBCs or Hz for 24 h, rested for 3 d, and challenged with Pam3CSK4 for 24 h. Cells were treated with control IgG or cytokine neutralizing antibody during the 24 h training stimulus (A) or throughout the entire 5 d experiment (B). Bars represent mean ± SEM for two donors (all comparisons to control IgG conditions and were not significant, paired *t*-test).

Differential epigenetic and metabolic regulation of malaria-induced trained immunity

Trained immunity is believed to be the result of intracellular metabolic shifts leading to changes in epigenetic regulation of proinflammatory and other genetic loci [reviewed in (150)]. To determine the role of naturally-acquired malaria infection on epigenetic remodeling at proinflammatory and metabolic promoters, we performed H3K4me3 ChIP on monocytes isolated from Kenyan children with acute febrile malaria, the same children PCR negative for malarial infection 6 weeks after antimalarial treatment, and healthy adult North American controls (Fig. 4.12A). Increased H3K4me3 was seen at the *TNF*, *IL6*, *MTOR*, and *GAPDH* promoters during acute malaria compared to healthy controls. These increased H3K4me3 levels were largely unchanged six weeks after antimalarial treatment. We performed a similar experiment using our *in vitro* model on adherent PBMCs given a 24 h first stimulation and then allowed to rest for three days. Similar to the increased number of transcripts for *TNF*, *PTGS2*, and *IL6* after both iRBC- and Hz-induced training (Fig. 4.6D), increased H3K4me3 was seen at the same promoters after iRBC (but not Hz) training as compared to RPMI+ training (Fig. 4.12B).

We utilized the methyltransferase inhibitor MTA as well as the mTOR inhibitor rapamycin, which have previously been demonstrated to inhibit BCG-induced training (96) and *C. albicans* β-glucan-induced training (102), respectively, to investigate the importance of these mechanisms in malaria-induced training. Treatment with 1 mM MTA during the 24 h first stimulation had no effect on iRBC-induced training (Fig. 4.12C). MTA treatment appeared to inhibit Hz-induced training, although this did not achieve statistical significance, presumably due to the relatively small sample size. Conversely,

treatment with 10 nM rapamycin during the 24 h first stimulation blocked iRBC-induced training as measured by IL-6 protein production but had no effect on malarial training as measured by TNFα protein levels (Fig. 4.12D).

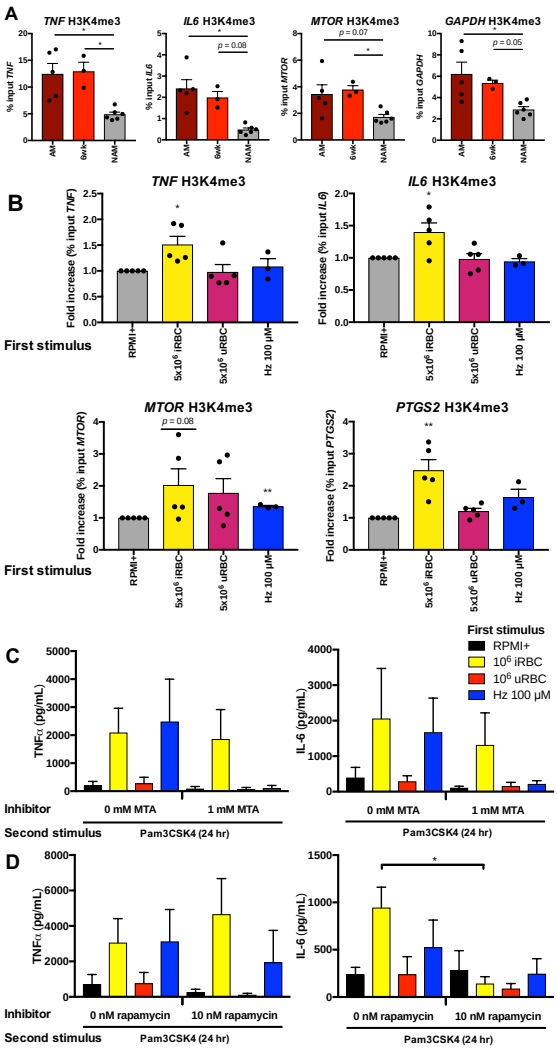

Figure 4.12. Epigenetic and metabolic regulation of malaria-induced training. (**A**) H3K4me3 ChIP was performed on monocytes isolated from Kenyan children with acute malarial disease (AM), the same children 6 weeks after antimalarial administration (6wk), or adult North American controls (NAM). Bars represent mean ± SEM for five (AM), three (6wk), or six (NAM) donors (*p<0.05, Kruskal-Wallis test). (**B**) H3K4me3 ChIP was performed on adherent PBMCs trained for 24 h and rested for 3 d. Bars represent mean ± SEM for five (RPMI+, iRBC, uRBC) or three (Hz) donors (all comparisons to RPMI+ trained, *p<0.05, **p<0.01, paired *t*-test) (**C, D**) Adherent PBMCs were co-treated with the methyltransferase inhibitor MTA (C), the mTOR inhibitor rapamycin (D) or relevant vehicle controls during the 24 h training stimulation. Cells were rested for 3 d and challenged with Pam3CSK4 for 24 h, after which supernatants were removed and cytokine concentrations were assessed by ELISA. Bars represent mean ± SEM for three or four donors (all comparisons to no inhibitor conditions and were not significant unless indicated, paired *t*-test).

Discussion

Malaria is an extraordinarily complicated disease. Individuals from endemic regions of the world have a clinical syndrome that is influenced by age and previous exposures. Young children who have little or no immunity to malaria are at highest risk for acute febrile disease that may be complicated by cerebral disease or other severe sequelae (13). This corresponds with our findings that Kenyan children have increased H3K4me3 at promoters relevant to inflammation and immunometabolism both during acute malaria and 6 weeks post-curative therapy as compared to healthy North American adult controls. Given that monocyte H3K4me3 levels are higher in adults than neonates at both proinflammatory and metabolic promoters (165), we expect monocytes from healthy adults to have higher baseline H3K4me3 levels than monocytes from healthy children. These data further support our hypothesis that malarial infection serves as a robust priming and training stimulus, and these children are most likely to hyperrespond to infection in ways that might be predicted based on the *in vitro* responses we have described above.

Older children and adults from endemic areas are likely to have experienced multiple episodes of malaria within their lifetime. These individuals will often have detectable parasitemia but no fever or other symptoms of disease (152). While the level of parasitemia in these asymptomatic malaria cases might be quite low (presumably due to acquired immunity), it is not uncommon for individuals to have levels of parasites in the blood that would require urgent treatment in the immunologically naïve. It is our hypothesis that the differences in outcome in disease between young individuals or

immunologically mature individuals who become infected for the first time later in life (*e.g.*, travelers) compared to multiply infected individuals, are to some extent due to epigenetic changes at proinflammatory and immunometabolic promoters.

In this work, we demonstrated that the malaria parasite and its crystal Hz can induce trained immunity as measured by proinflammatory gene expression after a secondary TLR ligand challenge. Although these two stimuli have similar effects on the inflammatory transcriptome post-Pam3CSK4 challenge, the differential regulation of iRBC- and Hz-induced training by known trained immunity inhibitors and differing levels of H3K4me3 at immunometabolic promoters indicate potentially divergent training mechanisms for the two stimuli. One potential explanation for this divergence is that the malaria parasite contains multiple additional ligands with innate immune stimulatory capacity. *P. falciparum* RNA is known to stimulate TLR7 (88), while GPI anchors in the parasite cell membrane can stimulate TLR2 (46). Although these TLRs utilize the same signaling cascades and transcription factors as the receptors stimulated by Hz, the balance in signaling between the cascades may be sufficiently different to explain these differences. For example, *IRF3* and *NFKB1*, but not *IRF7*, transcript levels are downregulated by malaria training (data not shown).

Rapamycin treatment only inhibited training as measured by IL-6 and not TNFα, which differs from previous studies on other training stimuli (102, 103). Given that the *TNF* and *IL6* loci have different initiation kinetics and epigenetic requirements for transcription (166), this discrepancy in rapamycin inhibition is not completely surprising, but this finding, along with the apparent dispensability of IFNγ signaling for malaria

training, provides further evidence that both malaria parasites and Hz induce innate immune training by mechanisms that differ from those described to date. Any hope for immunomodulation of malaria, either for the purposes of improving outcome in the critically ill or enhancing acquired immunity to the disease by immunization, requires a more thorough understanding of the basic pathogenesis of the disease. The methods for acquiring this understanding are at hand, and hence one can anticipate an era of improved approaches to reduce the morbidity and mortality of malaria.

Chapter V: Discussion

The work described in this dissertation attempted to answer two outstanding questions in the subfield of innate immune recognition of malaria:

1. **What is mechanism by which monocytes and macrophages recognize *P. falciparum* genomic DNA in the cytosol?**
2. **Does stimulation of monocytes and macrophages with *P. falciparum* induce innate immune memory?**

The experiments described in Chapter III of this dissertation demonstrate that the cytosolic DNA receptor cGAS is required for detection of *P. falciparum* gDNA in the cytosol of both human and mouse cells, and that the resulting production of 2'3'-cGAMP activates STING, leading to the phosphorylation of IRF3 and the transcription and translation of IFN-I. In Chapter IV of this dissertation, we demonstrated that stimulation of adherent PBMCs with *P. falciparum* iRBCs and Hz induces these cells to hyperrespond to a secondary TLR ligand challenge. We showed that this increased proinflammatory response to secondary TLR challenge included the increased production of proinflammatory cytokines and depressed production of an anti-inflammatory cytokine. We also demonstrated that training with malarial ligands induced widespread changes to the proinflammatory transcriptome after Pam3CSK4 second stimulus, and that these changes in transcription correlated with increased H3K4me3 marks at promoters of genes previously implicated in innate immune memory. We showed that these marks were also seen in Kenyan children naturally infected with malaria, and we generated preliminary data that began to tease apart the mechanism of this trained immunity. In the

rest of this discussion, I will examine each of these findings in more depth, draw conclusions about what they mean for the role of innate immunity in malaria sensing and pathogenesis, and indicate experiments that could strengthen these conclusions and move the projects in future directions.

The DNA receptor cGAS recognizes *P. falciparum* genomic DNA in the cytosol of monocytes and macrophages

Major results and conclusions

Plasmodial DNA has been recognized as an important PAMP for quite some time. Our group and others have demonstrated that *Plasmodium* DNA is sensed by TLR9 through delivery to the endosome by Hz (49, 50, 53). This DNA is complexed with malarial histones in the form of parasite chromatin (51, 52). Patients with febrile *P. falciparum* or *P. vivax* have increased levels of circulating immune complexes (ICs) containing parasite gDNA, and these ICs stimulate human monocytes to produce TNFα and other proinflammatory cytokines along with increased transcription of other NF-κB-dependent genes (119). Additionally, Hz is able to cause loss of phagolysosomal integrity, which allows DNA to escape into the cytosol, where it can be detected by the cytosolic DNA-sensing inflammasome protein AIM2 (53). Activated AIM2 inflammasomes, which are important for cleavage of pro-IL-1β into its active form, can also been seen in monocytes taken from patients with febrile *P. vivax* infection (119).

After escape from the phagolysosome, cytosolic gDNA can also trigger the production of IFN-I, and our group showed that this production of IFN-I by human PBMCs, HEK293, and THP-1 monocytes and mouse splenocytes and BMDMs was largely due to the recognition of AT-rich stem-loop structures in *P. falciparum* gDNA (55). In Figure 3.1, we demonstrate that purified human $CD14^+$ monocytes produce IFN-I in after stimulation with *P. falciparum* iRBCs or transfection with gDNA, Hz, and AT-rich DNA motifs, and in Figure 3.2, we show that IFN-I induction by Hz is abrogated by pretreatment of Hz with DNase.

In our previous work, BMDMs from various genetic knockouts or were used to demonstrate that this recognition of gDNA and the stem-loop motifs and the resulting IFN-I production required the adaptor protein STING, the kinase TBK1, and the transcription factors IRF3 and IRF7; however, further use of KO BMDMs and siRNA silencing of genes in human HEK293 demonstrated that this IFN-I production did not require the DNA sensors TLR9, RNA polymerase III, DAI, or p204 (55). Other potential DNA sensors that were not specifically evaluated in this earlier work include DDX41 (167), IFI16 (40), and cGAS (42, 43). Interestingly, all three of these cytosolic DNA sensors signal through STING, making them plausible receptors for *P. falciparum* gDNA in our model. In Figures 3.3 and 3.4, we conclusively show that cGAS is required for IFN-I production by *P. falciparum* gDNA. THP-1 human monocytes deficient in cGAS were not able to phosphorylate IRF3 or transcribe *IFNB* in response to transfection of *P. falciparum* gDNA or Hz. We also found that IFI16-deficient THP-1 human monocytes had no defect in their ability to recognize *P. falciparum* gDNA as measured by *IFNB*

transcription (Fig. 3.3). The role of IFI16 in cytosolic DNA recognition remains controversial. One recent study demonstrated that IFI16 has was required for cGAS-dependent IFN-I production after stimulation of THP-1 cells with dsDNA or viral ligands (168), while another study demonstrated that genetic deficiency of all 13 ALRs, including the mouse IFI16 ortholog p204, did not significantly affect IFN-I production induced by cytosolic DNA (169). In Figure 3.4, we demonstrate that cGAS is essential for production of IFNβ protein after transfection of AT-rich ODNs or *P. falciparum* gDNA into mouse BMDMs. In our previous work, we showed that knockdown of the mouse ortholog of IFI16, p204, did not inhibit IFNβ in response to transfection of AT-rich ODNs (55), and we found similar results with $p204^{-/-}$ BMDMs (data not shown). Therefore, we conclude that IFI16/p204 is not required for IFN-I production in response to Plasmodial DNA ligands, but cGAS is absolutely required. Finally, in Figure 5 we demonstrated that transfection of THP-1 cells or MDMs with *P. falciparum* gDNA induces the production of 2'3'-cGAMP, which has previously been described as the second messenger produced by cGAS that activates STING (44, 45).

Given the wealth of recent studies demonstrating the importance of cGAS in the immune response against a variety of pathogens, including HIV (144), herpes simples virus (HSV) (42), cytomegalovirus (CMV) (142), *Listeria monocytogenes* (146), *Neisseria gonorrhea* (122), *Mycobacterium tuberculosis* (170), and *Staphylococcus aureus* (171), it is perhaps not surprising that cGAS also recognizes *P. falciparum* gDNA. cGAS was originally described as a sensor that recognized dsDNA in a length-dependent, sequence-independent manner. In the original description of cytosolic DNA sensing by

Stetson and Medzhitov, they showed that 45 base pair (bp) double-stranded interferon-stimulatory DNA (ISD) induced a robust IFN-I response in mouse primary cells, but this IFN-I response was not seen to dsDNA sequences shorter than 25 bp (172) Other groups demonstrated IFN-I production by mouse and human cells after dsDNA sequences were delivered to the cytosol in a manner dependent on the dsDNA length, with the absolute minimum length required for induction of IFN-I production in human cells being between 20-40 bp (40, 173). Therefore, it is surprising that cGAS is required for recognition of the AT5 ODN, which is a mere 20 nucleotides long and single-stranded (55). Although the stem-loop structure of AT5 is required for its ability to induce IFN-I, the predicted double-stranded stem is only 4 bp long (55).

A recent paper in *Nature Immunology* may be able to explain the immunogenicity of the AT5 ODN. Herzner and colleagues demonstrated that step-loop DNA structures formed from the HIV-1 genome reverse-transcribed into ssDNA can activate cGAS (174). As they evaluated the mechanism by which these step-loop structures activated IFN-I production, they discovered that short dsDNA segments—as short as 12 bp—could induce IFN-I production when transfected into human PBMCs if the segments had three unpaired guanine residues adjoining the dsDNA segment in what the authors describe as Y-form short DNA (YSD)(174). As with AT5 ODN, induction of IFN-I production by YSD is dependent on cGAS/STING and is secondary to 2’3’-cGAMP synthesis; additionally, they used biotin-tagged YSD to demonstrate that cGAS bound to YSD but not to dsDNA of the same length (174). Although the loop formed by the putative secondary structure of AT5 ODN does not contain any guanine residues, the Y formed on

the other end of the 4 bp dsDNA segment contained three guanines on one end and two guanines on the other end (55). Additionally, lengthening the dsDNA segment of the YSD increased IFN-I production until the segment was 20 bp long, after which IFN-I production leveled off (174). In our data, we show that AT5 3x (a 60mer repeating the AT5 ODN sequence three times) induces increased *IFNB* transcription compared to AT5 in THP-1 cells, and this *IFNB* transcription is completely abrogated in cGAS-deficient THP-1 cells (Fig. 3.3C). This could be due to an increased dsDNA length or merely having three of the same Y-form structures connected in the same ODN. In either case, we tentatively conclude that cGAS is able to induce IFN-I production through the recognition of AT5 ODN.

Additional experiments and future directions

As stated in the title of this section of the discussion, we conclude that cGAS is the cytosolic receptor for *P. falciparum* gDNA and that cGAS/2’3’-cGAMP/STING signaling is required for IFN-I production in response to stimulation with cytosolic Plasmodial DNA. We also show provide strong evidence supporting cGAS as the sensor for AT-rich stem-loop ODNs like AT5; however, we could support this conclusion by creating a biotinylated version of AT5 and using a pull-down assay to determine if cGAS is able to bind AT5. We could also utilize biotinylated AT5 3x and dsAT5 4x to determine if the increased IFN-I transcription after transfection of these sequences was due to an enhanced ability to bind cGAS. To further demonstrate that AT5 and its derivatives activate cGAS to produce 2’3’-cGAMP, we could repeat the LC-MS/MS

experiment described in Figure 3.5 on supernatants from THP-1 cells transfected with AT5.

In this work, we demonstrated that IFN-I production by human and mouse monocytes and macrophages in response to Plasmodium DNA ligands required cGAS. Additionally, we showed that transfection of Hz induced IFN-I in a dose-dependent manner. This IFN-I production also required cGAS and was completely abrogated by DNAse treatment, indicating that the role of Hz in this IFN-I induction was really that of a DNA shuttle (53). What this work did not show was a definitive requirement for cGAS in iRBC-driven IFN-I production. We stimulated cGAS-competent and cGAS deficient THP-1 cells with iRBCs, but were unable to measure *IFNB* transcription (data not shown). Even though we use PMA to differentiate the THP-1 cells into macrophage-like cells, we did not see robust phagocytosis of iRBCs or Hz (J.E.S., unpublished observation). Presumably, this inability to phagocytose malaria or its products prevented delivery of *P. falciparum* gDNA to the cytosol for recognition by cGAS—hence the requirement for transfection of Hz.

As described in Figure 4.1A, stimulation of $CD14^{+}$ monocytes with iRBCs induces *IFNB* transcription; however, as elucidated in the introduction, *P. falciparum* can induce IFN-I expression through multiple PAMP-PRR interactions. There are a few tools that could be used to illuminate the role of cGAS in IFN-I production in response to iRBC stimulation. Future experiments could use genetic knockouts of other cell lines, such as the BLaER1 cells described in Figure 4.7. CRISPR-Cas9 technology has already been utilized to make multiple knockout lines from these cells (124). Mouse BMDMs

could also be used, but they produce little to no IFN-I after stimulation with *P. falciparum* iRBCs (data not shown). If primary cells are preferred, siRNA knockdown of cGAS in human $CD14^+$ monocytes could be attempted. Although transfection of human primary phagocytic cells has traditionally been difficult, a protocol purporting efficient siRNA gene knockdown in monocytes was recently published (175). Small molecule inhibition of cGAS would be another possible way to demonstrate the role of cGAS in iRBC sensing. Interestingly, multiple antimalarial drugs, including chloroquine, hydroxychloroquine, and primiquine, block DNA binding to cGAS and inhibit *IFNB* expression in THP-1 cells transfected with DNA (176); however, an antimalarial drug would not be the best choice to investigate cGAS activation by malaria parasites. In fact, Shizuo Akira's group demonstrated over a decade ago that chloroquine blocked Hz-mediated cytokine production (50). An indirect method for demonstrating the role of cGAS in recognizing *P. falciparum* iRBC would be to repeat the experiment described in Figure 3.5 by stimulating $CD14^+$ monocytes with iRBCs and utilizing LC-MS/MS to look for production of 2'3'-cGAMP.

The next question that needs to be addressed is the role of the cGAS/2'3'c-GAMP/STING in malaria immunity and disease. Our group has previously shown that PBMCs and neutrophils taken from patients naturally infected with malaria show increased expression of ISGs, indicating that production of IFN-I is involved in the acute response to malaria (55, 134). Given our group's access to clinical malaria patients in Columbia and Brazil, we are currently collecting serum samples from patients for future LC-MS/MS analysis to look for 2'3'-cGAMP. This would provide strong evidence for

cGAS activation in human disease. An alternative method for implicating cGAS in malarial disease *in vivo* is the use of one of the malaria mouse models. The *P. chaubaudi* model has been used to demonstrate the necessity of various cell types and PRRs for malaria-induced IFN-I production (87, 88), while *P. yoelii* N67 infection in mice induces cytosolic RNA sensor-dependent IFN-I production that is necessary for controlling parasitemia (177). As described in the introduction, IFN-I production is detected in mice infected with the ECM-inducing PbA species, and mice deficient in the IFN-I receptor are protected from ECM (85, 86). Our group has shown that TBK1- and IRF3/7-deficient mice are also spared from ECM lethality (55), and we hypothesize that the requirement for these molecules in ECM pathogenesis is due at least in part to their downstream activation after stimulation of the cGAS/2'3'cGAMP/STING axis in PbA infection.

Stimulation of adherent PBMCs with *P. falciparum* parasites or Hz induces trained innate immunity

Major results and conclusions

As described in Chapter I of this dissertation, the naturally-acquired immune response to malaria is complex. Those most at risk for severe outcomes from malarial infection are individuals whose immune systems have not been exposed to the parasite—such as infants in endemic areas and adults from non-endemic areas—or individuals who had developed natural immunity to malaria while living in an endemic area, moved to a non-endemic area for a period of years, and then are re-exposed to malarial infection. When the immune system encounters malarial parasites for the first time, a priming effect is

seen, and the immune system is hyperresponsive to a secondary challenge experienced during acute infection (106, 107). However, if the infection is allowed to progress and patients have multiple febrile paroxysms without sterilizing antimalarial treatment, their immune system can become hyporesponsive to subsequent innate immune challenge, as seen in historical studies examining the immune response to bacterial products after infection with malaria as treatment for neurosyphilis (115). Tolerance to malaria can also develop after experiencing multiple infections, as the parasite burden required to initiate fever increases with multiple infections (151), and many healthy individuals in endemic areas are infected with *P. falciparum* for weeks or even months with no fever or other symptoms (152). Given that priming and tolerance are two stages of the recently described model of innate immune memory (97), we hypothesized that malaria could also induce trained innate immunity; that is, stimulation with malaria could induce the innate immune system to hyperrespond to a later secondary challenge. To our knowledge, the results described in Chapter IV of this dissertation represent some of the first evidence in favor of trained innate immunity induction by *P. falciparum*.

We have developed a robust, reproducible *in vitro* assay in which pretreatment of adherent human PBMCs with *P. falciparum* iRBCs or Hz, followed by removal of these ligands and a rest period, induces these cells to hyperrespond to subsequent TLR stimulation. In Figure 4.1, we demonstrate that adherent PBMCs taken from leukapheresis products and trained with *P. falciparum* products produced increased proinflammatory cytokines after three or five days' rest to a secondary TLR stimulus. Overall, the effect of malarial training appeared more robust at three days' rest, so we

used that time point for the rest of our experiments. In Figure 4.2, we showed that malaria-induced training appeared to depend on the presence of multiple cell types, as monocytes alone did not display trained immunity; in fact, iRBC primary stimulation appeared to induce tolerance to subsequent LPS stimulation (Fig. 4.2D).

Given the drawbacks of using leukapheresis products, we shifted our model to using adherent PBMCs from blood freshly drawn in-house from healthy human donors. We demonstrated that malaria-induced training was reproducibly seen in adherent PBMCs from an individual donor drawn multiple times over a thirteen-month period (Fig. 4.3). We then expanded our donor pool and demonstrated that training with *P. falciparum* iRBCs or Hz induced increased TNFα and IL-6, but decreased IL-10 post-Pam3CSK4 challenge (Fig. 4.4 and 4.5). This differs slightly from the original description of trained immunity to *Candida albicans*, in which pretreatment with *C. albicans* and secondary challenge with Pam3CSK4 induced increased TNFα and IL-6, but had no effect on IL-10, as compared to control-trained cells (95). Given that IL-10 is produced at extremely high levels during malaria infection, especially severe malaria (178), while IL-10 is decreased during *in vitro* malaria-induced priming (106), I conclude that this decreased production of IL-10 after malaria training and TLR2 challenge represents immunomodulation by malarial ligands and not merely a synergistic effect between malaria ligands and Pam3CSK4 stimulation. We also demonstrated that malarial training induces wide-ranging changes to the inflammatory transcriptome post-Pam3CSK4 challenge (Fig. 4.6).

In order to broaden the scope of our *in vitro* assay, we attempted to replicate our results from human adherent PBMCs with two human immortalized monocyte-like cell lines, BLaER1 cells (124, 159) and THP-1 cells, and two different types of mouse primary cells, BMDMs and non-thioglycolate-elicited PECs. Our hope was that, by replicating our results in a cell line or mouse primary cells, we could use CRISPR-Cas9 or other genetic manipulation techniques to probe the PRR requirements for our training phenotype. We found increased production of TNFα and IL-6 after training with 10^6 iRBCs and LPS challenge in BLaER1 cells (Fig. 4.7B, C), but not after challenge with Pam3CSK4 (Fig. 4.7D), the secondary stimulus that gave us the most robust results in the human adherent PBMC assay. We also failed to see training or tolerance induction in THP-1 cells (Fig 4.8). In mouse BMDMs, we saw significant increase in TNFα after training with Hz/challenge with Pam3CSK4 (Fig. 4.9A) and RANTES after training with iRBCs and challenge with Pam3CSK4 or LPS (Fig. 4.9B). Interestingly, RANTES was highly expressed in Flt3 ligand-derived dendritic cells in a TLR9-dependent manner after stimulation with *P. falciparum* gDNA delivered to the endosome by Hz (49); however, training with various concentrations of Hz did not induce increase RANTES expression post-Pam3CSK4 or LPS challenge (Fig. 4.9B). Mouse PECs, on the other hand, after pretreatment with PbA iRBCs for 36 hours and three days' rest, produced significantly less TNFα after challenge with Pam3CSK4 and LPS as compared to control-pretreated cells (Fig. 4.9C).

There are few potential explanations for these seemingly conflicting results in mouse primary cells of training to iRBCs in BMDMs but tolerance in PECs. First, the

ligand usage was slightly different: *P. falciparum* iRBCs and Hz were used in BMDMs, while PbA iRBCs were used in PECs. As mentioned earlier, PbA infection in mice is used in the ECM model, which attempts to mimic CM in *P. falciparum* infection, but the diseases are not identical. One of the major arguments over the ECM model and its relevance to human disease is the role of the immune system in pathogenesis—it is absolutely required in PbA ECM, but its role is disputed in human CM [see Chapter I and (179, 180)]. This could indicate that PbA is more immunogenic—at least in mouse primary cells—than *P. falciparum*. Additionally, in our PEC experiment, we stimulated the cells with $2.4x10^6$ PbA iRBCs for 36 hrs instead of the usual 10^6 *P. falciparum* iRBCs for 24 hrs. Previous work in the field of innate immune memory has shown that increasing the dose of a stimulus can shift its effect from training to tolerance (105, 181), so this could play a role. Finally, BMDMs and PECs have different activation levels at baseline. PECs express significantly higher levels of *Tnf*, *Il6*, *Ptgs2*, *Ifnb1*, and *Il12a*—all genes previously discussed in this dissertation to be involved in malaria recognition and/or innate immune memory—than BMDMs before any stimulation (182). Increased expression of proinflammatory genes at baseline could cause PECs stimulated with PbA iRBCs to become activated to the point of tolerance induction rather than training.

Many early studies demonstrating trained immunity also utilized adherent PBMCs (95, 96, 105). We presumed that the adherent PBMCs would be primarily monocytes, as purities of ~90% monocytes from isolation through adherence have been reported (121). Surprisingly, we noticed almost no enrichment for monocytes after allowing the PBMCs to adhere in 96-well round-bottom plates for at least 1 h (Fig. 4.10B). As mentioned

previously, we noticed differences in cell numbers after training with different ligands. After looking more closely at the cells, we also noticed training ligand-dependent differences in cell morphology (Fig. 4.10A). To determine if there were differences in cell type proportions after training, we performed flow cytometric analysis on the remaining adherent PBMCs after the first stimulus and three-day rest. To our surprise, adherent PBMCs trained with iRBCs or Hz had increased numbers of $CD14^+$ monocytes compared to control-trained populations (Fig. 4.10C). Throughout our experiments, we utilized a MTS assay to normalize all cytokine values to cell number (see Chapter II). For all experiments in which we evaluated the trained cell population using flow and performed secondary stimulation, we normalized cytokine production to the ratio of $CD14^+CD45^+$ cells: $CD14^-CD45^+$ cells. The results of this normalization technique were almost identical to the results for the MTS normalization technique (Fig. 4.10D); therefore, it appears that the differences in cell numbers after training of adherent PBMCs is largely due to an overrepresentation of $CD14^+$ macrophages, and that even after normalizing for cell number—which appears to be due primarily to differences in macrophage cell number—we still see significant differences in cytokine production between malaria-trained adherent PBMCs and control-trained adherent PBMCs.

Given that there is a significant population of non-monocyte adherent PBMCs present during training (Fig. 4.10B) and malaria-induced training was not seen in negatively-selected monocytes (Fig. 4.2), we hypothesized that the requirement for non-monocyte cells was due to IFNγ production by NK cells or T cells (164). Surprisingly, there appeared to be no difference in training when the adherent PBMCs were treated

with neutralizing antibodies against IFNγ or the IL-12p40 subunit; however, these experiments were only performed on adherent PBMCs from two donors (Fig. 4.11). These results will be analyzed in further detail in the next section of this discussion.

The current paradigm for trained immunity holds that this phenomenon is at least in part epigenetically mediated. Concurrent with this model, we found increased H3K4me3 at important proinflammatory and metabolic promoters in our *in vitro* trained adherent PBMCs (Fig 4.12B). We also found increased H3K4me3 at these promoters in monocytes isolated from Kenyan children naturally infected with malaria and 6 weeks after sterilizing antimalarial treatment as compared to North American adult controls (Fig. 4.12B). The fact that these differences were seen in monocytes in infected Kenyan children lends support to the conclusions that a) the training phenotype seen in our *in vitro* model is due at least in part to monocytes, and b) that this training phenotype may be seen in naturally-acquired malarial disease. Finally, we found that co-treatment of adherent PBMCs with the methyltransferase inhibitor MTA appeared to abrogate Hz-induced training while not affecting iRBC-induced training (Fig 4.12C), while use of rapamycin as an inhibitor appeared not to have an effect on malaria-induced training as measured by TNFα, but significantly inhibited iRBC-induced training when measuring IL-6 (Fig. 4.12D). If these results are corroborated through further experimentation (see below), they could indicate that malaria induces training of the innate immune system through a novel mechanism.

Additional experiments and future directions

One of the most obvious actions we can take to strengthen the conclusions made in this work is to increase the numbers of donors tested, especially for some of the mechanistic experiments where large changes were seen, but the number of donors tested was too small to achieve statistical significance. I include the data showing differences between adherent PBMCs and monocytes (Fig 4.2), and the rapamycin and MTA inhibition studies in this group (Fig. 4.12C and D). However, I believe those trends are large enough that they will become statistically significant after increasing the number of donors tested.

The biggest caveat to the work presented in Chapter IV is that the trained immunity assay was primarily performed using adherent PBMCs. For this to be considered innate immune memory, we must demonstrate that the phenotype is due to innate immune cells. It is completely reasonable—and perhaps advantageous—for the training stimulus to occur in a heterogeneous population containing both innate and adaptive cells; after all, very few humans contracting malaria have completely deficient adaptive immune systems. However, our conclusions would be strengthened if we could more definitively show that the hyperresponsiveness to secondary challenge in our assay is due to an innate immune response, presumably increased cytokine production by the $CD14^+$ monocyte/macrophage compartment. Based on the fact that increased levels of proinflammatory cytokines are seen as a result of malarial training even after normalizing for cell number and the ratio of $CD14^+CD45^+$ cells/$CD14^-CD45^+$ cells present at the time of secondary stimulation (Fig 4.10D), I conclude that the phenotype seen in this assay

represents trained innate immunity. To confirm that the increased proinflammatory cytokine production after challenge is actually due to hyperresponsiveness of the innate compartment of the adherent PBMCs, further experiments are warranted.

Based on our hypothesis of epigenetic modifications at proinflammatory promoters, I expect that each trained macrophage should produce increased amounts of TNFα and IL-6 after secondary Pam3CSK4 challenge. This could be demonstrated by performing intracellular cytokine staining using florescent antibodies against these cytokines. We attempted this experiment, but had issues with the autofluorescence of phagocytosed Hz in the trained cells (data not shown). We are currently troubleshooting ways to get around this autofluorescence, but if we are unable to do so, another option would be to perform the training stimulation and three-day rest with adherent PBMCs and then separate the $CD14^+$ myeloid cells from the rest of the adherent PBMCs just before secondary challenge. Magnetic separation would be one way to do this, but it would have to utilize positive selection, as many of the trained macrophages still contain Hz in their lysosomes and/or cytoplasm and would thus be retained during magnetic separation (data not shown). In our trained immunity experiments on monocytes, we utilized negative selection in an effort to disturb the cells as little as possible before training; however, this positive selection would occur directly before secondary stimulation, so any inadvertent stimulation or physical disturbance of the cells as a result of the antibodies utilized for positive selection would have little time to affect the assay.

Another major caveat to our work related to the use of adherent PBMCs is that we did not control for potential changes in adherent PBMC composition when looking at

mRNA expression or epigenetic changes. As stated previously, it appears that our utilization of a MTS assay for cytokine normalization controls for changes in relative $CD14^+$ cell numbers within the adherent PBMC population, but we do not have a similar compensation mechanism for our other data. The mRNA expression data and ChIP data are normalized to cell number by using housekeeping genes and percent input, respectively, but the differences seen between training stimuli could conceivably be due merely to changes in the adherent PBMC composition, such as increased relative numbers of macrophages. However, the fact that increased H3K4me3 at proinflammatory promoters is seen in monocytes isolated from children with uncomplicated malaria and 6 weeks after sterilizing treatment (Fig. 4.12A) support our conclusion that the increase in H3K4me3 seen in our *in vitro* model is at least partially monocyte-dependent. Again though, the H3K4me3 levels in monocytes from Kenyan pediatric malaria patients were compared to healthy North American adults. Although previous studies indicate that H3K4me3 levels, particularly at proinflammatory promoters, are positively correlated with age (165), it is possible that monocytes from Kenyan children have higher baseline H3K4me3 levels than those from North American adults. An optimal control would be age-matched, malaria-naïve Kenyan children from the same community, but the prevalence of malaria in Kisumu Country drastically decreases the odds of finding such controls (183).

The above paragraphs focus on experimental methodologies to evaluate the importance of the $CD14^+$ monocyte/macrophage compartment to the training phenotype seen in this work. As shown in Figure 4.2, stimulating negatively selected monocytes

with malarial ligands does not appear to induce increased cytokine production after secondary TLR stimulation; therefore, another related question is what cell type(s) is(are) required during the training stimulation. To answer this question, we can utilize magnetic separation to selectively deplete other cell types, such as $CD3^+$, $CD19^+$, or $CD56^+$ cells, from PBMCs before adherence and then perform the trained immunity assay. Once we find that cells expressing one or more of these markers are required for trained immunity, we can then use additional cell markers, such as αβ vs γδ T-cell receptors (TCRs) to determine the exact cell population(s) required for the malaria-induced training phenotype.

If by using selective depletion of cell types from the parent PBMC population we can determine which cell types are required for malaria-induced trained immunity, we can then use transwell assays to determine if direct cell-cell contact between different cell types is required for the training phenotype. There is already evidence for direct contact as a requirement for cytokine production in malaria stimulation experiments. For example, an early study examining the production of TNFα by PBMCs in response to 24 h stimulation with *P. falciparum* iRBCs demonstrated that PBMCs depleted of $CD3^+$ cells produced lower levels of TNFα than the parent PBMC population (184), indicating synergy between $CD3^+$ and $CD14^+$ cells in producing TNFα. Experiments from Eleanor Riley's group revealed that robust IFNγ production by NK cells requires direct contact with other cell types present in PBMCs, presumably cells from the myeloid compartment (185).

Another possibility is that direct contact between different cell populations is not required, but that a soluble factor from a non-macrophage cell is required for trained immunity. The most obvious candidate for this soluble factor is a cytokine. As described earlier, trained immunity to *Candida albicans* required IFNγ from T cells or NK cells (164). In Figure 4.11, we presented data indicating that IFNγ-dependent signaling during the 24 h training period may not be required for malaria-induced trained immunity. In addition to repeating the neutralization antibody experiments in Figure 4.11, it would also strengthen our conclusion if we confirmed that the concentration and duration of neutralization antibody treatment were sufficient to truly neutralize the cytokine. We used similar concentrations to those that were recommended by the manufacturer or published previously (164), but we did not confirm complete cytokine neutralization. Neutralization of IL-12 could be evaluated by performing an IFNγ ELISA on the cell supernatants after anti-IL-12p40 antibody treatment. To confirm neutralization of all IFNγ, we could utilize a MHC II expression assay in human COLO-205 cells (186).

Multiple cell types have been demonstrated to produce IFNγ within the first 24 hrs of exposure to malaria. As mentioned in Chapter IV, IFNγ is produced by NK cells in as little as 6 hrs after initiating exposure to iRBCs, and that this IFNγ production is IL-12 and IL-18 dependent, but that this IL-18 production by macrophages is TLR2-independent (187). Another group demonstrated that γδ T cells produce IFNγ after 18 h of iRBC stimulation (188), and this production of IFNγ by γδ T cells is optimally induced by live iRBCs rather than killed iRBCs (189). When γδ T cells are depleted from PBMCs

before stimulation with iRBCs for 24 hrs, the majority of IFNγ production is lost, indicating that γδ T cells are the primary IFNγ-producing cells at this time point (190). Interestingly, both the number of Vδ2+ γδ T cells and the percentage of these cells producing TNFα and IFNγ decrease as an individual experiences increased malarial infections, leading to speculation that this phenomenon may play a role in malarial tolerance (191). An early study demonstrated that PBMCs stimulated with iRBCs produced large amounts of IFNγ but low levels of IL-12, and that transcript levels of *IFNG* remained high even after 48 hrs of stimulation (184). This raises the question of whether we used sufficient concentrations of neutralizing anti-IFNγ antibody or if the co-administration only during the 24 h first stimulation—and not throughout the entire duration of the assay—was sufficient to block all IFNγ, as the adherent PBMCs could be continuing to produce IFNγ even after extracellular iRBCs or Hz are removed by washing.

The previous pages in this section have discussed technical caveats to our findings: increasing sample size, confirming that the training phenotype is due to innate immune cells, and determining what other cell types/interactions are required for the training phenotype. However, the more philosophical caveat that can be made about this work concerns the definition of memory: does this assay, in which the majority of the training phenotype is seen with a three-day rest, really constitute memory?

In two of the early studies to demonstrate trained immunity in human adherent PBMCs, the rest period between the training stimulus and the secondary challenge was six days (95, 96). For one of the training stimuli utilized in these papers, the BCG

vaccine, it was shown that the training effects of BCG in vaccination of human subjects could last up to one year after vaccination (192). Indeed, in the 2011 *Cell, Host, and Microbe* paper in which they coin the phrase "trained immunity", Mihai Netea and colleagues point to epidemiological studies demonstrating the protective effect of BCG vaccination on all-cause mortality as *in vivo* evidence for trained immunity (97). In a later study, Netea and colleagues explore the effect of rest duration on trained immunity *in vitro* for a variety of training stimuli (193). In general, they find that rest periods of one, three, or six days have little effect on the training phenotype; however, for 24 hrs of BCG training and a secondary challenge of Pam3CSK4, there is significantly more IL-6 production compared to control-trained cells when the rest period is three days rather than 6 days (193). This finding mirrors our results using 10^5 iRBCs as a training stimulus: significantly increased IL-6 was seen after a three-day rest and Pam3CSK4 challenge, but not after five-day rest and Pam3CSK4 challenge (Fig. 4.1B). Also, our data using monocytes from Kenyan pediatric malaria patients indicate that increased H3K4me3 seen at proinflammatory promoters during acute malarial infection is also seen 6 weeks after initiation of curative treatment (Fig. 4.12A). These results support the conclusion that malarial trained immunity is a form of innate immune memory.

To summarize, in this work we demonstrate that cGAS is the cytosolic DNA sensor that recognizes *P. falciparum* DNA ligands. We also demonstrate that *P. falciparum* can induce trained innate immunity in an *in vitro* model and provide correlative evidence that this training phenotype is also seen during naturally acquired malarial infection. Given that malaria-induced IFN-I production has been demonstrated

to have immunomodulatory effects on both innate and adaptive immune cells (82, 83, 86, 134, 194, 195) it is tempting to speculate that IFN-I production by cGAS-dependent recognition of *P. falciparum* cytosolic DNA ligands could play a role in the trained innate immunity induced by malarial infection. Preliminary experiments utilizing *P. falciparum* gDNA and AT-rich ODN as priming stimuli are currently underway. As is often the case in scientific inquiry, more studies are needed.

References

1. World Health Organization. 2017. World Malaria Report 2016. 1–186.
2. White, N. J., S. Pukrittayakamee, T. T. Hien, M. A. Faiz, O. A. Mokuolu, and A. M. Dondorp. 2014. Malaria. *Lancet* 383: 723–735.
3. Aly, A. S. I., A. M. Vaughan, and S. H. I. Kappe. 2009. Malaria Parasite Development in the Mosquito and Infection of the Mammalian Host. *Annu. Rev. Microbiol.* 63: 195–221.
4. World Health Organization, Communicable Diseases Cluster. 2000. Severe falciparum malaria. *Trans. R. Soc. Trop. Med. Hyg.* 94 Suppl 1: S1–90.
5. Marsh, K., D. Forster, C. Waruiru, I. Mwangi, M. Winstanley, V. Marsh, C. Newton, P. Winstanley, P. Warn, and N. Peshu. 1995. Indicators of life-threatening malaria in African children. *N. Engl. J. Med.* 332: 1399–1404.
6. Miller, L. H., H. C. Ackerman, X.-Z. Su, and T. E. Wellems. 2013. Malaria biology and disease pathogenesis: insights for new treatments. *Nature Medicine* 19: 156–167.
7. Idro, R., K. Marsh, C. C. John, and C. R. J. Newton. 2010. Cerebral Malaria: Mechanisms of Brain Injury and Strategies for Improved Neurocognitive Outcome. *Pediatr Res* 68: 267–274.
8. White, N. J., White, N. J., G. D. H. Turner, G. D. H. Turner, N. P. J. Day, N. P. J. Day, A. M. Dondorp, and A. M. Dondorp. 2013. Lethal Malaria: Marchiafava and Bignami Were Right. *J. Infect. Dis.* 208: 192–198.
9. Taylor, T. E., W. J. Fu, R. A. Carr, R. O. Whitten, J. S. Mueller, N. G. Fosiko, S. Lewallen, N. G. Liomba, M. E. Molyneux, and J. G. Mueller. 2004. Differentiating the pathologies of cerebral malaria by postmortem parasite counts. *Nature Medicine* 10: 143–145.
10. Silamut, K., Silamut, K., N. H. Phu, N. H. Phu, C. Whitty, C. Whitty, G. D. Turner, G. D. H. Turner, K. Louwrier, K. Louwrier, N. T. Mai, N. T. H. Mai, J. A. Simpson, J. A. Simpson, T. T. Hien, T. T. Hien, N. J. White, and N. J. White. 1999. A Quantitative Analysis of the Microvascular Sequestration of Malaria Parasites in the Human Brain. *The American Journal of Pathology* 155: 395–410.
11. Patnaik, J. K., B. S. Das, S. K. Mishra, S. Mohanty, S. K. Satpathy, and D. Mohanty. 1994. Vascular clogging, mononuclear cell margination, and enhanced vascular permeability in the pathogenesis of human cerebral malaria. *Am. J. Trop. Med. Hyg.* 51: 642–647.
12. Gupta, S., R. W. Snow, C. A. Donnelly, K. Marsh, and C. Newbold. 1999. Immunity to non-cerebral severe malaria is acquired after one or two infections. *Nature Medicine* 5: 340–343.
13. Marsh, K., and S. Kinyanjui. 2006. Immune effector mechanisms in malaria. *Parasite Immunol.* 28: 51–60.
14. Janeway, C. A. 1989. Approaching the asymptote? Evolution and revolution in immunology. *Cold Spring Harb. Symp. Quant. Biol.* 54 Pt 1: 1–13.
15. Lemaitre, B., E. Nicolas, L. Michaut, J. M. Reichhart, and J. A. Hoffmann. 1996. The dorsoventral regulatory gene cassette spätzle/Toll/cactus controls the potent antifungal

response in Drosophila adults. *Cell* 86: 973–983.
16. Medzhitov, R., P. Preston-Hurlburt, and C. A. Janeway. 1997. A human homologue of the Drosophila Toll protein signals activation of adaptive immunity. *Nature* 388: 394–397.
17. Alexopoulou, L., A. C. Holt, R. Medzhitov, and R. A. Flavell. 2001. Recognition of double-stranded RNA and activation of NF-kappaB by Toll-like receptor 3. *Nature* 413: 732–738.
18. Heil, F., H. Hemmi, H. Hochrein, F. Ampenberger, C. Kirschning, S. Akira, G. Lipford, H. Wagner, and S. Bauer. 2004. Species-specific recognition of single-stranded RNA via toll-like receptor 7 and 8. *Science* 303: 1526–1529.
19. Hemmi, H., O. Takeuchi, T. Kawai, T. Kaisho, S. Sato, H. Sanjo, M. Matsumoto, K. Hoshino, H. Wagner, K. Takeda, and S. Akira. 2000. A Toll-like receptor recognizes bacterial DNA. *Nature* 408: 740–745.
20. Koblansky, A. A., D. Jankovic, H. Oh, S. Hieny, W. Sungnak, R. Mathur, M. S. Hayden, S. Akira, A. Sher, and S. Ghosh. 2013. Recognition of profilin by Toll-like receptor 12 is critical for host resistance to Toxoplasma gondii. *Immunity* 38: 119–130.
21. Andrade, W. A., M. do Carmo Souza, E. Ramos-Martinez, K. Nagpal, M. S. Dutra, M. B. Melo, D. C. Bartholomeu, S. Ghosh, D. T. Golenbock, and R. T. Gazzinelli. 2013. Combined Action of Nucleic Acid-Sensing Toll-like Receptors and TLR11/TLR12 Heterodimers Imparts Resistance to Toxoplasma gondii in Mice. *Cell Host and Microbe* 13: 42–53.
22. Zhang, D., G. Zhang, M. S. Hayden, M. B. Greenblatt, C. Bussey, R. A. Flavell, and S. Ghosh. 2004. A toll-like receptor that prevents infection by uropathogenic bacteria. *Science* 303: 1522–1526.
23. Aliprantis, A. O., R. B. Yang, M. R. Mark, S. Suggett, B. Devaux, J. D. Radolf, G. R. Klimpel, P. Godowski, and A. Zychlinsky. 1999. Cell activation and apoptosis by bacterial lipoproteins through toll-like receptor-2. *Science* 285: 736–739.
24. Brightbill, H. D., D. H. Libraty, S. R. Krutzik, R. B. Yang, J. T. Belisle, J. R. Bleharski, M. Maitland, M. V. Norgard, S. E. Plevy, S. T. Smale, P. J. Brennan, B. R. Bloom, P. J. Godowski, and R. L. Modlin. 1999. Host defense mechanisms triggered by microbial lipoproteins through toll-like receptors. *Science* 285: 732–736.
25. Takeuchi, O., S. Sato, T. Horiuchi, K. Hoshino, K. Takeda, Z. Dong, R. L. Modlin, and S. Akira. 2002. Cutting edge: role of Toll-like receptor 1 in mediating immune response to microbial lipoproteins. *The Journal of Immunology* 169: 10–14.
26. Takeuchi, O., T. Kawai, P. F. Mühlradt, M. Morr, J. D. Radolf, A. Zychlinsky, K. Takeda, and S. Akira. 2001. Discrimination of bacterial lipoproteins by Toll-like receptor 6. *International Immunology* 13: 933–940.
27. Yoshimura, A., E. Lien, R. R. Ingalls, E. Tuomanen, R. Dziarski, and D. Golenbock. 1999. Cutting edge: recognition of Gram-positive bacterial cell wall components by the innate immune system occurs via Toll-like receptor 2. *The Journal of Immunology* 163: 1–5.
28. Campos, M. A. S., I. C. Almeida, O. Takeuchi, S. Akira, E. P. Valente, D. O. Procopio, L. R. Travassos, J. A. Smith, D. T. Golenbock, and R. T. Gazzinelli. 2001. Activation of Toll-Like Receptor-2 by Glycosylphosphatidylinositol Anchors from a

Protozoan Parasite. *The Journal of Immunology* 167: 416–423.
29. Poltorak, A., X. He, I. Smirnova, M. Y. Liu, C. Van Huffel, X. Du, D. Birdwell, E. Alejos, M. Silva, C. Galanos, M. Freudenberg, P. Ricciardi-Castagnoli, B. Layton, and B. Beutler. 1998. Defective LPS signaling in C3H/HeJ and C57BL/10ScCr mice: mutations in Tlr4 gene. *Science* 282: 2085–2088.
30. Schromm, A. B., E. Lien, P. Henneke, J. C. Chow, A. Yoshimura, H. Heine, E. Latz, B. G. Monks, D. A. Schwartz, K. Miyake, and D. T. Golenbock. 2001. Molecular genetic analysis of an endotoxin nonresponder mutant cell line: a point mutation in a conserved region of MD-2 abolishes endotoxin-induced signaling. *J. Exp. Med.* 194: 79–88.
31. Hayashi, F., K. D. Smith, A. Ozinsky, T. R. Hawn, E. C. Yi, D. R. Goodlett, J. K. Eng, S. Akira, D. M. Underhill, and A. Aderem. 2001. The innate immune response to bacterial flagellin is mediated by Toll-like receptor 5. *Nature* 410: 1099–1103.
32. O'Neill, L. A. J., and A. G. Bowie. 2007. The family of five: TIR-domain-containing adaptors in Toll-like receptor signalling. *Nat Rev Immunol* 7: 353–364.
33. Hibino, T., M. Loza-Coll, C. Messier, A. J. Majeske, A. H. Cohen, D. P. Terwilliger, K. M. Buckley, V. Brockton, S. V. Nair, K. Berney, S. D. Fugmann, M. K. Anderson, Z. Pancer, R. A. Cameron, L. C. Smith, and J. P. Rast. 2006. The immune gene repertoire encoded in the purple sea urchin genome. *Developmental Biology* 300: 349–365.
34. Hoving, J. C., G. J. Wilson, and G. D. Brown. 2014. Signalling C-Type lectin receptors, microbial recognition and immunity. *Cell Microbiol* 16: 185–194.
35. Chen, G., M. H. Shaw, Y.-G. Kim, and G. Nuñez. 2009. NOD-Like Receptors: Role in Innate Immunity and Inflammatory Disease. *Annu. Rev. Pathol. Mech. Dis.* 4: 365–398.
36. Latz, E., T. S. Xiao, and A. Stutz. 2013. Activation and regulation of the inflammasomes. *Nat Rev Immunol* 13: 397–411.
37. Gack, M. U. 2014. Mechanisms of RIG-I-like receptor activation and manipulation by viral pathogens. *J. Virol.* 88: 5213–5216.
38. Hornung, V., A. Ablasser, M. Charrel-Dennis, F. Bauernfeind, G. Horvath, D. R. Caffrey, E. Latz, and K. A. Fitzgerald. 2009. AIM2 recognizes cytosolic dsDNA and forms a caspase-1-activating inflammasome with ASC. *Nature* 458: 514–518.
39. Fernandes-Alnemri, T., J.-W. Yu, P. Datta, J. Wu, and E. S. Alnemri. 2009. AIM2 activates the inflammasome and cell death in response to cytoplasmic DNA. *Nature* 458: 509–513.
40. Unterholzner, L., S. E. Keating, M. Baran, K. A. Horan, S. B. Jensen, S. Sharma, C. M. Sirois, T. Jin, E. Latz, T. S. Xiao, K. A. Fitzgerald, S. R. Paludan, and A. G. Bowie. 2010. IFI16 is an innate immune sensor for intracellular DNA. *Nature Publishing Group* 11: 997–1004.
41. Chiu, Y.-H., J. B. MacMillan, and Z. J. Chen. 2009. RNA Polymerase III Detects Cytosolic DNA and Induces Type I Interferons through the RIG-I Pathway. *Cell* 138: 576–591.
42. Sun, L., J. Wu, F. Du, X. Chen, and Z. J. Chen. 2013. Cyclic GMP-AMP synthase is a cytosolic DNA sensor that activates the type I interferon pathway. *Science* 339: 786–791.
43. Wu, J., L. Sun, X. Chen, F. Du, H. Shi, C. Chen, and Z. J. Chen. 2013. Cyclic GMP-AMP is an endogenous second messenger in innate immune signaling by cytosolic DNA.

Science 339: 826–830.
44. Zhang, X., H. Shi, J. Wu, X. Zhang, L. Sun, C. Chen, and Z. J. Chen. 2013. Cyclic GMP-AMP Containing Mixed Phosphodiester Linkages Is An Endogenous High-Affinity Ligand for STING. *Mol. Cell* 51: 226–235.
45. Ablasser, A., M. Goldeck, T. Cavlar, T. Deimling, G. Witte, I. Röhl, K.-P. Hopfner, J. Ludwig, and V. Hornung. 2013. cGAS produces a 2′-5′-linked cyclic dinucleotide second messenger that activates STING. *Nature* 498: 380–384.
46. Krishnegowda, G., A. M. Hajjar, J. Zhu, E. J. Douglass, S. Uematsu, S. Akira, A. S. Woods, and D. C. Gowda. 2005. Induction of Proinflammatory Responses in Macrophages by the Glycosylphosphatidylinositols of Plasmodium falciparum CELL SIGNALING RECEPTORS, GLYCOSYLPHOSPHATIDYLINOSITOL (GPI) STRUCTURAL REQUIREMENT, AND REGULATION OF GPI ACTIVITY. *J. Biol. Chem.* 280: 8606–8616.
47. Zheng, H., Z. Tan, T. Zhou, F. Zhu, Y. Ding, T. Liu, Y. Wu, and W. Xu. 2015. The TLR2 is activated by sporozoites and suppresses intrahepatic rodent malaria parasite development. *Sci Rep* 1–10.
48. Jaramillo, M., I. Plante, N. Ouellet, K. Vandal, P. A. Tessier, and M. Olivier. 2004. Hemozoin-Inducible Proinflammatory Events In Vivo: Potential Role in Malaria Infection. *The Journal of Immunology* 172: 3101–3110.
49. Parroche, P., F. N. Lauw, N. Goutagny, E. Latz, B. G. Monks, A. Visintin, K. A. Halmen, M. Lamphier, M. Olivier, D. C. Bartholomeu, R. T. Gazzinelli, and D. T. Golenbock. 2007. Malaria hemozoin is immunologically inert but radically enhances innate responses by presenting malaria DNA to Toll-like receptor 9. *Proc. Natl. Acad. Sci. U.S.A.* 104: 1919–1924.
50. Coban, C., K. J. Ishii, T. Kawai, H. Hemmi, S. Sato, S. Uematsu, M. Yamamoto, O. Takeuchi, S. Itagaki, N. Kumar, T. Horii, and S. Akira. 2005. Toll-like receptor 9 mediates innate immune activation by the malaria pigment hemozoin. *J. Exp. Med.* 201: 19–25.
51. Wu, X., N. M. Gowda, S. Kumar, and D. C. Gowda. 2010. Protein-DNA Complex Is the Exclusive Malaria Parasite Component That Activates Dendritic Cells and Triggers Innate Immune Responses. *The Journal of Immunology* 184: 4338–4348.
52. Gowda, N. M., X. Wu, and D. C. Gowda. 2011. The Nucleosome (Histone-DNA Complex) Is the TLR9-Specific Immunostimulatory Component of Plasmodium falciparum That Activates DCs. *PLoS ONE* 6: e20398–14.
53. Kalantari, P., R. B. DeOliveira, J. Chan, Y. Corbett, V. Rathinam, A. Stutz, E. Latz, R. T. Gazzinelli, D. T. Golenbock, and K. A. Fitzgerald. 2014. Dual engagement of the NLRP3 and AIM2 inflammasomes by plasmodium-derived hemozoin and DNA during malaria. *CellReports* 6: 196–210.
54. Ataide, M. A., W. A. Andrade, D. S. Zamboni, D. Wang, M. D. C. Souza, B. S. Franklin, S. Elian, F. S. Martins, D. Pereira, G. Reed, K. A. Fitzgerald, D. T. Golenbock, and R. T. Gazzinelli. 2014. Malaria-induced NLRP12/NLRP3-dependent caspase-1 activation mediates inflammation and hypersensitivity to bacterial superinfection. *PLoS Pathog* 10: e1003885.
55. Sharma, S., R. B. DeOliveira, P. Kalantari, P. Parroche, N. Goutagny, Z. Jiang, J.

Chan, D. C. Bartholomeu, F. Lauw, J. P. Hall, G. N. Barber, R. T. Gazzinelli, K. A. Fitzgerald, and D. T. Golenbock. 2011. Innate immune recognition of an AT-rich stem-loop DNA motif in the Plasmodium falciparum genome. *Immunity* 35: 194–207.
56. Stevenson, M. M., and E. M. Riley. 2004. Innate immunity to malaria. *Nat Rev Immunol* 4: 169–180.
57. Hunt, N. H., and G. E. Grau. 2003. Cytokines: accelerators and brakes in the pathogenesis of cerebral malaria. *Trends in Immunology* 24: 491–499.
58. Grau, G. E., T. E. Taylor, M. E. Molyneux, J. J. Wirima, P. Vassalli, M. Hommel, and P. H. Lambert. 1989. Tumor necrosis factor and disease severity in children with falciparum malaria. *N. Engl. J. Med.* 320: 1586–1591.
59. Lyke, K. E., R. Burges, Y. Cissoko, L. Sangare, M. Dao, I. Diarra, A. Kone, R. Harley, C. V. Plowe, O. K. Doumbo, and M. B. Sztein. 2004. Serum Levels of the Proinflammatory Cytokines Interleukin-1 Beta (IL-1), IL-6, IL-8, IL-10, Tumor Necrosis Factor Alpha, and IL-12(p70) in Malian Children with Severe Plasmodium falciparum Malaria and Matched Uncomplicated Malaria or Healthy Controls. *Infect. Immun.* 72: 5630–5637.
60. Idro, R., N. E. Jenkins, and C. R. Newton. 2005. Pathogenesis, clinical features, and neurological outcome of cerebral malaria. *The Lancet Neurology* 4: 827–840.
61. Lundie, R. J., Lundie, R. J., T. F. de Koning-Ward, T. F. de Koning-Ward, G. M. Davey, G. M. Davey, C. Q. Nie, C. Q. Nie, D. S. Hansen, D. S. Hansen, L. S. Lau, L. S. Lau, J. D. Mintern, J. D. Mintern, G. T. Belz, G. T. Belz, L. Schofield, L. Schofield, F. R. Carbone, F. R. Carbone, J. A. Villadangos, J. A. Villadangos, B. S. Crabb, B. S. Crabb, W. R. Heath, and W. R. Heath. 2008. Blood-stage Plasmodium infection induces CD8+ T lymphocytes to parasite-expressed antigens, largely regulated by CD8 + dendritic cells. *Proc. Natl. Acad. Sci. U.S.A.* 105: 14509–14514.
62. Piva, L., Piva, L., P. Tetlak, P. Tetlak, C. Claser, C. Claser, K. Karjalainen, K. Karjalainen, L. Rénia, L. Renia, C. Ruedl, and C. Ruedl. 2012. Cutting Edge: Clec9A+ Dendritic Cells Mediate the Development of Experimental Cerebral Malaria. *The Journal of Immunology* 189: 1128–1132.
63. Miyakoda, M., D. Kimura, M. Yuda, Y. Chinzei, Y. Shibata, K. Honma, and K. Yui. 2008. Malaria-specific and nonspecific activation of CD8+ T cells during blood stage of Plasmodium berghei infection. *The Journal of Immunology* 181: 1420–1428.
64. Campanella, G. S. V., A. M. Tager, J. K. El Khoury, S. Y. Thomas, T. A. Abrazinski, L. A. Manice, R. A. Colvin, and A. D. Luster. 2008. Chemokine receptor CXCR3 and its ligands CXCL9 and CXCL10 are required for the development of murine cerebral malaria. *Proc. Natl. Acad. Sci. U.S.A.* 105: 4814–4819.
65. Howland, S. W., C. M. Poh, S. Y. Gun, C. Claser, B. Malleret, N. Shastri, F. Ginhoux, G. M. Grotenbreg, and L. Rénia. 2013. Brain microvessel cross-presentation is a hallmark of experimental cerebral malaria. *EMBO Mol Med* 5: 984–999.
66. Nitcheu, J., O. Bonduelle, C. Combadiere, M. Tefit, D. Seilhean, D. Mazier, and B. Combadiere. 2003. Perforin-Dependent Brain-Infiltrating Cytotoxic CD8+ T Lymphocytes Mediate Experimental Cerebral Malaria Pathogenesis. *The Journal of Immunology* 170: 2221–2228.
67. Haque, A., Haque, A., S. E. Best, S. E. Best, K. Unosson, K. Unosson, F. H. Amante,

F. H. Amante, F. de Labastida, F. de Labastida, N. M. Anstey, N. M. Anstey, G. Karupiah, G. Karupiah, M. J. Smyth, M. J. Smyth, W. R. Heath, W. R. Heath, C. R. Engwerda, and C. R. Engwerda. 2011. Granzyme B Expression by CD8+ T Cells Is Required for the Development of Experimental Cerebral Malaria. *The Journal of Immunology* 186: 6148–6156.
68. Yañez, D. M., D. D. Manning, A. J. Cooley, W. P. Weidanz, and H. C. van der Heyde. 1996. Participation of lymphocyte subpopulations in the pathogenesis of experimental murine cerebral malaria. *Journal of immunology (Baltimore, Md. : 1950)* 157: 1620–1624.
69. Belnoue, E., Belnoue, E., M. Kayibanda, M. Kayibanda, A. M. Vigário, A. M. Vigario, J.-C. Deschemin, J. C. Deschemin, N. V. Rooijen, N. van Rooijen, M. Viguier, M. Viguier, G. Snounou, G. Snounou, L. Rénia, and L. Renia. 2002. On the Pathogenic Role of Brain-Sequestered CD8+ T Cells in Experimental Cerebral Malaria. *The Journal of Immunology* 169: 6369–6375.
70. Grau, G. E., H. Heremans, P. F. Piguet, P. Pointaire, P. H. Lambert, A. Billiau, and P. Vassalli. 1989. Monoclonal antibody against interferon gamma can prevent experimental cerebral malaria and its associated overproduction of tumor necrosis factor. *Proc. Natl. Acad. Sci. U.S.A.* 86: 5572–5574.
71. Villegas-Mendez, A., Villegas-Mendez, A., R. Greig, R. Greig, T. N. Shaw, T. N. Shaw, J. B. De Souza, J. B. de Souza, E. Gwyer Findlay, E. Gwyer Findlay, J. S. Stumhofer, J. S. Stumhofer, J. C. R. Hafalla, J. C. R. Hafalla, D. G. Blount, D. G. Blount, C. A. Hunter, C. A. Hunter, E. M. Riley, E. M. Riley, K. N. Couper, and K. N. Couper. 2012. IFN- -Producing CD4+ T Cells Promote Experimental Cerebral Malaria by Modulating CD8+ T Cell Accumulation within the Brain. *The Journal of Immunology* 189: 968–979.
72. Ball, E. A., M. R. Sambo, M. Martins, M. J. Trovoada, C. Benchimol, J. Costa, L. Antunes Goncalves, A. Coutinho, and C. Penha-Goncalves. 2013. IFNAR1 Controls Progression to Cerebral Malaria in Children and CD8+ T Cell Brain Pathology in Plasmodium berghei-Infected Mice. *The Journal of Immunology* 190: 5118–5127.
73. Palomo, J., M. Fauconnier, L. Coquard, M. L. Gilles, S. Meme, F. Szeremeta, L. Fick, J.-F. O. Franetich, M. Jacobs, D. E. Togbe, J.-C. Beloeil, D. Mazier, B. Ryffel, and V. F. J. Quesniaux. 2013. Type I interferons contribute to experimental cerebral malaria development in response to sporozoite or blood-stage Plasmodium bergheiANKA. *European Journal of Immunology* 43: 2683–2695.
74. Haque, A., S. E. Best, A. Ammerdorffer, L. Desbarrieres, M. M. de Oca, F. H. Amante, F. de Labastida Rivera, P. Hertzog, G. M. Boyle, G. R. Hill, and C. R. Engwerda. 2011. Type I interferons suppress CD4+ T-cell-dependent parasite control during blood-stage Plasmodium infection. *European Journal of Immunology* 41: 2688–2698.
75. ISAACS, A., and J. LINDENMANN. 1957. Virus interference. I. The interferon. *Proceedings of the Royal Society of London. Series B, Containing papers of a Biological character. Royal Society (Great Britain)* 147: 258–267.
76. Pestka, S., C. D. Krause, and M. R. Walter. 2004. Interferons, interferon-like cytokines, and their receptors. *Immunol Rev* 202: 8–32.

77. González-Navajas, J. M., J. Lee, M. David, and E. Raz. 2012. Immunomodulatory functions of type I interferons. *Nat Rev Immunol* 12: 97–135.
78. Stetson, D. B., and R. Medzhitov. 2006. Type I Interferons in Host Defense. *Immunity* 25: 373–381.
79. Ojo-Amaize, E. A., L. S. Salimonu, A. I. Williams, O. A. Akinwolere, R. Shabo, G. V. Alm, and H. Wigzell. 1981. Positive correlation between degree of parasitemia, interferon titers, and natural killer cell activity in Plasmodium falciparum-infected children. *Journal of immunology (Baltimore, Md. : 1950)* 127: 2296–2300.
80. Aucan, C., A. J. Walley, B. J. W. Hennig, J. Fitness, A. Frodsham, L. Zhang, D. Kwiatkowski, and A. V. S. Hill. 2003. Interferon-alpha receptor-1 (IFNAR1) variants are associated with protection against cerebral malaria in The Gambia. *Genes Immun* 4: 275–282.
81. Vigário, A. M., E. Belnoue, A. C. Grüner, M. Mauduit, M. Kayibanda, J.-C. Deschemin, M. Marussig, G. Snounou, D. Mazier, I. Gresser, and L. Rénia. 2007. Recombinant human IFN-alpha inhibits cerebral malaria and reduces parasite burden in mice. *Journal of immunology (Baltimore, Md. : 1950)* 178: 6416–6425.
82. Haque, A., S. E. Best, A. Ammerdorffer, L. Desbarrieres, M. M. de Oca, F. H. Amante, F. de Labastida Rivera, P. Hertzog, G. M. Boyle, G. R. Hill, and C. R. Engwerda. 2011. Type I interferons suppress CD4$^+$ T-cell-dependent parasite control during blood-stage Plasmodium infection. *European Journal of Immunology* 41: 2688–2698.
83. de Oca, M. M., R. Kumar, F. de Labastida Rivera, F. H. Amante, M. Sheel, R. J. Faleiro, P. T. Bunn, S. E. Best, L. Beattie, S. S. Ng, C. L. Edwards, G. M. Boyle, R. N. Price, N. M. Anstey, J. R. Loughland, J. Burel, D. L. Doolan, A. Haque, J. S. McCarthy, and C. R. Engwerda. 2016. Type I Interferons Regulate Immune Responses in Humans with Blood-Stage Plasmodium falciparum Infection. *CellReports* 17: 399–412.
84. Liehl, P., V. Zuzarte-Luís, J. Chan, T. Zillinger, F. Baptista, D. Carapau, M. Konert, K. K. Hanson, C. Carret, C. Lassnig, M. Müller, U. Kalinke, M. Saeed, A. F. Chora, D. T. Golenbock, B. Strobl, M. Prudêncio, L. P. Coelho, S. H. Kappe, G. Superti-Furga, A. Pichlmair, A. M. Vigário, C. M. Rice, K. A. Fitzgerald, W. Barchet, and M. M. Mota. 2013. Host-cell sensors for Plasmodium activate innate immunity against liver-stage infection. *Nature Medicine* 20: 47–53.
85. deWalick, S., F. H. Amante, K. A. McSweeney, L. M. Randall, A. C. Stanley, A. Haque, R. D. Kuns, K. P. A. MacDonald, G. R. Hill, and C. R. Engwerda. 2007. Cutting Edge: Conventional Dendritic Cells Are the Critical APC Required for the Induction of Experimental Cerebral Malaria. *The Journal of Immunology* 178: 6033–6037.
86. Haque, A., S. E. Best, M. Montes de Oca, K. R. James, A. Ammerdorffer, C. L. Edwards, F. de Labastida Rivera, F. H. Amante, P. T. Bunn, M. Sheel, I. Sebina, M. Koyama, A. Varelias, P. J. Hertzog, U. Kalinke, S. Y. Gun, L. Rénia, C. Ruedl, K. P. A. MacDonald, G. R. Hill, and C. R. Engwerda. 2014. Type I IFN signaling in CD8– DCs impairs Th1-dependent malaria immunity. *J. Clin. Invest.* 124: 2483–2496.
87. Kim, C. C., C. S. Nelson, E. B. Wilson, B. Hou, A. L. DeFranco, and J. L. DeRisi. 2012. Splenic Red Pulp Macrophages Produce Type I Interferons as Early Sentinels of Malaria Infection but Are Dispensable for Control. *PLoS ONE* 7: e48126.

88. Baccarella, A., M. F. Fontana, E. C. Chen, and C. C. Kim. 2013. Toll-like receptor 7 mediates early innate immune responses to malaria. *Infect. Immun.* 81: 4431–4442.
89. Franklin, B. S., Franklin, B. S., S. T. Ishizaka, S. T. Ishizaka, M. Lamphier, M. Lamphier, F. Gusovsky, F. Gusovsky, H. Hansen, H. Hansen, J. Rose, J. Rose, W. Zheng, W. Zheng, M. A. Ataíde, M. A. Ataide, R. B. de Oliveira, R. B. de Oliveira, D. T. Golenbock, D. T. Golenbock, R. T. Gazzinelli, and R. T. Gazzinelli. 2011. Therapeutical targeting of nucleic acid-sensing Toll-like receptors prevents experimental cerebral malaria. *Proc. Natl. Acad. Sci. U.S.A.* 108: 3689–3694.
90. Coban, C., Coban, C., K. J. Ishii, K. J. Ishii, S. Uematsu, S. Uematsu, N. Arisue, N. Arisue, S. Sato, S. Sato, M. Yamamoto, M. Yamamoto, T. Kawai, T. Kawai, O. Takeuchi, O. Takeuchi, H. Hisaeda, H. Hisaeda, T. Horii, T. Horii, S. Akira, and S. Akira. 2006. Pathological role of Toll-like receptor signaling in cerebral malaria. *International Immunology* 19: 67–79.
91. Togbe, D., L. Schofield, G. E. Grau, B. Schnyder, V. Boissay, S. Charron, S. Rose, B. Beutler, V. F. J. Quesniaux, and B. Ryffel. 2007. Murine Cerebral Malaria Development Is Independent of Toll-Like Receptor Signaling. *The American Journal of Pathology* 170: 1640–1648.
92. Griffith, J. W., C. O'Connor, K. Bernard, T. Town, D. R. Goldstein, and R. Bucala. 2007. Toll-Like Receptor Modulation of Murine Cerebral Malaria Is Dependent on the Genetic Background of the Host. *J. Infect. Dis.* 196: 1553–1564.
93. Kordes, M., Kordes, M., K. Matuschewski, K. Matuschewski, J. C. R. Hafalla, and J. C. R. Hafalla. 2011. Caspase-1 Activation of Interleukin-1 (IL-1) and IL-18 Is Dispensable for Induction of Experimental Cerebral Malaria. *Infect. Immun.* 79: 3633–3641.
94. Tanaka, Y., and Z. J. Chen. 2012. STING Specifies IRF3 Phosphorylation by TBK1 in the Cytosolic DNA Signaling Pathway. *Science Signaling* 5: ra20–ra20.
95. Quintin, J., S. Saeed, J. H. A. Martens, E. J. Giamarellos-Bourboulis, D. C. Ifrim, C. Logie, L. Jacobs, T. Jansen, B.-J. Kullberg, C. Wijmenga, L. A. B. Joosten, R. J. Xavier, J. W. M. van der Meer, H. G. Stunnenberg, and M. G. Netea. 2012. Candida albicans infection affords protection against reinfection via functional reprogramming of monocytes. *Cell Host and Microbe* 12: 223–232.
96. Kleinnijenhuis, J., J. Quintin, F. Preijers, L. A. B. Joosten, D. C. Ifrim, S. Saeed, C. Jacobs, J. van Loenhout, D. de Jong, H. G. Stunnenberg, R. J. Xavier, J. W. M. van der Meer, R. van Crevel, and M. G. Netea. 2012. Bacille Calmette-Guerin induces NOD2-dependent nonspecific protection from reinfection via epigenetic reprogramming of monocytes. *Proc. Natl. Acad. Sci. U.S.A.* 109: 17537–17542.
97. Netea, M. G., J. Quintin, and J. W. M. van der Meer. 2011. Trained immunity: a memory for innate host defense. *Cell Host and Microbe* 9: 355–361.
98. Cavaillon, J.-M., and M. Adib-Conquy. 2006. Bench-to-bedside review: endotoxin tolerance as a model of leukocyte reprogramming in sepsis. *Critical Care* 10: 233.
99. Carson, W. F., K. A. Cavassani, Y. Dou, and S. L. Kunkel. 2011. Epigenetic regulation of immune cell functions during post-septic immunosuppression. *Epigenetics* 6: 273–283.
100. Foster, S. L., D. C. Hargreaves, and R. Medzhitov. 2007. Gene-specific control of

inflammation by TLR-induced chromatin modifications. *Nature* 447: 972–978.
101. Saeed, S., J. Quintin, H. H. D. Kerstens, N. A. Rao, A. Aghajanirefah, F. Matarese, S.-C. Cheng, J. Ratter, K. Berentsen, M. A. van der Ent, N. Sharifi, E. M. Janssen-Megens, M. Ter Huurne, A. Mandoli, T. van Schaik, A. Ng, F. Burden, K. Downes, M. Frontini, V. Kumar, E. J. Giamarellos-Bourboulis, W. H. Ouwehand, J. W. M. van der Meer, L. A. B. Joosten, C. Wijmenga, J. H. A. Martens, R. J. Xavier, C. Logie, M. G. Netea, and H. G. Stunnenberg. 2014. Epigenetic programming of monocyte-to-macrophage differentiation and trained innate immunity. *Science* 345: 1251086.
102. Cheng, S.-C., J. Quintin, R. A. Cramer, K. M. Shepardson, S. Saeed, V. Kumar, E. J. Giamarellos-Bourboulis, J. H. A. Martens, N. A. Rao, A. Aghajanirefah, G. R. Manjeri, Y. Li, D. C. Ifrim, R. J. W. Arts, B. M. J. W. van der Veer, B. M. J. W. van der Meer, P. M. T. Deen, C. Logie, L. A. O'Neill, P. Willems, F. L. van de Veerdonk, J. W. M. van der Meer, A. Ng, L. A. B. Joosten, C. Wijmenga, H. G. Stunnenberg, R. J. Xavier, and M. G. Netea. 2014. mTOR- and HIF-1α-mediated aerobic glycolysis as metabolic basis for trained immunity. *Science* 345: 1250684–1250684.
103. Arts, R. J. W., A. Carvalho, C. La Rocca, C. Palma, F. Rodrigues, R. Silvestre, J. Kleinnijenhuis, E. Lachmandas, L. G. Gonçalves, A. Belinha, C. Cunha, M. Oosting, L. A. B. Joosten, G. Matarese, R. van Crevel, and M. G. Netea. 2016. Immunometabolic Pathways in BCG-Induced Trained Immunity. *CellReports* 17: 2562–2571.
104. Cheng, S.-C., B. P. Scicluna, R. J. W. Arts, M. S. Gresnigt, E. Lachmandas, E. J. Giamarellos-Bourboulis, M. Kox, G. R. Manjeri, J. A. L. Wagenaars, O. L. Cremer, J. Leentjens, A. J. van der Meer, F. L. van de Veerdonk, M. J. Bonten, M. J. Schultz, P. H. G. M. Willems, P. Pickkers, L. A. B. Joosten, T. van der Poll, and M. G. Netea. 2016. Broad defects in the energy metabolism of leukocytes underlie immunoparalysis in sepsis. *Nat Immunol* 17: 406–413.
105. Ifrim, D. C., J. Quintin, L. A. B. Joosten, C. Jacobs, T. Jansen, L. Jacobs, N. A. R. Gow, D. L. Williams, J. W. M. van der Meer, and M. G. Netea. 2014. Trained immunity or tolerance: opposing functional programs induced in human monocytes after engagement of various pattern recognition receptors. *Clin. Vaccine Immunol.* 21: 534–545.
106. McCall, M. B. B., M. G. Netea, C. C. Hermsen, T. Jansen, L. Jacobs, D. Golenbock, A. J. A. M. van der Ven, and R. W. Sauerwein. 2007. Plasmodium falciparum Infection Causes Proinflammatory Priming of Human TLR Responses. *The Journal of Immunology* 179: 162–171.
107. Franklin, B. S., P. Parroche, M. A. Ataíde, F. Lauw, C. Ropert, R. B. de Oliveira, D. Pereira, M. S. Tada, P. Nogueira, L. H. P. da Silva, H. Bjorkbacka, D. T. Golenbock, and R. T. Gazzinelli. 2009. Malaria primes the innate immune response due to interferon-gamma induced enhancement of toll-like receptor expression and function. *Proc. Natl. Acad. Sci. U.S.A.* 106: 5789–5794.
108. Luty, A. J., B. Lell, R. Schmidt-Ott, L. G. Lehman, D. Luckner, B. Greve, P. Matousek, K. Herbich, D. Schmid, F. Migot-Nabias, P. Deloron, R. S. Nussenzweig, and P. G. Kremsner. 1999. Interferon-gamma responses are associated with resistance to reinfection with Plasmodium falciparum in young African children. *J. Infect. Dis.* 179: 980–988.

109. Dodoo, D., F. M. Omer, J. Todd, B. D. Akanmori, K. A. Koram, and E. M. Riley. 2002. Absolute levels and ratios of proinflammatory and anti-inflammatory cytokine production in vitro predict clinical immunity to Plasmodium falciparum malaria. *J. Infect. Dis.* 185: 971–979.
110. Boutlis, C. S., T. W. Yeo, and N. M. Anstey. 2006. Malaria tolerance – for whom the cell tolls? *Trends in Parasitology* 22: 371–377.
111. Gatton, M. L., and Q. Cheng. 2003. Evaluation of the pyrogenic threshold for Plasmodium falciparum malaria in naive individuals. *Am. J. Trop. Med. Hyg.* 66: 467–473.
112. Mabey, D. C., A. Brown, and B. M. Greenwood. 1987. Plasmodium falciparum malaria and Salmonella infections in Gambian children. *J. Infect. Dis.* 155: 1319–1321.
113. Williamson, W. A., and B. M. Greenwood. 1978. IMPAIRMENT OF THE IMMUNE RESPONSE TO VACCINATION AFTER ACUTE MALARIA. *The Lancet* 311: 1328–1329.
114. Culley, W. J., and E. T. Mertz. 2016. Effect of Restricted Food Intake on Growth and Composition of Preweanling Rat Brain.∗. *Proceedings of the Society for Experimental Biology and Medicine* 118: 283–287.
115. Heyman, A., and P. B. Beeson. 1949. Influence of various disease states upon the febrile response to intravenous injection of typhoid bacterial pyrogen; with particular reference to malaria and cirrhosis of the liver. *J. Lab. Clin. Med.* 34: 1400–1403.
116. Perry, J. A., C. S. Olver, R. C. Burnett, and A. C. Avery. 2005. Cutting Edge: The Acquisition of TLR Tolerance during Malaria Infection Impacts T Cell Activation. *The Journal of Immunology* 174: 5921–5925.
117. Trager, W., and J. B. Jensen. 1976. Human malaria parasites in continuous culture. *Science* 193: 673–675.
118. Singh, B., A. Bobogare, J. Cox-Singh, G. Snounou, M. S. Abdullah, and H. A. Rahman. 1999. A genus- and species-specific nested polymerase chain reaction malaria detection assay for epidemiologic studies. *Am. J. Trop. Med. Hyg.* 60: 687–692.
119. Hirako, I. C., C. Gallego-Marin, M. A. Ataide, W. A. Andrade, H. Gravina, B. C. Rocha, R. B. de Oliveira, D. B. Pereira, J. Vinetz, B. Diamond, S. Ram, D. T. Golenbock, and R. T. Gazzinelli. 2015. DNA-Containing Immunocomplexes Promote Inflammasome Assembly and Release of Pyrogenic Cytokines by CD14+ CD16+ CD64high CD32low Inflammatory Monocytes from Malaria Patients. *mBio* 6: e01605–15–e01605–15.
120. Fitzgerald, K. A., D. C. Rowe, B. J. Barnes, D. R. Caffrey, A. Visintin, E. Latz, B. Monks, P. M. Pitha, and D. T. Golenbock. 2003. LPS-TLR4 Signaling to IRF-3/7 and NF-κB Involves the Toll Adapters TRAM and TRIF. *J. Exp. Med.* 198: 1043–1055.
121. Wahl, L. M., S. M. Wahl, L. E. Smythies, and P. D. Smith. 2006. Isolation of human monocyte populations. *Curr Protoc Immunol* Chapter 7: Unit 7.6A–7.6A.10.
122. Andrade, W. A., S. Agarwal, S. Mo, S. A. Shaffer, J. P. Dillard, T. Schmidt, V. Hornung, K. A. Fitzgerald, E. A. Kurt-Jones, and D. T. Golenbock. 2016. Type I Interferon Induction by Neisseria gonorrhoeae: Dual Requirement of Cyclic GMP-AMP Synthase and Toll-like Receptor 4. *CellReports* 15: 2438–2448.
123. Park, E. K., H. S. Jung, H. I. Yang, M. C. Yoo, C. Kim, and K. S. Kim. 2007. Optimized THP-1 differentiation is required for the detection of responses to weak

stimuli. *Inflamm. res.* 56: 45–50.
124. Gaidt, M. M., T. S. Ebert, D. Chauhan, T. Schmidt, J. L. Schmid-Burgk, F. Rapino, A. A. B. Robertson, M. A. Cooper, T. Graf, and V. Hornung. 2016. Human Monocytes Engage an Alternative Inflammasome Pathway. *Immunity* 44: 833–846.
125. Fuss, I. J., M. E. Kanof, P. D. Smith, and H. Zola. 2009. Isolation of whole mononuclear cells from peripheral blood and cord blood. *Curr Protoc Immunol* Chapter 7: Unit7.1.
126. Roberts, Z. J., N. Goutagny, P.-Y. Perera, H. Kato, H. Kumar, T. Kawai, S. Akira, R. Savan, D. van Echo, K. A. Fitzgerald, H. A. Young, L.-M. Ching, and S. N. Vogel. 2007. The chemotherapeutic agent DMXAA potently and specifically activates the TBK1–IRF-3 signaling axis. *J. Exp. Med.* 204: 1559–1569.
127. Seth, R. B., L. Sun, C.-K. Ea, and Z. J. Chen. 2005. Identification and Characterization of MAVS, a Mitochondrial Antiviral Signaling Protein that Activates NF-κB and IRF3. *Cell* 122: 669–682.
128. MPH, C. C., H. J. S. PhD, M. S. H. MD, J. L. PhD, A. A. P. BA, J. H. MD, C. S. G. MPH, N. F. MPH, R. D. G. MD, and P. S. R. G. F. D. Med. 2013. The changing epidemiology of malaria elimination: new strategies for new challenges. *The Lancet* 382: 900–911.
129. Lu, F., R. Culleton, M. Zhang, A. Ramaprasad, L. von Seidlein, H. Zhou, G. Zhu, J. Tang, Y. Liu, W. Wang, Y. Cao, S. Xu, Y. Gu, J. Li, C. Zhang, Q. Gao, D. Menard, A. Pain, H. Yang, Q. Zhang, and J. Cao. 2017. Emergence of Indigenous Artemisinin-Resistant Plasmodium falciparum in Africa. *N. Engl. J. Med.* 376: 991–993.
130. Ashley, E. A., M. Dhorda, R. M. Fairhurst, C. Amaratunga, P. Lim, S. Suon, S. Sreng, J. M. Anderson, S. Mao, B. Sam, C. Sopha, C. M. Chuor, C. Nguon, S. Sovannaroth, S. Pukrittayakamee, P. Jittamala, K. Chotivanich, K. Chutasmit, C. Suchatsoonthorn, R. Runcharoen, T. T. Hien, N. T. Thuy-Nhien, N. V. Thanh, N. H. Phu, Y. Htut, K.-T. Han, K. H. Aye, O. A. Mokuolu, R. R. Olaosebikan, O. O. Folaranmi, M. Mayxay, M. Khanthavong, B. Hongvanthong, P. N. Newton, M. A. Onyamboko, C. I. Fanello, A. K. Tshefu, N. Mishra, N. Valecha, A. P. Phyo, F. Nosten, P. Yi, R. Tripura, S. Borrmann, M. Bashraheil, J. Peshu, M. A. Faiz, A. Ghose, M. A. Hossain, R. Samad, M. R. Rahman, M. M. Hasan, A. Islam, O. Miotto, R. Amato, B. MacInnis, J. Stalker, D. P. Kwiatkowski, Z. Bozdech, A. Jeeyapant, P. Y. Cheah, T. Sakulthaew, J. Chalk, B. Intharabut, K. Silamut, S. J. Lee, B. Vihokhern, C. Kunasol, M. Imwong, J. Tarning, W. J. Taylor, S. Yeung, C. J. Woodrow, J. A. Flegg, D. Das, J. Smith, M. Venkatesan, C. V. Plowe, K. Stepniewska, P. J. Guerin, A. M. Dondorp, N. P. Day, N. J. White, Tracking Resistance to Artemisinin Collaboration (TRAC). 2014. Spread of artemisinin resistance in Plasmodium falciparum malaria. *N. Engl. J. Med.* 371: 411–423.
131. Bhattarai, A., A. S. Ali, S. P. Kachur, A. Mårtensson, A. K. Abbas, R. Khatib, A.-W. Al-mafazy, M. Ramsan, G. Rotllant, J. F. Gerstenmaier, F. Molteni, S. Abdulla, S. M. Montgomery, A. Kaneko, and A. Björkman. 2007. Impact of Artemisinin-Based Combination Therapy and Insecticide-Treated Nets on Malaria Burden in Zanzibar. *PLoS Med* 4: e309–7.
132. Lozano, R., M. Naghavi, K. Foreman, S. Lim, K. Shibuya, V. Aboyans, J. Abraham, T. Adair, R. Aggarwal, S. Y. Ahn, M. Alvarado, H. R. Anderson, L. M. Anderson, K. G.

Andrews, C. Atkinson, L. M. Baddour, S. Barker-Collo, D. H. Bartels, M. L. Bell, E. J. Benjamin, D. Bennett, K. Bhalla, B. Bikbov, A. Bin Abdulhak, G. Birbeck, F. Blyth, I. Bolliger, S. Boufous, C. Bucello, M. Burch, P. Burney, J. Carapetis, H. Chen, D. Chou, S. S. Chugh, L. E. Coffeng, S. D. Colan, S. Colquhoun, K. E. Colson, J. Condon, M. D. Connor, L. T. Cooper, M. Corriere, M. Cortinovis, K. C. de Vaccaro, W. Couser, B. C. Cowie, M. H. Criqui, M. Cross, K. C. Dabhadkar, N. Dahodwala, D. De Leo, L. Degenhardt, A. Delossantos, J. Denenberg, D. C. Des Jarlais, S. D. Dharmaratne, E. R. Dorsey, T. Driscoll, H. Duber, B. Ebel, P. J. Erwin, P. Espindola, M. Ezzati, V. Feigin, A. D. Flaxman, M. H. Forouzanfar, F. G. R. Fowkes, R. Franklin, M. Fransen, M. K. Freeman, S. E. Gabriel, E. Gakidou, F. Gaspari, R. F. Gillum, D. Gonzalez-Medina, Y. A. Halasa, D. Haring, J. E. Harrison, R. Havmoeller, R. J. Hay, B. Hoen, P. J. Hotez, D. Hoy, K. H. Jacobsen, S. L. James, R. Jasrasaria, S. Jayaraman, N. Johns, G. Karthikeyan, N. Kassebaum, A. Keren, J.-P. Khoo, L. M. Knowlton, O. Kobusingye, A. Koranteng, R. Krishnamurthi, M. Lipnick, S. E. Lipshultz, S. L. Ohno, J. Mabweijano, M. F. MacIntyre, L. Mallinger, L. March, G. B. Marks, R. Marks, A. Matsumori, R. Matzopoulos, B. M. Mayosi, J. H. McAnulty, M. M. McDermott, J. McGrath, G. A. Mensah, T. R. Merriman, C. Michaud, M. Miller, T. R. Miller, C. Mock, A. O. Mocumbi, A. A. Mokdad, A. Moran, K. Mulholland, M. N. Nair, L. Naldi, K. M. V. Narayan, K. Nasseri, P. Norman, M. O'Donnell, S. B. Omer, K. Ortblad, R. Osborne, D. Ozgediz, B. Pahari, J. D. Pandian, A. P. Rivero, R. P. Padilla, F. Perez-Ruiz, N. Perico, D. Phillips, K. Pierce, C. A. Pope, E. Porrini, F. Pourmalek, M. Raju, D. Ranganathan, J. T. Rehm, D. B. Rein, G. Remuzzi, F. P. Rivara, T. Roberts, F. R. De León, L. C. Rosenfeld, L. Rushton, R. L. Sacco, J. A. Salomon, U. Sampson, E. Sanman, D. C. Schwebel, M. Segui-Gomez, D. S. Shepard, D. Singh, J. Singleton, K. Sliwa, E. Smith, A. Steer, J. A. Taylor, B. Thomas, I. M. Tleyjeh, J. A. Towbin, T. Truelsen, E. A. Undurraga, N. Venketasubramanian, L. Vijayakumar, T. Vos, G. R. Wagner, M. Wang, W. Wang, K. Watt, M. A. Weinstock, R. Weintraub, J. D. Wilkinson, A. D. Woolf, S. Wulf, P.-H. Yeh, P. Yip, A. Zabetian, Z.-J. Zheng, A. D. Lopez, C. J. L. Murray, M. A. AlMazroa, and Z. A. Memish. 2012. Global and regional mortality from 235 causes of death for 20 age groups in 1990 and 2010: a systematic analysis for the Global Burden of Disease Study 2010. *Lancet* 380: 2095–2128.

133. Gazzinelli, R. T., P. Kalantari, K. A. Fitzgerald, and D. T. Golenbock. 2014. Innate sensing of malaria parasites. *Nat Rev Immunol* 14: 744–757.

134. Rocha, B. C., P. E. Marques, F. M. de Souza Leoratti, C. Junqueira, D. B. Pereira, L. R. do Valle Antonelli, G. B. Menezes, D. T. Golenbock, and R. T. Gazzinelli. 2015. Type I Interferon Transcriptional Signature in Neutrophils and Low-Density Granulocytes Are Associated with Tissue Damage in Malaria. *CellReports* 13: 2829–2841.

135. Barbalat, R., S. E. Ewald, M. L. Mouchess, and G. M. Barton. 2011. Nucleic Acid Recognition by the Innate Immune System. *Annu. Rev. Immunol.* 29: 185–214.

136. Chen, Q., L. Sun, and Z. J. Chen. 2016. Regulation and function of the cGAS–STING pathway of cytosolic DNA sensing. *Nat Immunol* 17: 1142–1149.

137. Barber, G. N. 2014. STING-dependent cytosolic DNA sensing pathways. *Trends in Immunology* 35: 88–93.

138. Ishikawa, H., Z. Ma, and G. N. Barber. 2009. STING regulates intracellular DNA-mediated, type I interferon-dependent innate immunity. *Nature* 461: 788–792.

139. Zhong, B., Y. Yang, S. Li, Y.-Y. Wang, Y. Li, F. Diao, C. Lei, X. He, L. Zhang, P. Tien, and H.-B. Shu. 2008. The Adaptor Protein MITA Links Virus-Sensing Receptors to IRF3 Transcription Factor Activation. *Immunity* 29: 538–550.
140. Ishii, K. J., T. Kawagoe, S. Koyama, K. Matsui, H. Kumar, T. Kawai, S. Uematsu, O. Takeuchi, F. Takeshita, C. Coban, and S. Akira. 2008. TANK-binding kinase-1 delineates innate and adaptive immune responses to DNA vaccines. *Nature* 451: 725–729.
141. Gun, S. Y., C. Claser, K. S. W. Tan, and L. Rénia. 2014. Interferons and Interferon Regulatory Factors in Malaria. *Mediators of Inflammation* 2014: 1–21.
142. Lio, C.-W. J., B. McDonald, M. Takahashi, R. Dhanwani, N. Sharma, J. Huang, E. Pham, C. A. Benedict, and S. Sharma. 2016. cGAS-STING Signaling Regulates Initial Innate Control of Cytomegalovirus Infection. *J. Virol.* 90: 7789–7797.
143. Wiens, K. E., and J. D. Ernst. 2016. The Mechanism for Type I Interferon Induction by Mycobacterium tuberculosis is Bacterial Strain-Dependent. *PLoS Pathog* 12: e1005809–20.
144. Gao, D., J. Wu, Y.-T. Wu, F. Du, C. Aroh, N. Yan, L. Sun, and Z. J. Chen. 2013. Cyclic GMP-AMP synthase is an innate immune sensor of HIV and other retroviruses. *Science* 341: 903–906.
145. Andrade, W. A., A. Firon, T. Schmidt, V. Hornung, K. A. Fitzgerald, E. A. Kurt-Jones, P. Trieu-Cuot, D. T. Golenbock, and P.-A. Kaminski. 2016. Group B Streptococcus Degrades Cyclic-di-AMP to Modulate STING-Dependent Type I Interferon Production. *Cell Host and Microbe* 20: 49–59.
146. Hansen, K., T. Prabakaran, A. Laustsen, S. E. Jorgensen, S. H. Rahbaek, S. B. Jensen, R. Nielsen, J. H. Leber, T. Decker, K. A. Horan, M. R. Jakobsen, and S. R. Paludan. 2014. Listeria monocytogenes induces IFN expression through an IFI16-, cGAS- and STING-dependent pathway. *The EMBO Journal* 33: 1654–1666.
147. Zhang, Y., L. Yeruva, A. Marinov, D. Prantner, P. B. Wyrick, V. Lupashin, and U. M. Nagarajan. 2014. The DNA Sensor, Cyclic GMP–AMP Synthase, Is Essential for Induction of IFN-β during Chlamydia trachomatisInfection. *The Journal of Immunology* 193: 2394–2404.
148. Pichyangkul, S., K. Yongvanitchit, U. Kum-arb, H. Hemmi, S. Akira, A. M. Krieg, D. G. Heppner, V. A. Stewart, H. Hasegawa, S. Looareesuwan, G. D. Shanks, and R. S. Miller. 2004. Malaria Blood Stage Parasites Activate Human Plasmacytoid Dendritic Cells and Murine Dendritic Cells through a Toll-Like Receptor 9-Dependent Pathway. *The Journal of Immunology* 172: 4926–4933.
149. Vigario, A. M., E. Belnoue, A. C. Gruner, M. Mauduit, M. Kayibanda, J. C. Deschemin, M. Marussig, G. Snounou, D. Mazier, I. Gresser, and L. Renia. 2007. Recombinant Human IFN- Inhibits Cerebral Malaria and Reduces Parasite Burden in Mice. *The Journal of Immunology* 178: 6416–6425.
150. Netea, M. G., L. A. B. Joosten, E. Latz, K. H. G. Mills, G. Natoli, H. G. Stunnenberg, L. A. J. ONeill, and R. J. Xavier. 2016. Trained immunity: A program of innate immune memory in health and disease. *Science* 352: aaf1098–aaf1098.
151. Gatton, M. L., and Q. Cheng. 2002. Evaluation of the pyrogenic threshold for Plasmodium falciparum malaria in naive individuals. *Am. J. Trop. Med. Hyg.* 66: 467–

473.
152. Portugal, S., T. M. Tran, A. Ongoiba, A. Bathily, S. Li, S. Doumbo, J. Skinner, D. Doumtabe, Y. Kone, J. Sangala, A. Jain, D. H. Davies, C. Hung, L. Liang, S. Ricklefs, M. V. Homann, P. L. Felgner, S. F. Porcella, A. Färnert, O. K. Doumbo, K. Kayentao, B. M. Greenwood, B. Traore, and P. D. Crompton. 2017. Treatment of Chronic Asymptomatic Plasmodium falciparum Infection Does Not Increase the Risk of Clinical Malaria Upon Reinfection. *Clin. Infect. Dis.* 64: 645–653.
153. Li, Y., M. Oosting, P. Deelen, I. R. N. o-Ponce, S. Smeekens, M. Jaeger, V. Matzaraki, M. A. Swertz, R. J. Xavier, L. Franke, C. Wijmenga, L. A. B. Joosten, V. Kumar, and M. G. Netea. 2016. Inter-individual variability and genetic influences on cytokine responses to bacteria and fungi. *Nature Medicine* 22: 952–960.
154. Ayimba, E., J. Hegewald, A. Y. S gb na, R. G. Gantin, C. J. Lechner, A. Agosssou, M. Banla, and P. T. Soboslay. 2011. Proinflammatory and regulatory cytokines and chemokines in infants with uncomplicated and severe Plasmodium falciparum malaria. *Clin. Exp. Immunol.* 166: 218–226.
155. Prakash, D., C. Fesel, R. Jain, P.-A. Cazenave, G. C. Mishra, and S. Pied. 2006. Clusters of cytokines determine malaria severity in Plasmodium falciparum-infected patients from endemic areas of Central India. *J. Infect. Dis.* 194: 198–207.
156. Portugal, S., J. Moebius, J. Skinner, S. Doumbo, D. Doumtabe, Y. Kone, S. Dia, K. Kanakabandi, D. E. Sturdevant, K. Virtaneva, S. F. Porcella, S. Li, O. K. Doumbo, K. Kayentao, A. Ongoiba, B. Traore, and P. D. Crompton. 2014. Exposure-Dependent Control of Malaria-Induced Inflammation in Children. *PLoS Pathog* 10: e1004079–16.
157. Ishida, H., T. Imai, K. Suzue, M. Hirai, T. Taniguchi, A. Yoshimura, Y. Iwakura, H. Okada, T. Suzuki, C. Shimokawa, and H. Hisaeda. 2013. IL-23 protection against Plasmodium bergheiinfection in mice is partially dependent on IL-17 from macrophages. *European Journal of Immunology* 43: 2696–2706.
158. Sellau, J., C. F. Alvarado, S. Hoenow, M. S. Mackroth, D. Kleinschmidt, S. Huber, and T. Jacobs. 2016. IL-22 dampens the T cell response in experimental malaria. *Nature Publishing Group* 1–11.
159. Rapino, F., E. F. Robles, J. A. Richter-Larrea, E. M. Kallin, J. A. Martinez-Climent, and T. Graf. 2013. C/EBPα Induces Highly Efficient Macrophage Transdifferentiation of B Lymphoma and Leukemia Cell Lines and Impairs Their Tumorigenicity. *CellReports* 3: 1153–1163.
160. Zhang, X., R. Goncalves, and D. M. Mosser. 2008. The isolation and characterization of murine macrophages. *Curr Protoc Immunol* Chapter 14: Unit 14.1.
161. Artavanis-Tsakonas, K., and E. M. Riley. 2002. Innate immune response to malaria: rapid induction of IFN-gamma from human NK cells by live Plasmodium falciparum-infected erythrocytes. *The Journal of Immunology* 169: 2956–2963.
162. Artavanis-Tsakonas, K., K. Eleme, K. L. McQueen, N. W. Cheng, P. Parham, D. M. Davis, and E. M. Riley. 2003. Activation of a Subset of Human NK Cells upon Contact with Plasmodium falciparum-Infected Erythrocytes. *The Journal of Immunology* 171: 5396–5405.
163. Korbel, D. S., K. C. Newman, C. R. Almeida, D. M. Davis, and E. M. Riley. 2005. Heterogeneous Human NK Cell Responses to Plasmodium falciparum-Infected

Erythrocytes. *The Journal of Immunology* 175: 7466–7473.
164. Ifrim, D. C., J. Quintin, L. Meerstein-Kessel, T. S. Plantinga, L. A. B. Joosten, J. W. M. van der Meer, F. L. van de Veerdonk, and M. G. Netea. 2015. Defective trained immunity in patients with STAT-1-dependent chronic mucocutaneaous candidiasis. *Clin. Exp. Immunol.* 181: 434–440.
165. Bermick, J. R., N. J. Lambrecht, A. D. denDekker, S. L. Kunkel, N. W. Lukacs, C. M. Hogaboam, and M. A. Schaller. 2016. Neonatal monocytes exhibit a unique histone modification landscape. *Clinical Epigenetics* 1–15.
166. Ramirez-Carrozzi, V. R., D. Braas, D. M. Bhatt, C. S. Cheng, C. Hong, K. R. Doty, J. C. Black, A. Hoffmann, M. Carey, and S. T. Smale. 2009. A Unifying Model for the Selective Regulation of Inducible Transcription by CpG Islands and Nucleosome Remodeling. *Cell* 138: 114–128.
167. Zhang, Z., B. Yuan, M. Bao, N. Lu, T. Kim, and Y.-J. Liu. 2011. The helicase DDX41 senses intracellular DNA mediated by the adaptor STING in dendritic cells. *Nat Immunol* 12: 959–965.
168. Jønsson, K. L., A. Laustsen, C. Krapp, K. A. Skipper, K. Thavachelvam, D. Hotter, J. H. Egedal, M. Kjolby, P. Mohammadi, T. Prabakaran, L. K. Sørensen, C. Sun, S. B. Jensen, C. K. Holm, R. J. Lebbink, M. Johannsen, M. Nyegaard, J. G. Mikkelsen, F. Kirchhoff, S. R. Paludan, and M. R. Jakobsen. 2017. IFI16 is required for DNA sensing in human macrophages by promoting production and function of cGAMP. *Nat Commun* 8: 14391.
169. Gray, E. E., D. Winship, J. M. Snyder, S. J. Child, A. P. Geballe, and D. B. Stetson. 2016. The AIM2-like Receptors Are Dispensable for the Interferon Response to Intracellular DNA. *Immunity* 45: 255–266.
170. Collins, A. C., H. Cai, T. Li, L. H. Franco, X.-D. Li, V. R. Nair, C. R. Scharn, C. E. Stamm, B. Levine, Z. J. Chen, and M. U. Shiloh. 2015. Cyclic GMP-AMP Synthase Is an Innate Immune DNA Sensor for Mycobacterium tuberculosis. *Cell Host and Microbe* 17: 820–828.
171. Scumpia, P. O., G. A. Botten, J. S. Norman, K. M. Kelly-Scumpia, R. Spreafico, A. R. Ruccia, P. K. Purbey, B. J. Thomas, R. L. Modlin, and S. T. Smale. 2017. Opposing roles of Toll-like receptor and cytosolic DNA-STING signaling pathways for Staphylococcus aureus cutaneous host defense. *PLoS Pathog* 13: e1006496.
172. Stetson, D. B., and R. Medzhitov. 2006. Recognition of Cytosolic DNA Activates an IRF3-Dependent Innate Immune Response. *Immunity* 24: 93–103.
173. Ablasser, A., F. Bauernfeind, G. Hartmann, E. Latz, K. A. Fitzgerald, and V. Hornung. 2009. RIG-I-dependent sensing of poly(dA:dT) through the induction of an RNA polymerase III-transcribed RNA intermediate. *Nature Publishing Group* 10: 1065–1072.
174. Herzner, A.-M., C. A. Hagmann, M. Goldeck, S. Wolter, K. Kübler, S. Wittmann, T. Gramberg, L. Andreeva, K.-P. Hopfner, C. Mertens, T. Zillinger, T. Jin, T. S. Xiao, E. Bartok, C. Coch, D. Ackermann, V. Hornung, J. Ludwig, W. Barchet, G. Hartmann, and M. Schlee. 2015. Sequence-specific activation of the DNA sensor cGAS by Y-form DNA structures as found in primary HIV-1 cDNA. *Nat Immunol* 16: 1025–1033.
175. Troegeler, A., C. Lastrucci, C. Duval, A. Tanne, C. E. L. Cougoule, I. Maridonneau-

Parini, O. Neyrolles, and G. Lugo-Villarino. 2014. An efficient siRNA-mediated gene silencing in primary human monocytes, dendritic cells and macrophages. *Immunology and Cell Biology* 92: 699–708.
176. An, J., J. J. Woodward, T. Sasaki, M. Minie, and K. B. Elkon. 2015. Cutting Edge: Antimalarial Drugs Inhibit IFN-β Production through Blockade of Cyclic GMP-AMP Synthase–DNA Interaction. *The Journal of Immunology* 194: 4089–4093.
177. Wu, J., L. Tian, X. Yu, S. Pattaradilokrat, J. Li, M. Wang, W. Yu, Y. Qi, A. E. Zeituni, S. C. Nair, S. P. Crampton, M. S. Orandle, S. M. Bolland, C.-F. Qi, C. A. Long, T. G. Myers, J. E. Coligan, R. Wang, and X.-Z. Su. 2014. Strain-specific innate immune signaling pathways determine malaria parasitemia dynamics and host mortality. *Proc. Natl. Acad. Sci. U.S.A.* 111: E511–E520.
178. Peyron, F., N. Burdin, P. Ringwald, J. P. Vuillez, F. Rousset, and J. Banchereau. 1994. High levels of circulating IL-10 in human malaria. *Clin. Exp. Immunol.* 95: 300–303.
179. Craig, A. G., G. E. Grau, C. Janse, J. W. Kazura, D. Milner, J. W. Barnwell, G. Turner, J. Langhorne, on behalf of the participants of the Hinxton Retreat meeting on "Animal Models for Research on Severe Malaria." 2012. The Role of Animal Models for Research on Severe Malaria. *PLoS Pathog* 8: e1002401–9.
180. White, N. J., G. D. H. Turner, I. M. Medana, A. M. Dondorp, and N. P. J. Day. 2010. The murine cerebral malaria phenomenon. *Trends in Parasitology* 26: 11–15.
181. Yuan, R., S. Geng, and L. Li. 2016. Molecular Mechanisms That Underlie the Dynamic Adaptation of Innate Monocyte Memory to Varying Stimulant Strength of TLR Ligands. *Front. Immunol.* 7: 38–12.
182. Bisgaard, L. S., C. K. Mogensen, A. Rosendahl, H. Cucak, L. B. Nielsen, S. E. Rasmussen, and T. X. Pedersen. 2016. Bone marrow-derived and peritoneal macrophages have different inflammatory response to oxLDL and M1/M2 marker expression – implications for atherosclerosis research. *Sci Rep* 1–10.
183. Jenkins, R., R. Omollo, M. Ongecha, P. Sifuna, C. Othieno, L. Ongeri, J. Kingora, and B. Ogutu. 2015. Prevalence of malaria parasites in adults and its determinants in malaria endemic area of Kisumu County, Kenya. *Malaria Journal* 1–6.
184. Scragg, I. G., M. Hensmann, C. A. Bate, and D. Kwiatkowski. 1999. Early cytokine induction by Plasmodium falciparum is not a classical endotoxin-like process. *European Journal of Immunology* 29: 2636–2644.
185. Newman, K. C., D. S. Korbel, J. C. Hafalla, and E. M. Riley. 2006. Cross-Talk with Myeloid Accessory Cells Regulates Human Natural Killer Cell Interferon-γ Responses to Malaria. *PLoS Pathog* 2: e118–14.
186. Schreiber, R. D. 2001. Measurement of mouse and human interferon gamma. *Curr Protoc Immunol* Chapter 6: Unit 6.8.
187. Baratin, M., S. Roetynck, C. Lépolard, C. Falk, S. Sawadogo, S. Uematsu, S. Akira, B. Ryffel, J.-G. Tiraby, L. Alexopoulou, C. J. Kirschning, J. Gysin, E. Vivier, and S. Ugolini. 2005. Natural killer cell and macrophage cooperation in MyD88-dependent innate responses to Plasmodium falciparum. *Proc. Natl. Acad. Sci. U.S.A.* 102: 14747–14752.
188. Hensmann, M., and D. Kwiatkowski. 2001. Cellular Basis of Early Cytokine

Response to Plasmodium falciparum. *Infect. Immun.* 69: 2364–2371.
189. Waterfall, M., A. Black, and E. Riley. 1998. Gammadelta+ T cells preferentially respond to live rather than killed malaria parasites. *Infect. Immun.* 66: 2393–2398.
190. D'Ombrain, M. C., D. S. Hansen, K. M. Simpson, and L. Schofield. 2007. γδ-T cells expressing NK receptors predominate over NK cells and conventional T cells in the innate IFN-γ response to Plasmodium falciparum malaria. *European Journal of Immunology* 37: 1864–1873.
191. Jagannathan, P., C. C. Kim, B. Greenhouse, F. Nankya, K. Bowen, I. Eccles-James, M. K. Muhindo, E. Arinaitwe, J. W. Tappero, M. R. Kamya, G. Dorsey, and M. E. Feeney. 2014. Loss and dysfunction of Vδ2$^+$ γδ T cells are associated with clinical tolerance to malaria. *Sci Transl Med* 6: 251ra117–251ra117.
192. Kleinnijenhuis, J., J. Quintin, F. Preijers, C. S. Benn, L. A. B. Joosten, C. Jacobs, J. van Loenhout, R. J. Xavier, P. Aaby, J. W. M. van der Meer, R. van Crevel, and M. G. Netea. 2014. Long-lasting effects of BCG vaccination on both heterologous Th1/Th17 responses and innate trained immunity. *J Innate Immun* 6: 152–158.
193. Bekkering, S., B. A. Blok, L. A. B. Joosten, N. P. Riksen, R. van Crevel, and M. G. Netea. 2016. In VitroExperimental Model of Trained Innate Immunity in Human Primary Monocytes. *Clin. Vaccine Immunol.* 23: 926–933.
194. Liehl, P., V. Zuzarte-Luís, J. Chan, T. Zillinger, F. Baptista, D. Carapau, M. Konert, K. K. Hanson, C. Carret, C. Lassnig, M. Müller, U. Kalinke, M. Saeed, A. F. Chora, D. T. Golenbock, B. Strobl, M. Prudêncio, L. P. Coelho, S. H. Kappe, G. Superti-Furga, A. Pichlmair, A. M. Vigário, C. M. Rice, K. A. Fitzgerald, W. Barchet, and M. M. Mota. 2013. Host-cell sensors for Plasmodium activate innate immunity against liver-stage infection. *Nature Medicine* 20: 47–53.
195. Yáñez, A., N. Hassanzadeh Kiabi, M. Y. Ng, J. Megías, A. Subramanian, G. Y. Liu, D. M. Underhill, M. L. Gil, and H. S. Goodridge. 2013. Detection of a TLR2 agonist by hematopoietic stem and progenitor cells impacts the function of the macrophages they produce. *European Journal of Immunology* 43: 2114–2125.